National Library of Canada
Canadian Theses Service
Ottawa, Canada
K1A 0N4

Bibliothèque nationale du Canada
Service des thèses canadiennes

NOTICE

The quality of this microform is heavily dependent upon the quality of the original thesis submitted for microfilming. Every effort has been made to ensure the highest quality of reproduction possible.

If pages are missing, contact the university which granted the degree.

Some pages may have indistinct print especially if the original pages were typed with a poor typewriter ribbon or if the university sent us an inferior photocopy.

Reproduction in full or in part of this microform is governed by the Canadian Copyright Act, R.S.C. 1970, c. C-30, and subsequent amendments.

AVIS

La qualité de cette microforme dépend grandement de la qualité de la thèse soumise au microfilmage. Nous avons tout fait pour assurer une qualité supérieure de reproduction.

S'il manque des pages, veuillez communiquer avec l'université qui a conféré le grade.

La qualité d'impression de certaines pages peut laisser à désirer, surtout si les pages originales ont été dactylographiées à l'aide d'un ruban usé ou si l'université nous a fait parvenir une photocopie de qualité inférieure.

La reproduction, même partielle, de cette microforme est soumise à la Loi canadienne sur le droit d'auteur, SRC 1970, c. C-30, et ses amendements subséquents.

NL-339 (r. 88/04) c

Canada

National Library of Canada
Canadian Theses Service
Ottawa Canada
K1A 0N4

Bibliothèque nationale du Canada
Service des thèses canadiennes

The author has granted an irrevocable non-exclusive licence allowing the National Library of Canada to reproduce, loan, distribute or sell copies of his/her thesis by any means and in any form or format, making this thesis available to interested persons.

The author retains ownership of the copyright in his/her thesis. Neither the thesis nor substantial extracts from it may be printed or otherwise reproduced without his/her permission.

L'auteur a accordé une licence irrévocable et non exclusive permettant à la Bibliothèque nationale du Canada de reproduire, prêter, distribuer ou vendre des copies de sa thèse de quelque manière et sous quelque forme que ce soit pour mettre des exemplaires de cette thèse à la disposition des personnes intéressées.

L'auteur conserve la propriété du droit d'auteur qui protège sa thèse. Ni la thèse ni des extraits substantiels de celle-ci ne doivent être imprimés ou autrement reproduits sans son autorisation.

ISBN 0-315-55481-9

Canada

THE UNIVERSITY OF ALBERTA

UNSTEADY FLOW ASPECTS OF RIVER ICE BREAKUP

BY

DESMOND WILLIAMSON

A THESIS
SUBMITTED TO THE FACULTY OF GRADUATE STUDIES AND RESEARCH
IN PARTIAL FULFILMENT OF THE REQUIREMENTS FOR THE DEGREE
OF MASTER OF SCIENCE

DEPARTMENT OF CIVIL ENGINEERING

EDMONTON, ALBERTA

FALL 1989

UNIVERSITY OF ALBERTA

RELEASE FORM

NAME OF AUTHOR DESMOND WILLIAMSON

TITLE OF THESIS UNSTEADY FLOW ASPECTS OF RIVER ICE BREAKUP

DEGREE FOR WHICH THESIS WAS PRESENTED MASTER OF SCIENCE

YEAR THIS DEGREE GRANTED FALL, 1989

Permission is hereby granted to THE UNIVERSITY OF ALBERTA LIBRARY to reproduce single copies of this thesis and to lend or sell such copies for private, scholarly or scientific research purposes only.

The author reserves other publication rights, and neither the thesis nor extensive extracts from it may be printed or otherwise reproduced without the author's written permission.

(SIGNED) D. Williamson....

PERMANENT ADDRESS:

.12136...129 st.............

.EDMONTON..AB.............

....

DATED Oct..12...1989

THE UNIVERSITY OF ALBERTA

FACULTY OF GRADUATE STUDIES AND RESEARCH

The undersigned certify that they have read, and recommend to the Faculty of Graduate Studies and Research for acceptance, a thesis entitled

UNSTEADY FLOW ASPECTS OF RIVER ICE BREAKUP

submitted by Desmond Williamson in partial fulfillment of the requirements for the degree of Master of Science.

(Supervisor)

Date : 10 Oct 89

ABSTRACT

The dynamic breakup of a solid ice cover in a river can be catastrophic, causing peak flood levels and destroying riverine structures. It is therefore of great interest to develop an understanding and to quantify the processes involved in such a breakup event.

A finite difference numerical model has been developed and used to examine the flow associated with the triggering and sustenance of a dynamic breakup. The numerical algorithm used is a four point implicit scheme using the Newton Raphson solution procedure. The model can be used for both open water and ice covered channels.

The model was used to study the river waves generated by a change in discharge, and a change in stage, both of which can trigger dynamic breakup. The change in discharge was intended to model flows such as power plant or dam releases and natural floods; the change in stage models the sudden failure of an ice jam. Dimensionless plots were developed to allow prediction of the nature of the river waves generated by these changes.

A modified version of this model was then used to investigate a possible mechanism for the sustenance of breakup and ice run. This mechanism is the additional force applied to the breakup front due to the rough ice pack and the passage of water released from channel storage as the breakup moves downstream. It was found that force applied to

the ice cover downstream of the breakup front can be increased by an order of magnitude over that for steady flow.

ACKNOWLEDGEMENT

The author would like to thank his supervisor Dr. R. Gerard for the guidance, wisdom, and encouragement he provided throughout this study. The opportunity to participate in field studies at Hay River and to attend the 5th Workshop on Hydraulics of River Ice/Ice Jams in Winnipeg is greatly appreciated. The author would also like to thank Dr. Gerard and Mr. M. Ferrick for arranging the visit to the US Army Cold Regions Research and Engineering Laboratory at Hanover, New Hampshire. Mr. Ferrick's knowledge and experience was invaluable and his hospitality, and that of the staff at CRREL, is greatly appreciated. Also, the author is grateful to Dr. P. Steffler for his advice and input on numerical modelling and to Mr. P. Banks of Alberta Environment for his assistance with the DAMBRK model.

TABLE OF CONTENTS

Chapter Page No.

ABSTRACT iv

ACKNOWLEDGEMENT vi

TABLE OF CONTENTS vii

LIST OF TABLES ix

LIST OF FIGURES x

1 INTRODUCTION

1.1 Introduction 1
1.2 The Breakup Process 2
1.3 Dynamic Breakup 3
1.4 Unsteady Flow and Breakup 7
1.5 Scope of Study 9

2 MODEL

2.1 Introduction 11
2.2 Modifications due to Ice Cover 12
2.3 The Scheme 15
2.4 Boundary and Initial Conditions 19
2.5 Input and Output 21
2.6 Model Testing 22

3 HYDROGRAPH ROUTING

3.1 Introduction 28
3.2 Parameter Definition 29
3.3 Dimensional Analysis 29
3.4 Results 36
3.5 Application 43

4 ICE JAM FAILURE

4.1 Introduction 53
4.2 Parameter Definition 56
4.3 Dimensional Analysis 57
4.4 Results 58
4.5 Application 72

5 BREAKUP

5.1 Introduction 77
5.2 Modelling Breakup 79
5.3 Parameter Definition 82
5.4 Dimensional Analysis 83
5.5 Results-Unsteady Flow 85
5.6 Results-Model of Strength-dominated breakup 90
5.7 Discussion 95

6 CONCLUSION 97

LIST OF REFERENCES 101

APPENDIX A : DETAILS OF COMPUTER PROGRAM

A.1 Numerical Solution Technique 107
A.2 Program Structure 109
A.3 Data Requirements 110
A.4 Running the Program 115
A.5 Program Listing 123

APPENDIX B : DATA FOR DIAGNOSTIC PLOTS

B.1 - Ch.3 146
B.2 - Ch.4 148

APPENDIX C : DATA FOR PREDICTIVE PLOTS

C.1 - Ch.3 149
C.2 - Ch.4 155

LIST OF TABLES

Table		Page No.
2.1	Data for numerical model runs	19
B.1	Data for Diagnostic Plots - Ch.3	146
B.2	Data for Diagnostic Plots - Ch.4	148
C.1	Data for Predictive Plots - Ch.3	149
C.2	Data for Predictive Plots - Ch.4	155

LIST OF FIGURES

Fig. Page No.

1.1 Schematic of Model of Support-dominated breakup 6

1.2 Schematic of Current Model of Strength-dominated breakup 6

2.1 Four Point Implicit Finite Difference Scheme 16

2.2 Comparison with Liland's results for the North Saskatchewan River: hydrograph at 80 km 24

2.3 Comparison with Liland's results for the North Saskatchewan River: profile at 40 hours 24

2.4a Connecticut River-station #1, open water 26

2.4b Connecticut River-station #2, open water 26

2.4c Connecticut River-station #3, open water 26

2.5a Connecticut River-station #1, ice cover 27

2.5b Connecticut River-station #2, ice cover 27

2.5c Connecticut River-station #3, ice cover 27

3.1 Schematic Showing Assumed Inflow Hydrograph 30

3.2 Hydrograph Routing - F_o=0.3, Q'=3, T_p'=1, T_b'=2 37

3.3a Effect of T_p' on Peak Depth at x'=1, T_b'=2, F_o=0.3 40

3.3b Effect of T_p' on Peak Friction Slope at x'=1,T_b'=2,F_o=0.3 40

3.3c Effect of T_p' on Wave Velocity at x'=1, T_b'=2, F_o=0.3 40

3.4a Effect of Q'
on Peak Depth at $x'=1$, $T_b'=2$, $F_o=0.3$ 41
3.4b Effect of Q'
on Peak Friction Slope at $x'=1, T_b'=2, F_o=0.3$ 41
3.4c Effect of Q'
on Wave Velocity at $x'=1$, $T_b'=2$, $F_o=0.3$ 41
3.5 Effect of T_b'
on Peak Depth at $x'=1$, $T_p'=1$, $F_o=0.3$ 42
3.6 Effect of F_o
on Wave Velocity at $x'=1$, $Tp'=1$, $Tb'=2$ 42
3.7a Attenuation of Peak Depth at $Q'=3$ 44
3.7b Attenuation of Peak Discharge at $Q'=3$ 44
3.7c Attenuation of Peak Friction Slope at $Q'=3$ 45
3.7d Attenuation of Wave Velocity at $Q'=3$ 45
3.8a Attenuation of Peak Depth at $Q'=5$ 46
3.8b Attenuation of Peak Discharge at $Q'=5$ 46
3.8c Attenuation of Peak Friction Slope at $Q'=5$ 47
3.8d Attenuation of Wave Velocity at $Q'=5$ 47
3.9a Attenuation of Peak Depth at $Q'=7$ 48
3.9b Attenuation of Peak Discharge at $Q'=7$ 48
3.9c Attenuation of Peak Friction Slope at $Q'=7$ 49
3.9d Attenuation of Wave Velocity at $Q'=7$ 49
4.1 Schematic Describing Jam Profile at Failure 55
4.2 Ice Jam Release - $F_o=0.3$, $X'=1$, $Y'=2$, $L'=0.1$ 59
4.3 Effect of X'
on Peak Depth at $x'=1$, $F_o=0.3$, $L'=0.2$ 1

4.4a Effect of Y' on Peak Depth at x'=1, F_o=0.3, L'=0.2 61
4.4b Effect of Y' on Peak Friction Slope at x'=1,X'=5,L'=0.2 62
4.4c Effect of Y' on Wave Velocity at x'=1, X'=5, L'=0.2 62
4.5a Effect of F_o on Peak Friction Slope at x'=1, X'=5, L'=0.2 63
4.5b Effect of F_o on Wave Velocity at x'=1, X'=5, L'=0.2 63
4.6a Effect of L' on Peak Friction Slope at x'=1, X'=5, L'=0.2 64
4.6b Effect of L' on Wave Velocity at x'=1, X'=5, L'=0.2 64
4.7a Attenuation of Peak Depth at Y'=2 66
4.7b Attenuation of Peak Discharge at Y'=2 66
4.7c Attenuation of Peak Friction Slope at Y'=2 67
4.7d Attenuation of Wave Velocity at Y'=2 67
4.8a Attenuation of Peak Depth at Y'=4 68
4.8b Attenuation of Peak Discharge at Y'=4 68
4.8c Attenuation of Peak Friction Slope at Y'=4 69
4.8d Attenuation of Wave Velocity at Y'=4 69
4.9a Attenuation of Peak Depth at Y'=6 70
4.9b Attenuation of Peak Discharge at Y'=6 70
4.9c Attenuation of Peak Friction Slope at Y'=6 71
4.9d Attenuation of Wave Velocity at Y'=6 71

4.10 Ice Jam Release

Athabasca River @ Fort McMurray 73

5.1a Effect of Ice Cover Removal on Depth 86

5.1b Effect of Roughness Change on Depth 86

5.2a Effect of Ice Cover Removal on Velocity 87

5.2b Effect of Roughness Change on Velocity 87

5.3a Effect of Ice Cover Removal on Discharge 88

5.3b Effect of Roughness Change on Discharge 88

5.4 Effect of Pack Length and Breakup Velocity on Force Applied at Breaking Front $F_o=0.3$, $Y'=1.5$ 91

5.5 Effect of Initial Froude Number and Breakup Velocity on Force Applied at Breaking Front $L'=0.75$, $Y'=1.5$ 92

5.6 Effect of Pack Roughness and Breakup Velocity on Force Applied at Breaking Front $F_o=0.3$, $L'=0.75$ 93

1 INTRODUCTION

1.1 Introduction

Break-up of a solid ice cover is an important and commonplace event, occurring at least once a year on most rivers and streams in Canada. Flooding, constraints to hydro-power production, interference with navigation, and damage to river structures are all problems associated with break-up. However, the current quantitative understanding of the break-up process is limited (Gerard and Flato, 1988).

Ferrick and Mulherin (1988) state that it is widely acknowledged that river waves are important in the ice break-up process, citing several references (Doyle and Andres, 1979 ; Henderson and Gerard, 1981 ; Beltaos and Krishnappan, 1982 ; Billfalk, 1982 ; Wong et al., 1985; and Prowse et al., 1986). Ferrick (1985) defines river waves as long period, shallow water waves that are a consequence of unsteady flow. It is therefore apparent that a quantitative analysis of the ice break-up process will involve solution of the equations governing unsteady flow in open channels. In this study, a computer model which solves the unsteady flow equations using a finite difference algorithm has been developed and is used to analyze selected aspects of the break-up process.

1.2 The Breakup Process

Gerard and Flato (1988) indicate three ways that a river ice cover may break up. The first is that no breakup will occur at all. This is possible in broad shallow streams that become frozen to the bed during winter. In this case, spring runoff will run in melt channels on top of the ice cover, and there is little movement of the bottomfast ice.

The second type is a thermal break-up. This consists of the floating ice cover essentially deteriorating and melting in place with only minor ice runs. This type f break-up tends to occur when there is relatively low and constant discharge during spring.

The third type is known as a dynamic break-up. This is when a strong competent ice cover is physically broken by large hydraulic forces associated with a well-defined river wave. This type of break-up is associated with large ice runs, major ice jams, and high water levels. As a result, this type is the most important and will be the type considered in this study.

All three types of break-up can be present in a river in a given year in different reaches of the river. Also, different types can occur in the same reach in different years. For example, Prowse et al. (1986) observed that in the seven years between 1978 and 1984 there were five dynamic breakups and two thermal breakups on the Liard River near its confluence with the Mackenzie River at Fort Simpson, N.W.T.

1.3 Dynamic Breakup

Gerard and Flato (1988) isolate four distinct stages of a dynamic breakup. These are : conditioning of the ice cover, triggering of the ice run, progression and sustenance of the ice run, and stall of the ice run. Conditioning of the ice cover includes an increase in forces applied to the ice cover by the flow and a decrease in the strength of the ice cover by decay and melt. Triggering is the stage when the forces on the ice cover exceed the cover's resistance. The accumulation of ice broken from the solid ice cover will then be accelerated by the flow. The progression and sustenance stage is when the ice run is moving downstream, breaking up a solid ice cover. It may move just a short distance or hundreds of kilometres, as observed by Parkinson (1982) on the Mackenzie River and Gerard et al. (1984) on the Yukon River. The sustenance of the ice run is likely related to the release of water from channel storage as the ice cover is removed. The final stage of an ice run is stall, at which point an ice jam is formed.

Ferrick and Mulherin (1989) classify the type of dynamic breakup according to the mode of failure of the ice cover. The two types they have observed are a support-dominated breakup and a strength-dominated breakup. A support-dominated breakup is a high energy event characterized by the failure of the ice cover at its supports resulting in a bank to bank release of the ice. The upstream end of the stationary ice cover is known as the breaking front. This type of breakup travels faster than the flow velocity, preventing the participation of broken ice in the breakup event. A strength-dominated breakup, however, is a low energy process, involving smaller hydraulic forces and lower breakup speeds. The ice broken off the solid cover interacts with the solid ice cover, breaking relatively small pieces from the intact cover.

These stages and types of breakup have been studied in various ways. Billfalk (1982) studied the case of a linearly sloping surge wave passing the end of an ice cover. When the induced bending moment exceeds the flexural strength of the ice cover, a crack leading to the triggering of breakup is assumed to occur. Beltaos (1984) following Shulyakovskii (1972) analysed the triggering stage of a dynamic breakup by relating it to the water surface width available for large broken ice sheets to pass. As a result, ice cover dimensions and channel geometry were considered to be of primary importance.

Ferrick and Mulherin (1989) have developed a numerical model intended to predict the triggering, sustenance and stall of a support-dominated breakup on the Connecticut River near Windsor, Vermont. The hydraulic forces applied to the ice cover are calculated by an unsteady flow model and when these forces exceed an empirical breakup criteria, the ice run is triggered. The movement of the ice run is modelled by considering the portion of the river upstream of the breaking front to be open water, thereby releasing water from storage and sustaining the ice run (see Fig. 1.1). When the forces at the breakup front no longer exceed the breakup criteria, the ice run is considered to have stalled, forming an ice jam. The empirical breakup criteria is based on the force required to fail the ice cover in shear along its hinge cracks. These hinge cracks are longitudinal cracks near the banks which are formed as the ice cover is repeatedly lifted and lowered by changes in discharge. Comparison with measured field data showed this model to quantify the dynamic breakup process at this site reasonably well.

Gerard and Flato (1988) present a model for analysing a strength-dominated type of breakup. This conceptual model of breakup considers a water mass balance, a force balance, and an ice mass balance. This model consists of a pack of broken ice interacting with a solid ice cover. The pack is bounded by open water upstream and the breaking front downstream (see Fig. 1.2). The force applied to the solid ice cover at the breaking front is affected by the shear applied by the flow to the pack of rough ice. This model and Ferrick and Mulherin's model form the two extremes possible in terms of dealing with the effect of the broken ice on the hydraulics.

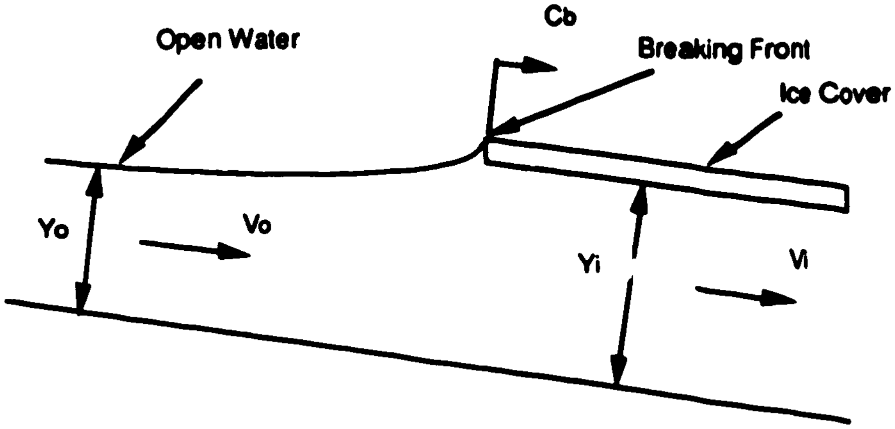
Open Water
Cb
Breaking Front
Ice Cover
Yo
Vo
Yi
Vi

Fig. 1.1 Schematic of Model of Support-dominated Breakup

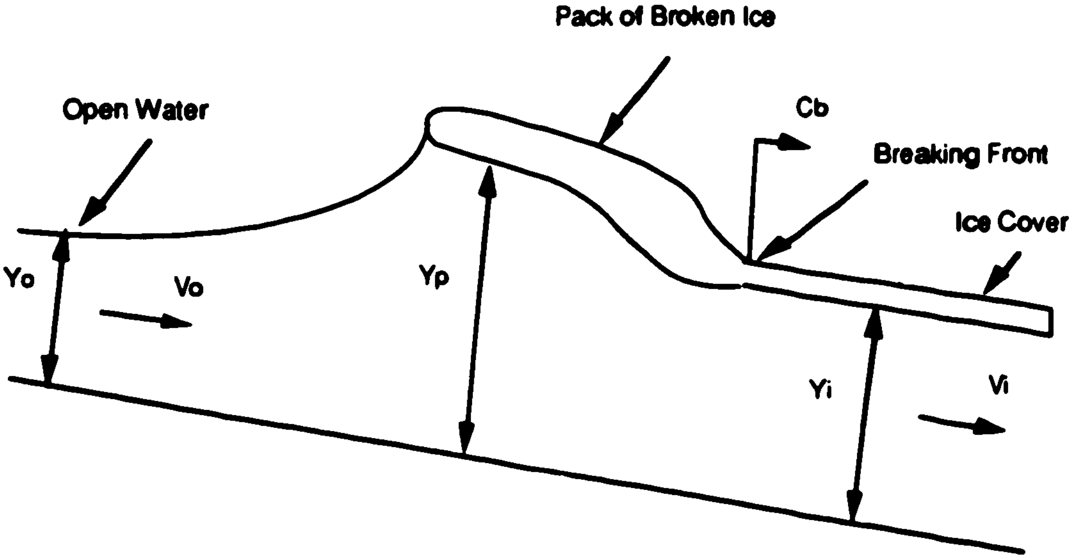
Pack of Broken Ice
Open Water
Cb
Breaking Front
Ice Cover
Yo
Vo
Yp
Yi
Vi

Fig. 1.2 Schematic of Current Model of Strength-dominated Breakup

1.4 Unsteady Flow and Breakup

There are two unsteady flow components of interest in studying the dynamic breakup process. One is the unsteady flow that may trigger breakup. The other is the self-generated unsteady flow associated with the ice run, which may affect the progression of breakup.

The unsteady flow required to initiate a dynamic breakup can be generated in two ways. The first is a sudden increase in discharge due to either natural events such as rain or snowmelt or releases from hydraulic structures such as hydroelectric plants. The second is the river wave resulting from the failure of an ice jam.

These surges are also of interest in ice jam flood forecasting. A river wave passing under an ice jam can be responsible for the peak flood levels. For example, this is often the case on the Hay River at the town of Hay River, N.W.T.(Gerard and Stanley, 1988). Here, an ice jam usually forms at the town because of its location on the delta of the river at Great Slave Lake. This ice jam is formed from an ice run that usually occurs first on the lower reaches of the river. As breakup progresses on the upper reaches, ice jams form and fail and thereby release surges that move downriver in to the ice jam at the delta. When these surges arrive, the highest water levels are experienced. Gerard and Stanley found it necessary to include the effect of such surges in their empirical flood forecasting model.

Once triggered, an ice run generates unsteady flow within itself and this may be the process responsible for sustaining a dynamic breakup after the river wave that triggered the run has moved ahead of the breaking front. Little work has been done in this area. Knowledge of the depth and shear stress distribution through the ice run would allow calculation of the force applied to the solid ice cover at the breaking front. This may provide insight into the sustenance of breakup.

Ferrick and Mulherin (1989) have used an unsteady flow model to quantify the increase in force applied to the solid ice cover during a support-dominated breakup. This analysis does not consider the presence of the pack of rough, broken ice upstream of the breaking front. However, an unsteady flow model can also be used to examine a strength-dominated breakup which does consider this pack.

When the pack is considered, the nature of the resulting unsteady flow is as follows. For a pack velocity between zero and the flow velocity, water is being released from storage at the upstream end of the ice cover, and going into storage at the downstream end of the pack (just upstream of the breaking front). Therefore, water released from upstream must reach the breaking front in order to sustain breakup. As this water passes under the rough ice of the pack, the shear stress applied to the ice pack will increase. The net increase in force applied to the pack is balanced by shear at the river banks and the solid ice cover downstream. This increase in the force applied to the solid ice cover from the increase in shear force on the pack may be a factor in the sustenance of breakup. An unsteady flow analysis can be used to investigate the magnitude of the increase in force at the breaking front.

1.5 Scope of Study

There are two cases of unsteady flow that are of interest in analysing the dynamic breakup process. First is the flow that may trigger breakup such as surges released by hydro-electric plant operation or ice jam failure upstream.

Numerical analysis of the movement and development of such waves has been performed before. However, the interest in this study is in carrying out a parametric study of these waves and to investigate if they can be generalized somewhat on the basis of dimensional analysis. Based on the latter, curves are generated that allow quick assessment of peak depth, peak discharge, peak friction slope, and wave velocity.

The second aspect of unsteady flow considered is the unsteady flow generated by a change in ice cover characteristics during breakup. The two significant changes in ice cover that occur during breakup are the increase in roughness of the broken ice, and the change from ice covered to open water conditions. Profiles of depth, discharge, and shear stress at different times are presented for a given set of flow conditions for both of these changes. These plots show the typical nature of the unsteady flow associated with each of these changes. Also, these two processes are combined in an attempt to model a strength-dominated breakup in a similar but simplified manner to the model of Gerard and Flato (1988). The simplifications used in this study are that only packs of fixed length are considered, and the change in thickness of the pack is not taken into account. Plots are presented which show the magnitude of the increase in force applied to the solid ice cover resulting from the increase in shear applied to the pack as a function of certain dimensionless parameters.

2 MODEL

2.1 Introduction

The unsteady flow model developed for this study is a four point implicit finite difference model based on a scheme introduced by Amein (1968). The formulation has been modified for application to non-prismatic channels by Chaudry and Contractor (1973). The solution of the set of finite difference equations is achieved by using the generalized Newton Raphson procedure. This method has been used extensively and is the basis of the National Weather Service models DWOPER and DAMBRK. Neglecting lateral inflow, the two non-linear partial differential equations which govern unsteady flow in open channels are the continuity equation :

$$B\frac{\partial Y}{\partial t} + A\frac{\partial V}{\partial x} + V\frac{\partial A}{\partial x} = 0 \qquad (2.1)$$

which describes the conservation of water mass, and the momentum equation :

$$\frac{\partial V}{\partial t} + V\frac{\partial V}{\partial x} + g\frac{\partial Y}{\partial x} - g(S_o - S_f) = 0 \qquad (2.2)$$

In these equations, Y is the flow depth, V cross-section-averaged flow velocity, B surface width, A flow cross section area, x longitudinal distance along the channel, g acceleration due to gravity, S_0 channel bed slope, and S_f friction slope (energy gradient).

2.2 Modifications due to Ice Cover

An ice cover affects the total waterway roughness, the hydraulic radius, and the depth of flow. These effects must be accounted for in the unsteady flow model.

The waterway roughness must be modified to account for the roughness of the underside of the ice cover. Daly and Ashton (1983) use the formula :

$$n_c = \left(\frac{n_b^{2/3}+n_i^{2/3}}{2}\right)^{3/2}$$

where n_c is the composite Manning's roughness coefficient, n_i is the roughness coefficient of the underside of the ice cover, and n_b is the roughness coefficient of the bed. As pointed out by Gerard and Andres (1982), this can be recast in more general terms as :

$$k_c = \left(\frac{k_b{}^p + k_i{}^p}{2}\right)^{1/p}$$

where k_c is the composite roughness height, k_b is the bed roughness height, and k_i is the roughness height of the underside of the ice cover. The exponent p is given by :

$$p = \frac{2m}{2m+1}$$

in which m is the exponent in a power law approximation of the semi-logarithmic equation for the conveyance coefficient C_* of the form :

$$C_* = 2.5 \ln \left(\frac{12R}{k_c}\right) \alpha \left(\frac{R}{k}\right)^m$$

where R is the hydraulic radius. The Manning equation is such a power law approximation with m = 1/6 which corresponds to p = 1/4. For the range of R/k found in ice jams, m = 1/4 (p = 1/3) is appropriate.

As usual, the hydraulic radius is calculated by :

$$R = \frac{A}{P}$$

where A is the cross-sectional area and P the wetted perimeter, which includes the ice cover. Generally the ice cover width is simply taken as the surface width although this is an approximation in non-rectangular channels in which the top width varies with stage but the ice cover has a fixed width. For wide rectangular channels, the presence of an ice cover means the hydraulic radius is approximately half the hydraulic radius for open water conditions.

S_f can then be calculated using the composite roughness ght and the hydraulic radius in the rearranged form of the dimensionless Chezy equation:

$$S_f = \frac{V^2}{gRC_*^2}$$

The other consideration is the effect of the submerged thickness of ice on the depth of flow. The total depth in the $g\frac{\partial Y}{\partial x}$ term of the momentum equation is equal to the waterway depth, used in the rest of the calculations, plus the submerged thickness of the ice. In the absence of snow cover or effect of attachment to shore, the submerged thickness t_s of an ice cover or ice pack is given by :

$$t_s = \left(\frac{\rho_i}{\rho}\right) t_i$$

where ρ_i is the density of ice, ρ the density of water, and t_i the ice thickness. In this program, the ratio $\frac{\rho_i}{\rho}$ is set equal to 0.92. The only time this consideration is important i when the ice thickness changes from section to section.

2.3 The Scheme

The four point implicit finite difference scheme (Fig. 2.1) approximates the dependent variables and the partial derivatives of the continuity and momentum equations. The dependent variables (B, A, V, S_f) are approximated by :

$$f(x,t) = \frac{\theta}{2}\left(f_{j+1}^{i+1} + f_{j+1}^{i} \right) + \frac{(1-\theta)}{2}\left(f_{j}^{i+1} + f_{j}^{i} \right)$$

where θ is a weighting factor, i represents the spatial interval along the channel, and j represents the time step.. The spatial derivatives are approximated by :

$$\frac{\partial f}{\partial x} = \frac{\theta}{\Delta x}\left(f_{j+1}^{i+1} - f_{j+1}^{i} \right) + \frac{(1-\theta)}{\Delta x}\left(f_{j}^{i+1} - f_{j}^{i} \right)$$

where Δx is the distance increment, and the temporal derivatives are evaluated by :

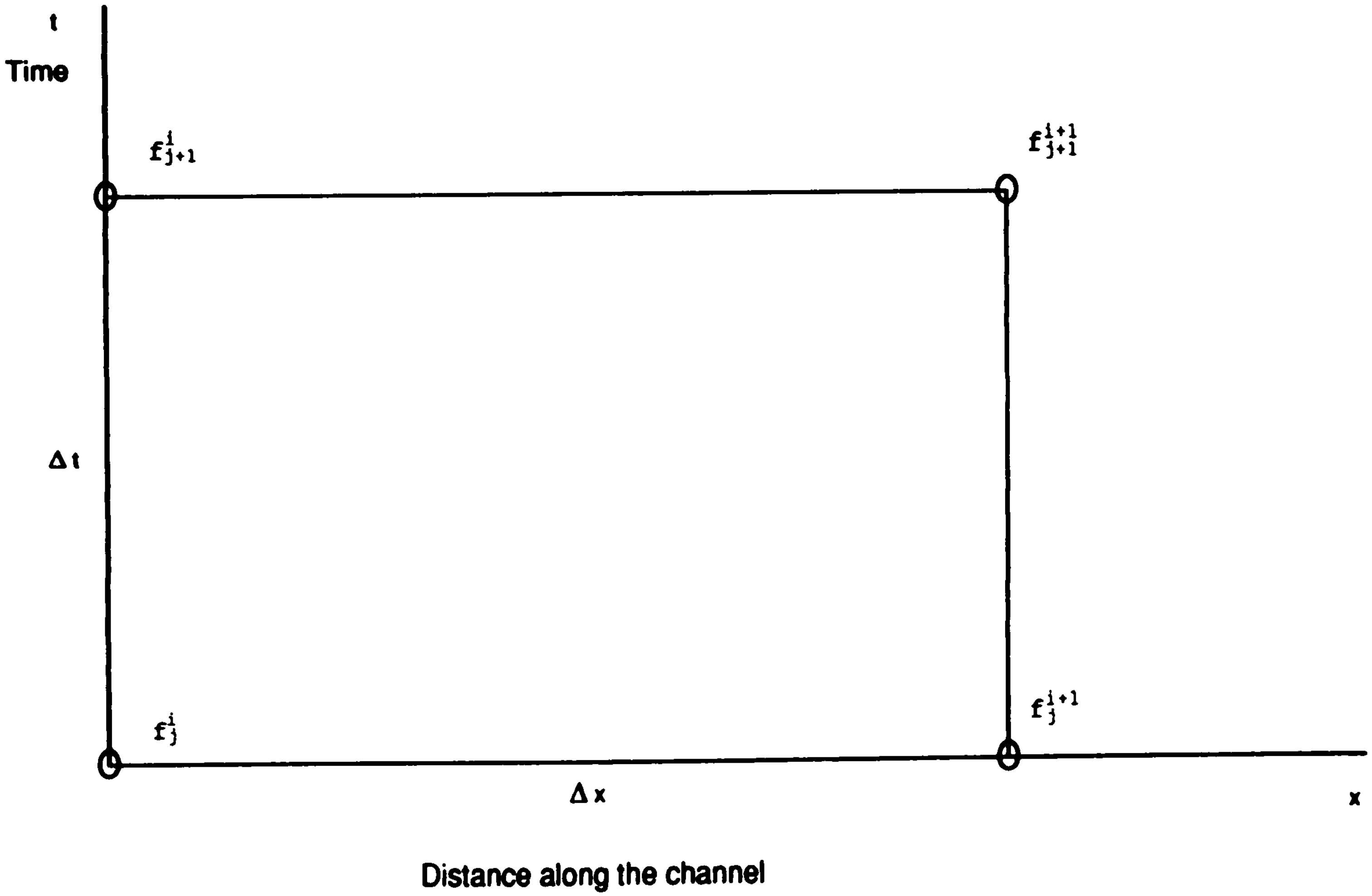
t
Time
f^{i}_{j+1}
f^{i+1}_{j+1}
Δt
f^{i}_{j}
f^{i+1}_{j}
Δx
x
Distance along the channel

Fig. 2.1 Four Point Implicit Finite Difference Scheme

$$\frac{\partial f}{\partial t} = \frac{1}{2\Delta t}\left(f_{j+1}^{i+1} + f_{j+1}^{i} - f_{j}^{i+1} - f_{j}^{i} \right)$$

where Δt is the time increment.

These approximations are used to transform the two governing partial differential equations into a set of algebraic equations. A pair of algebraic equations is formed for each pair of computational nodes along the channel. For a channel with N nodes, the result is (N-1) pairs of equations with 2N unknowns. Therefore, two boundary conditions are required to obtain a unique solution. For subcritical flow, one boundary condition must be supplied at both the upstream and downstream nodes.

The weighting factor, θ, plays a role in the accuracy and stability of the model. If the factor is set to 0.5, the derivative approximations are second order accurate. When θ moves away from 0.5, the approximations are only first order accurate and numerical diffusion is added to the model. However, Joliffe (1982) reports on studies that have found it desirable to increase the weighting coefficient slightly above 0.5. Test runs using this model for extreme cases of the hydrograph routing and ice jam failure studies found the change in accuracy between $\theta = 0.5$ and $\theta = 0.6$ to be insignificant. The maximum observed changes in results were as follows : peak flow depth 0.8%, peak discharge 1.8%, and peak friction slope 4%. Differences in results of these magnitudes only existed over small portions of the entire solution. The change in wave velocity was not measurable. All results presented in this study were calculated with a value of $\theta = 0.6$.

Choice of discretization parameters can also affect the accuracy of the solution. The discretization parameters are the spacial discretization (Δx) and the temporal discretization (Δt). Δx is the distance between the nodes that define the channel and Δt is the increase in total time for each step of the solution. Fread (1984) provides some rules of thumb to aid in the selection of these parameters. He suggests that a good first estimate of Δt is 1/20 of the time to peak discharge for routing inflow hydrographs. For Δx, he recommends $\Delta x \leq c\Delta t$ where c is wave speed.

However, the approach used to select Δx and Δt in this study was to try certain values and then either reduce or increase the parameters to evaluate the sensitivity of the solution to Δx and Δt. If a significant change in results was observed, the steps were reduced until a change was no longer observed. If a significant change in results was not observed, the parameters were sometimes increased to reduce computational effort. This selection procedure was used for each major channel situation used in the production of all plots presented in Ch.3 and Ch.4. The five major channel situations and discretizations used for the plots presented in this study are shown in Table 2.1. Other situations were used to check the generality of the dimensionless presentation.

Table 2.1 - Data for numerical model runs

Yo (m)	So	Qo (m^3/s)	Vo (m/s)	B (m)	Fo	Ice	Time Step (hr.)	Distance Step (m)
1.674	0.0002	700	0.418	1000	0.1	Y	0.5	2000
1.042	0.0004	600	0.640	900	0.2	N	0.2	750
1.379	0.0007	600	1.088	400	0.3	N	0.1	500
1.207	0.0006	500	1.381	300	0.4	N	0.025	200
0.977	0.0010	700	1.551	330	0.5	N	0.025	200

2.4 Boundary and Initial Conditions

As mentioned above, for subcritical flow a boundary condition is required at both the upstream and downstream ends of the reach being modelled. The upstream boundary condition can be provided by specifying either the discharge or the depth at the first node. A table of discrete values for various times ((Q,t) or (Y,t)) is supplied to the computer program in the input file. The program linearly interpolates between these points to calculate the value at the upstream node at each time step.

There are four options available for the downstream boundary condition. The first option, a channel-controlled stage-discharge relationship, is used frequently in the analysis presented in this report. The discharge at the downstream node is calculated by :

$$Q = C.A\sqrt{gRS_f}$$

where S_f is approximated from the change in depth between the last two nodes by :

$$S_f \approx S_o - \frac{\partial Y}{\partial x}$$

This equation reproduces the hysteresis which is characteristic of river wave rating curves (Fread, 1984).

The second option is for critical flow at the downstream node. This option may be needed if the reach ends at a fall, rapids, or an engineering structure which causes the flow to become supercritical. The third and fourth options are for the depth or the discharge at the downstream node to be specified with time in a manner similar to the upstream boundary conditions. Specifying depth may be applicable if the end of the [illegible] is at a large body of water such as a lake. Specifying discharge is appropriate if there is a dam or structure at the downstream node with a known release pattern.

The initial conditions over the reach can be given in one of two ways. The first is for the stage at each section to be given in the input data file. Assuming steady state initial conditions, the initial discharge is then used to calculate the velocity at each node. This option is necessary for the study of the release of an ice jam, where the initial stage profile is given. The second option is to calculate the initial depths using the initial discharge, channel geometry, and downstream boundary condition. The calculation procedure used for this in this program is the standard step gradually varied flow algorithm.

2.5 Input and Output

Data required to define channel geometry can be input in two ways. The first assumes a trapezoidal channel with a constant bed slope. The bottom width, side slope, and bed slope are read in prior to the cross section data. The cross section data for each section consists of the distance along the channel, the initial flow depth, the initial discharge, the ice thickness, the channel roughness, and the roughness of the bottom of the ice cover. If the program is used to calculate the initial profile, the flow depths will be ignored except at the downstream section; this is needed if the fixed elevation downstream boundary condition is being used. For open water routing the ice thickness should be input as zero and the roughness of the bottom of the ice cover will be ignored.

The other method of input is applicable to irregular channels. With this option, a table containing cross section coordinates is included with each set of cross section data. The program will select the minimum elevation from each table to establish the thalweg profile and from this the bed slope for each reach is calculated.

The program output is controlled by options selected in the input data file. In all cases, the initial flow conditions are output, as is a table of the maximum flow characteristics at each section. However, the input file controls when profiles are written and at which sections hydrographs are stored. The table of maximum conditions can be used to trace the amplitude of the wave as it moves down the river. This data is used to create the dimensionless depth profiles presented in the hydrograph routing and the ice jam release sections. The hydrographs can be used to calculate the time of arrival of the wave at various distances downstream.

2.6 Model Testing

The first test applied to the model was a comparison with the dynamic routing portion of the NWS model DAMBRK. As stated earlier, DAMBRK uses the same scheme and solution procedure as this model, making it a good test for open water conditions. The results of several different hydrograph routing runs were compared and were found to agree very well.

To test the ice cover portion of the model, a comparison was made to the results for the North Saskatchewan River upstream of Edmonton generated by a model developed by Liland (1971). This model solves the governing equations by the method of characteristics. The channel was approximated as trapezoidal with a base width of 64m and side slopes of 15 horizontal to 1 vertical. The initial discharge was 27 m^3/s, bed slope 0.00095, and Manning roughness coefficient 0.023. The initial conditions were read from plots. The results from the present model compare well with those of Liland, as can be seen in Fig. 2.2 and 2.3. The maximum difference was approximately 7%.

A final test was conducted by comparing the model results with data gathered in the field for both open water and ice covered conditions. Ferrick, Lemieux, Weyrick and Demont (1988) present stage data measured on the Connecticut River near Windsor, Vermont during controlled dam release tests for both open water and ice covered conditions. Using channel data gathered by Ferrick et al. and the initial conditions shown in their plots, the boundary conditions were

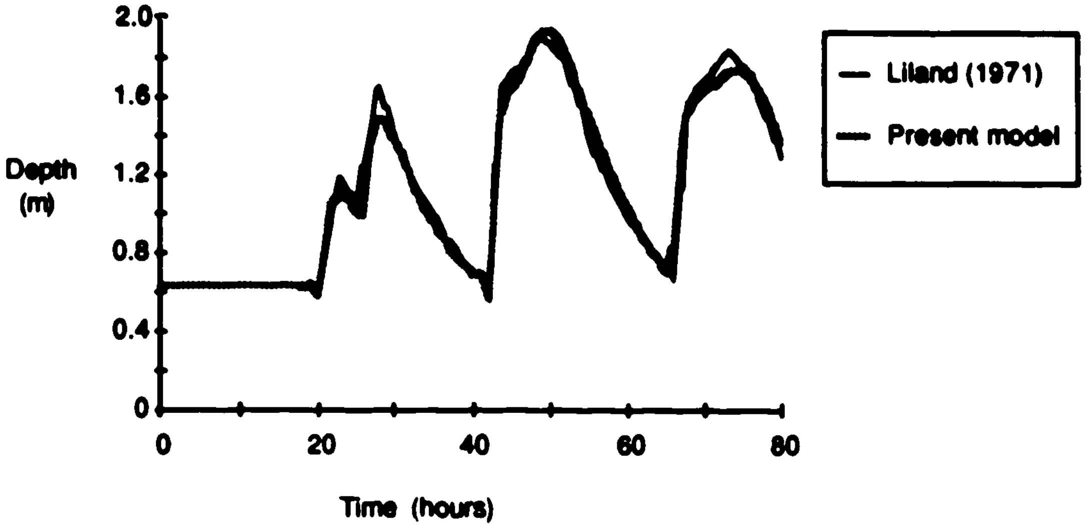

Fig. 2.2 Comparison with Liland's results for the North Saskatchewan River : hydrograph at 80 km

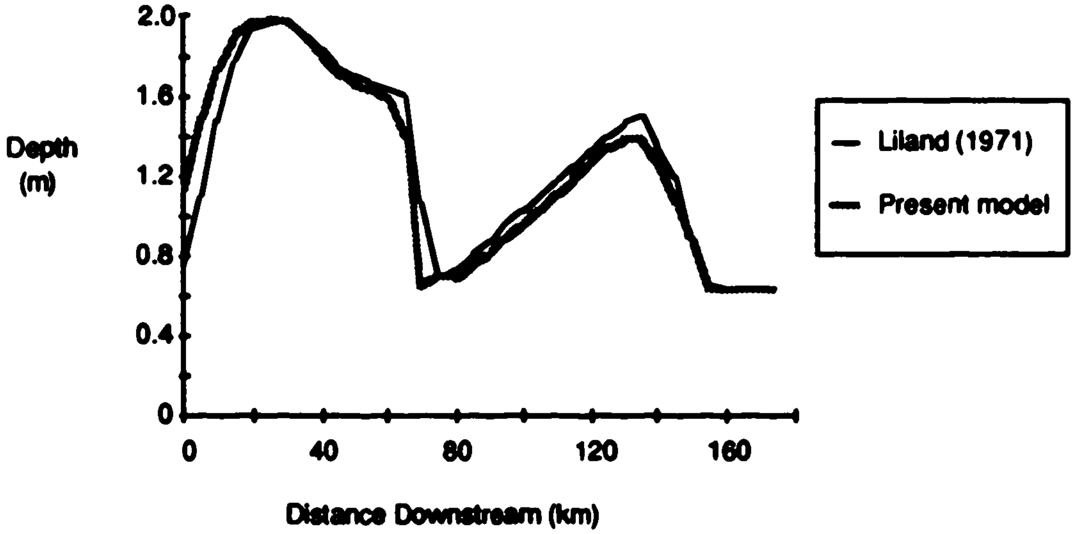

Fig. 2.3 Comparison with Liland's results for the North Saskatchewan River : profile at 40 hours

adjusted to match the hydrograph measured at the gauging station near the upstream end of the study reach. The program was then run and the hydrographs stored as the river wave passed the three measurement stations in the reach. In the ice covered case, an ice cover was present from just downstream of station #1 (≈ 15 km downstream from the start of the reach) to the downstream end of the reach. The distance from the upstream end of the reach is approximately 25 km. to station #2 and 35km. to station #3. Plots of increase in stage against time are presented in Fig.2.4a - Fig 2.5c for all three stations for both the open water and the ice covered cases. The present model computes the attenuation and velocity of the river waves quite well in both cases. As might be expected, the ice cover increases the attenuation of the river wave and reduces its velocity.

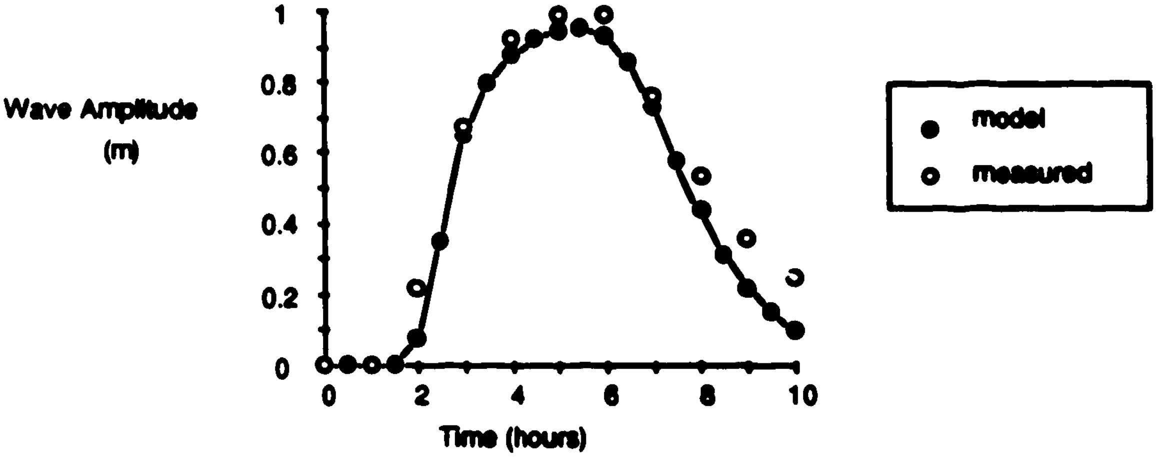

Fig. 2.4a CONNECTICUT RIVER - station #1
open water

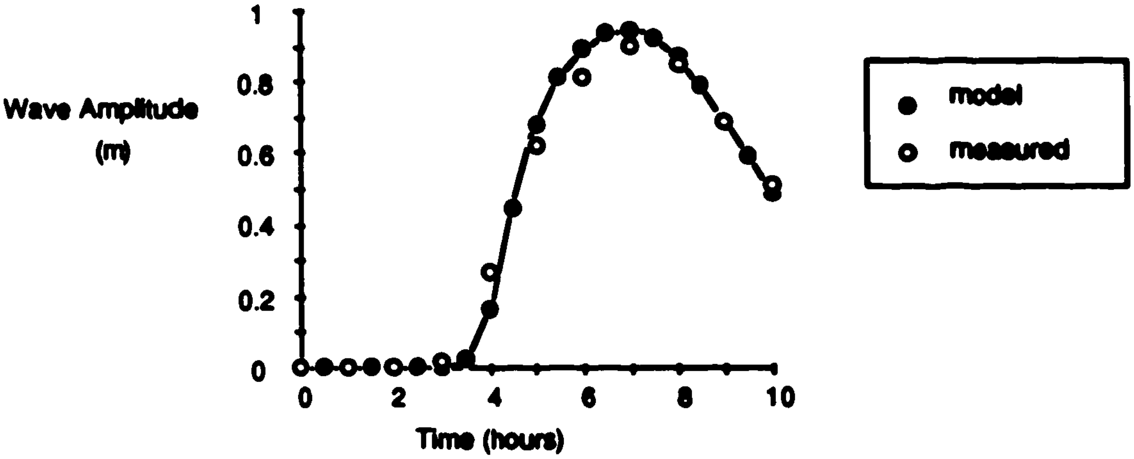

Fig. 2.4b CONNECTICUT RIVER - station #2
open water

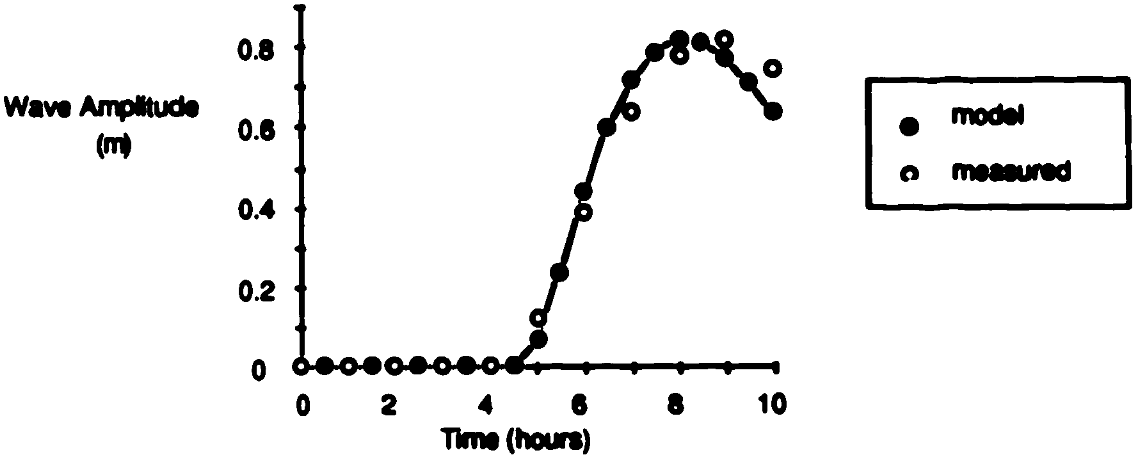

Fig. 2.4c CONNECTICUT RIVER - station #3
open water

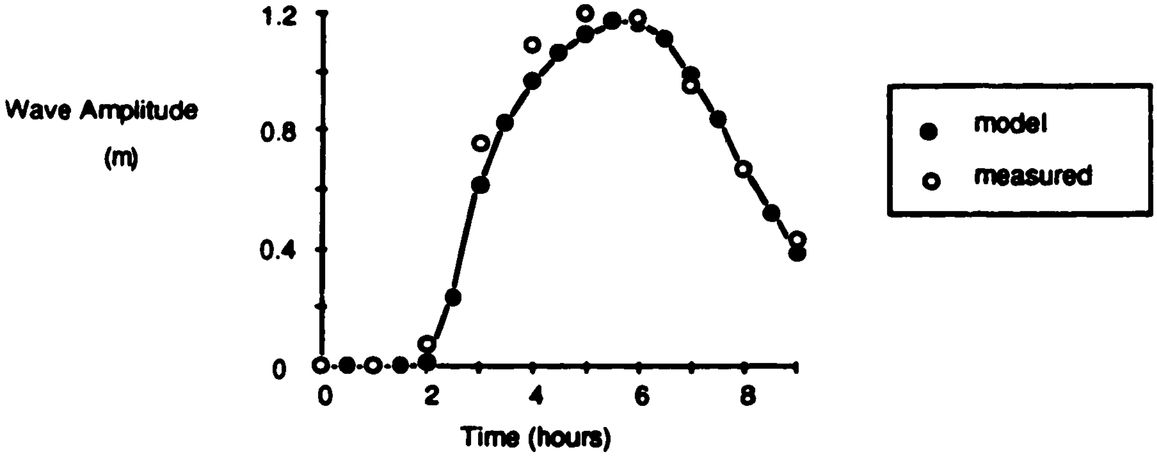

Fig. 2.5a CONNECTICUT RIVER - station #1
ice cover

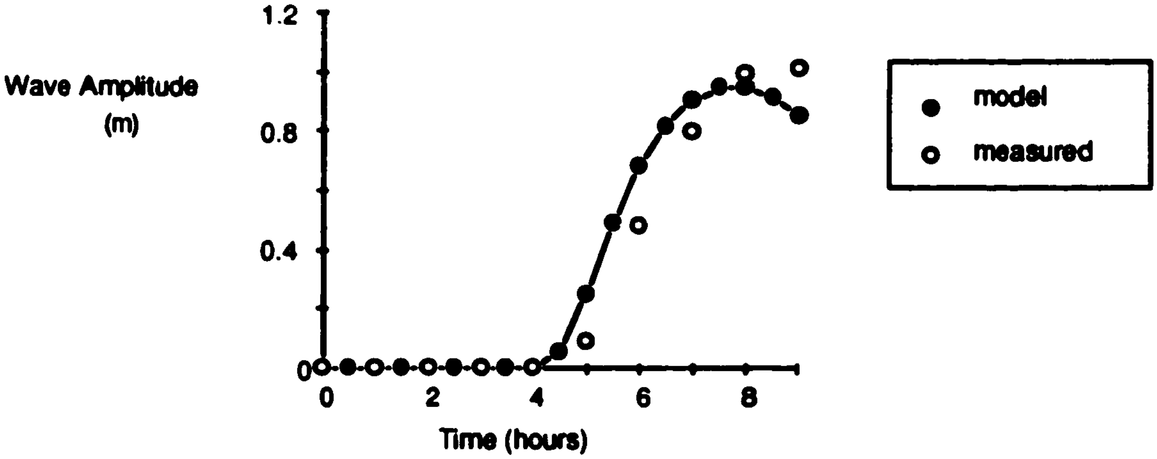

Fig. 2.5b CONNECTICUT RIVER - station #2
ice cover

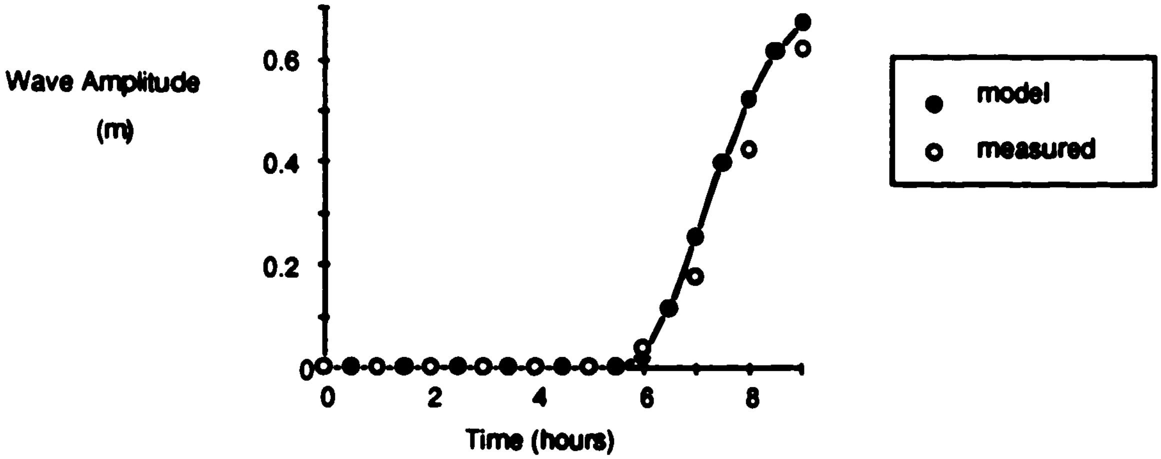

Fig. 2.5c CONNECTICUT RIVER - station #3
ice cover

3 HYDROGRAPH ROUTING

3.1 Introduction

In this section, a parametric study is carried out on the first situation of interest- a sudden change in discharge generated by hydro-electric plant releases or natural flood waves. To simplify the analysis, the shape of the hydrographs associated with the sudden change in discharge has been idealised as triangular. This allows the hydrograph to be characterized by only two parameters. Also, the channels considered are rectangular and have constant slope and roughness. As well as providing an indication of sensitivity to certain parameters, the results can be used for preliminary estimates of the characteristics of the unsteady flow that results in these circumstances.

A wide range of physical variables is involved in this analysis, requiring a technique for presenting the results systematically. This is achieved by developing dimensionless parameters to describe the river wave characteristics, such as the variation in the peak depth (Y), peak discharge (Q), peak energy gradient (S_f), and wave speed (C_w) as the wave moves downstream.

3.2 Parameter Definition

Fig. 3.1 shows the parameters that describe the inflow hydrograph. The discharge rises linearly from the initial flow rate (Q_o) to a maximum (Q_p) in a prescribed time (T_p). It then falls linearly until it returns to Q_o at time T_b.

The parameters required to define the channel are the bed slope (S_o), width (B), channel roughness (k_b), and ice cover roughness (k_i). Variation in ice cover thickness was not considered.

3.3 Dimensional Analysis

An appropriate set of dimensionless parameters that will allow complete presentation of the results can be found by non-dimensionalizing the governing unsteady flow equations (equations 2.1 and 2.2) and boundary conditions. A previous attempt at non-dimensionalizing the open channel unsteady flow equations in order to present results from a numerical model was made by Kabir and Orsborn (1984), but this approach was not applicable to the present situation.

Taking X_s as a distance scale, V_s as a velocity scale, T_s as a time scale, and Y_s as a depth scale, the momentum equation (2.2) becomes :

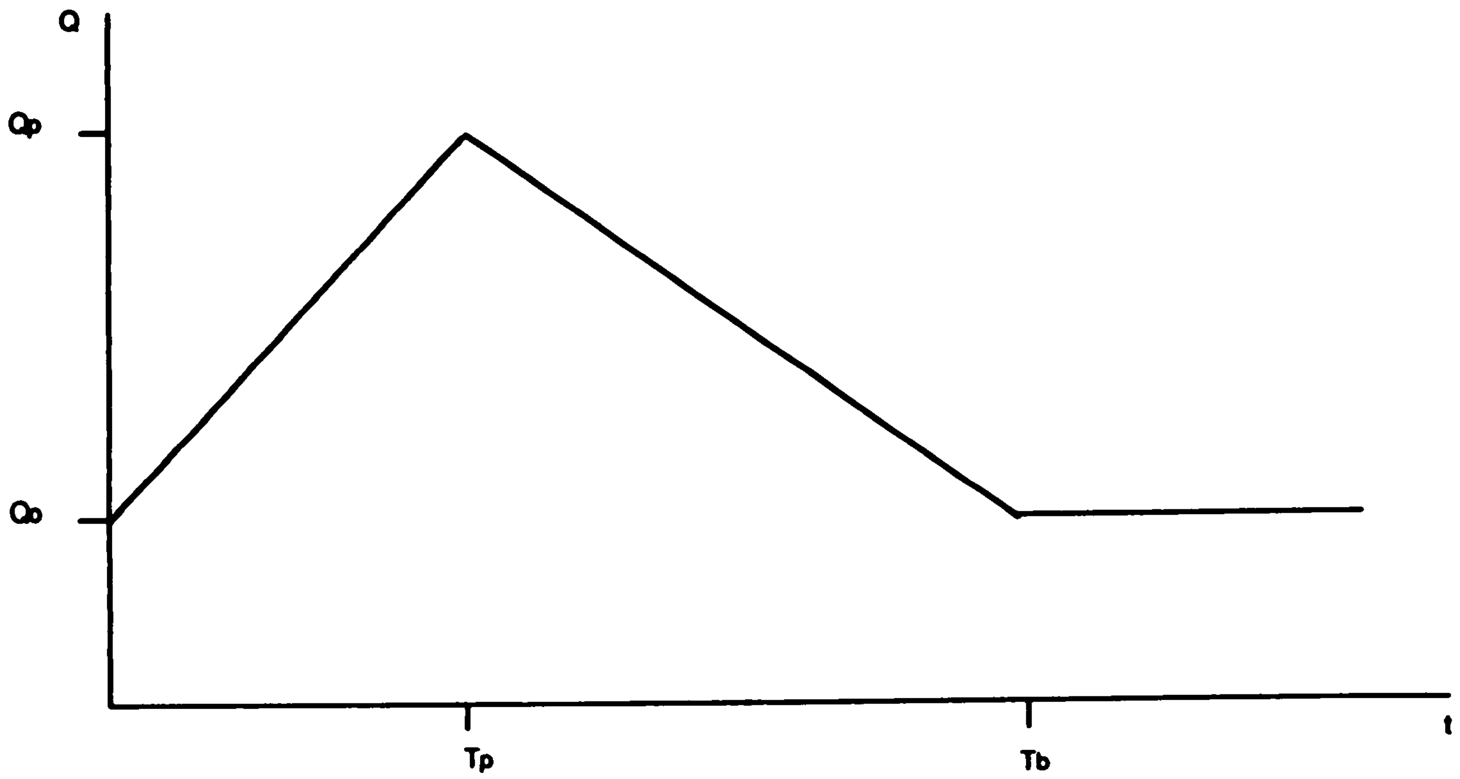

Fig. 3.1 Schematic Showing Assumed Inflow Hydrograph

$$\frac{V_s}{T_s}\frac{\partial V'}{\partial t'} + \frac{V_s^2}{X_s} V'\frac{\partial V'}{\partial x'} + \frac{gY_s}{X_s}\frac{\partial Y'}{\partial x'} - g(S_o - S_f) = 0$$

where :

$$t' = \frac{t}{T_s}$$

$$V' = \frac{V}{V_s}$$

$$Y' = \frac{Y}{Y_s}$$

and $x' = \dfrac{x}{X_s}$.

Dividing both sides by $\dfrac{V_s^2}{X_s}$ yields :

$$\frac{X_s}{V_s T_s}\frac{\partial V'}{\partial t'} + V'\frac{\partial V'}{\partial x'} + \frac{gY_s}{V_s^2}\frac{\partial Y'}{\partial x'} - \frac{gX_s(S_o - S_f)}{V_s^2} = 0$$

Defining the time scale $T_s \equiv \dfrac{X_s}{V_s}$ reduces this equation to :

$$\frac{\partial V'}{\partial t'} + V'\frac{\partial V'}{\partial x'} + \frac{gY_s}{V_s^2}\frac{\partial Y'}{\partial x'} - \frac{gX_s S_o}{V_s^2} + \frac{gX_s S_f}{V_s^2} = 0$$

and defining the distance scale $X_s \equiv \dfrac{Y_s}{S_o}$ gives :

$$\frac{\partial V'}{\partial t'} + V'\frac{\partial V'}{\partial x'} + \frac{gY_s}{V_s^2}\frac{\partial Y'}{\partial x'} - \frac{gY_s}{V_s^2} + \frac{gY_s}{V_s^2}\left(\frac{S_f}{S_o}\right) = 0$$

Using the approximation that the conveyance coefficient C_* is given by :

$$C_* \alpha \left(\frac{R}{k}\right)^m$$

where k is the waterway roughness and recognizing that :

$$S_o = \frac{V_o^2}{gR_oC_{*o}^2} \quad \text{and} \quad S_f = \frac{V^2}{gRC_*^2}$$

leads to :

$$\frac{S_f}{S_o} = \left(\frac{V}{V_o}\right)^2 \left(\frac{R_o}{R}\right)^{(1+2m)} \left(\frac{k_o}{k}\right)^{2m} = \left(\frac{V}{V_o}\right)^2 \left(\frac{R_o}{R}\right)^{(1+2m)}$$

where k_o is the initial waterway roughness. Applying the scales, using the wide channel approximation R = Y for open channels ($R = \frac{Y}{2}$ for ice covered channels) and assuming the waterway roughness is constant, yields :

$$\frac{S_f}{S_o} = \left(\frac{V'V_s}{V_o}\right)^2 \left(\frac{Y_o}{Y'Y_s}\right)^{(1+2m)}$$

Substituting for $\frac{S_f}{S_o}$, the momentum equation becomes :

$$\frac{\partial V'}{\partial t'} + V'\frac{\partial V'}{\partial x'} + \frac{gY_s}{V_s^2}\frac{\partial Y'}{\partial x'} - \frac{gY_s}{V_s^2} + \frac{gY_s}{V_s^2}\left(\frac{V'V_s}{V_o}\right)^2 \left(\frac{Y_o}{Y'Y_s}\right)^{(1+2m)} = 0$$

It is now necessary to select an appropriate velocity scale and vertical length scale. The obvious choice for the latter is the normal depth Y_o. For the velocity scale either the normal velocity V_o or the dynamic celerity $\sqrt{gY_o}$ may be used. The celerity of dynamic waves scales on $\sqrt{gY_o}$ but the celerity of diffusive waves scales on V_o. The waves that result in this analysis range between diffusive waves and dynamic waves so either scale would be as convenient as the other. Herein, V_o is taken as the velocity scale. Finally, therefore, equation 2.2 reduces to :

$$F_o^2 \left(\frac{\partial V'}{\partial t'} + V'\frac{\partial V'}{\partial x'}\right) + \frac{\partial Y'}{\partial x'} + V'^2 \left(\frac{1}{Y'}\right)^{(1+2m)} - 1 = 0$$

where $F_o^2 = \dfrac{V_o^2}{gY_o}$, F_o being the initial Froude number.

Applying the Y_s, V_s, X_s, and T_s scales to the continuity equation (2.1) yields :

$$\frac{BY_s}{T_s}\frac{\partial Y'}{\partial t'} + \frac{BY_sV_sY'}{X_s}\frac{\partial V'}{\partial x'} + \frac{V_sBY_sV'}{X_s}\frac{\partial Y'}{\partial x'} = 0$$

Dividing by B gives :

$$\frac{Y_s}{T_s}\frac{\partial Y'}{\partial t'} + \frac{Y_sV_sY'}{X_s}\frac{\partial V'}{\partial x'} + \frac{Y_sV_sV'}{X_s}\frac{\partial Y'}{\partial x'} = 0$$

Since $T_s = \frac{X_s}{V_s}$, equation 2.1 becomes :

$$\frac{Y_sV_s}{X_s}\frac{\partial Y'}{\partial t'} + \frac{Y_sV_sY'}{X_s}\frac{\partial V'}{\partial x'} + \frac{Y_sV_sV'}{X_s}\frac{\partial Y'}{\partial x'} = 0$$

Dividing both sides by $\frac{Y_sV_s}{X_s}$ reduces equation 2.1 to :

$$\frac{\partial Y'}{\partial t'} + Y'\frac{\partial V'}{\partial x'} + V'\frac{\partial Y'}{\partial x} = 0$$

When made dimensionless, the longitudinal distance variable x becomes :

$$x' = \frac{x}{\frac{Y_o}{S_o}} = \frac{xS_o}{Y_o}$$

and time t becomes :

$$t' = \frac{t}{\frac{Y_o}{V_oS_o}} = \frac{tV_oS_o}{Y_o}$$

The variables that define the boundary conditions in this section are T_p, T_b, and $q_p = Q_p/B$. Non-dimensionalizing T_p yields :

$$T_p' = \frac{T_p}{T_s} = \frac{T_p V_o S_o}{Y_o}$$

and non-dimensionalizing q_p by the appropriate scales gives :

$$\frac{q_p}{V_s Y_s} = \frac{q_p}{V_o Y_o} = \frac{q_p}{q_o} = \frac{Q_p}{Q_o} = Q'$$

The other time variable T_b can be made dimensionless by dividing by T_p yielding a hydrograph shape parameter :

$$\frac{T_b}{T_p} = T_b'$$

Finally, then, assuming m is constant over the range of interest, any dimensionless feature of the solution, say χ, will depend on :

$$\chi = f(F_o , T_p' , Q' , T_b' , x' , t')$$

The results of interest in this section are the peak waterway depth Y, peak discharge Q, peak energy gradient S_f, and wave velocity C_w. These results are of interest because Y and Q are good indicators of the magnitude of the wave, S_f is related to the force applied by the flow to the ice cover (Ferrick and Mulherin , 1989), and wave velocity can be used to predict time of arrival of the wave. The wave velocity in this study is calculated by :

$$C_w = \frac{x}{t}$$

where x is the distance to a given section, and t is the time at which the depth has risen by 1 % over the initial depth at that section. Care was taken to assure this 1% increase was indicative of wave arrival. The appropriate dimensionless form of these results is :

$$\frac{Y}{Y_o},\ \frac{Q}{Q_o},\ \frac{S_f}{S_o},\ \text{and}\ \frac{C_w}{V_o}$$

3.4 Results

Fig. 3.2 shows the changes to a hydrograph as it is routed downstream for a given set of conditions. It is evident that the wave becomes broader and less peaked with distance. The following plots show the effect of certain

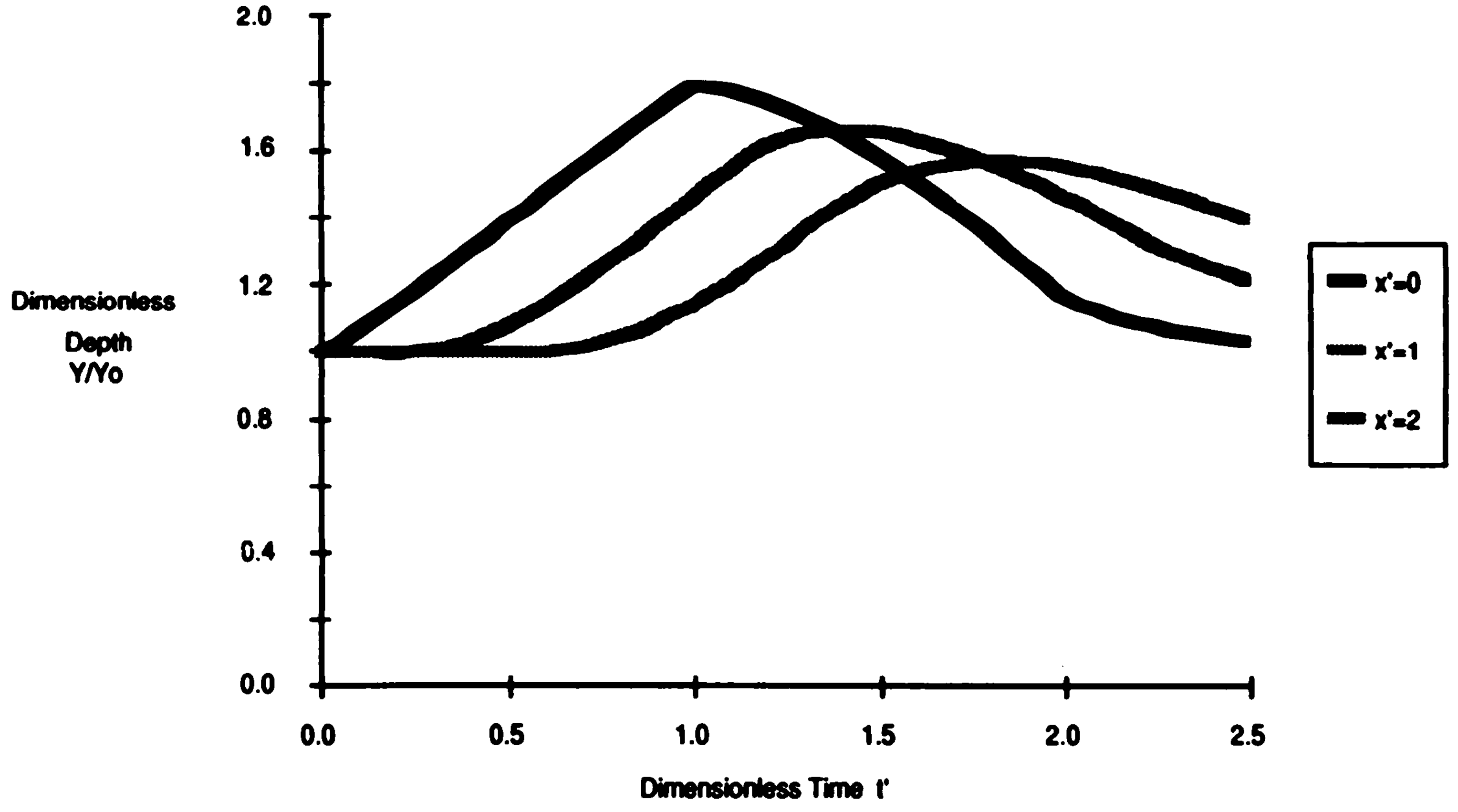

Fig. 3.2 Hydrograph Routing - Fo=0.3, Q'=3, Tp'=1, Tb'=2

variables on this attenuation process and quantify the changes that occur.

The results of this chapter are presented in two parts. The first set of plots are 'diagnostic plots'. These plots attempt to isolate the effect of each dimensionless parameter on the solution to allow an assessment of the sensitivity and to aid in interpolating between the second set of plots, the 'predictive' plots. These plots can be used to predict the variation in the above salient features of a river wave as it propagates downstream. They are intended to cover a wide range of practical cases of unsteady flow. Because of the manner of non-dimensionalizing utilized in this analysis, the effect of an ice cover on these dimensionless plots is negligible and therefore they are applicable to both open water and ice cover cases. In fact, some of the plots have been generated with an ice cover present.

Fig. 3.3 to Fig. 3.6 are the diagnostic plots. Selected data for these plots can be found in Appendix B. The effect of T_p' is investigated in the three plots of Fig. 3.3. With Q' and T_b' held constant, T_p' represents both the steepness and volume of the inflow hydrograph. Fig. 3.3a shows the effect of T_p' on the peak depth at a selected dimensionless distance. When T_p' is large, attenuation of depth is small and the flow approaches steady state. However, when T_p' becomes smaller, attenuation of peak depth increases. Fig. 3.3b and Fig 3.3c show the effect of T_p' on the peak friction slope and wave velocity. As T_p' becomes smaller, the steepness of the inflow hydrograph increases resulting in higher peak friction slopes and wave velocities. However, a decrease in peak friction slope and wave velocity occurs as T_p' becomes very small. This is because rapid attenuation of the wave under these circumstances is affecting the results. This decrease can be seen in Fig. 3.3c. The theoretical wave velocity limits suggest that the waves in this study range from diffusive to dynamic waves.

The three plots of Fig. 3.4 show the effect of Q'. All results show an increase as Q' increases. The effect of Q' is more noticeable on depth and friction slope than on wave velocity. Also, the plots show that a linear interpolation between the range of Q' presented in the practical plots can be used.

Fig. 3.5 shows the effect of the T_b' parameter on peak depth at a short distance downstream. The effect of Tb' on the other results is not shown because it is even less significant. A slight increase in peak depth is shown as the T_b' parameter increases. This is expected since an increase in T_b' represents an increase in the volume of the inflow hydrograph, thereby reducing attenuation. The magnitude of the effect of T_b' increases with distance. The effect of T_b' on friction slope is negligible and the maximum effect on wave velocity is 6%.

Fig. 3.6 shows the effect of F_o on wave velocity at a certain distance. Again, the effect on the other results is not shown since it is very small. A slight decrease in wave

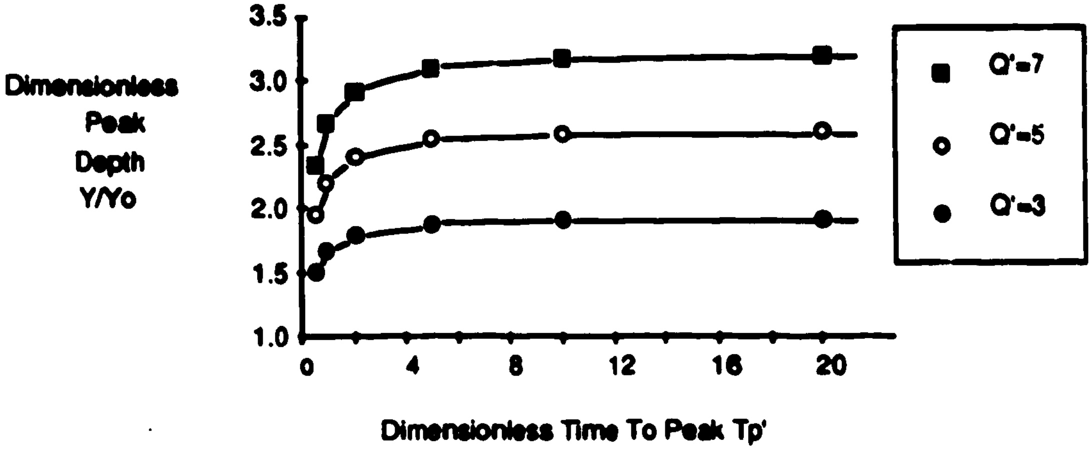

Fig. 3.3a Effect of Tp'
on Peak Depth at x'=1,Tb'=2, Fo=0.3

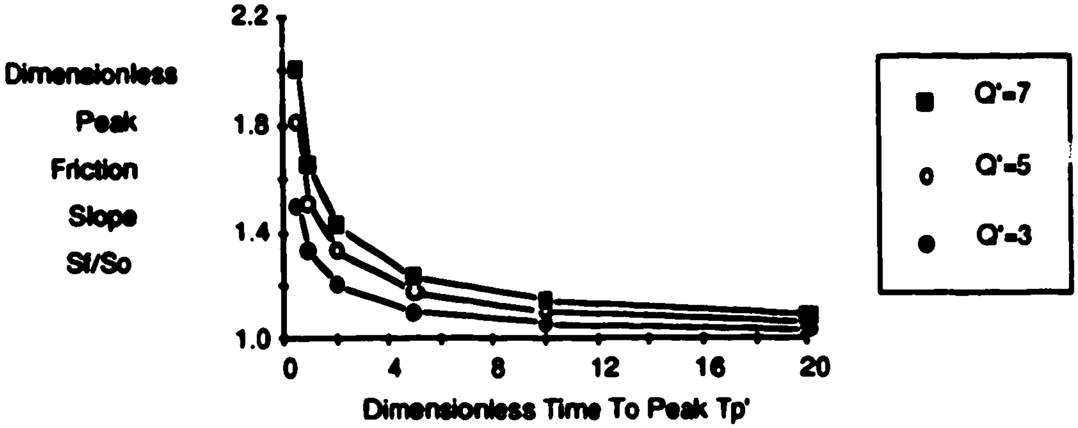

Fig. 3.3b Effect of Tp'
on Peak Friction Slope at x'=1, Tb'=2, Fo=0.3

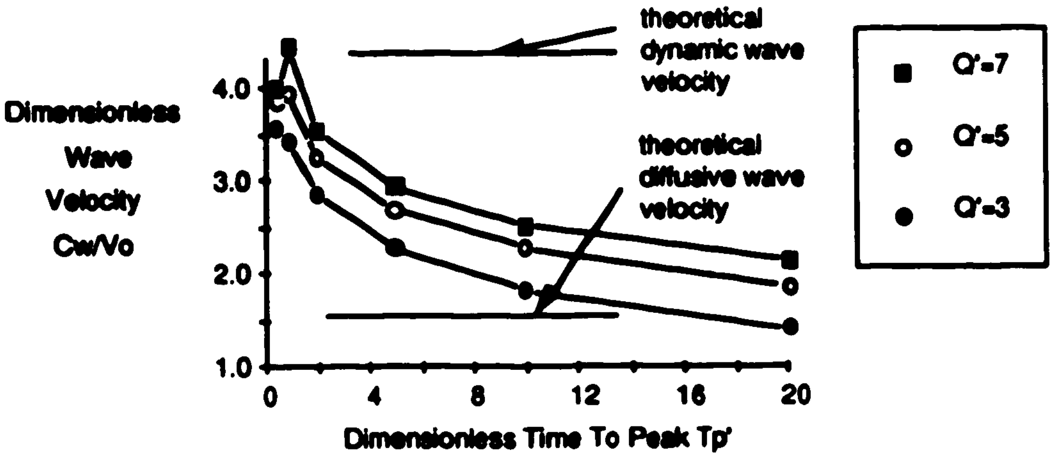

Fig. 3.3c Effect of Tp'
on Wave Velocity at x'=1, Tb'=2, Fo=0.3

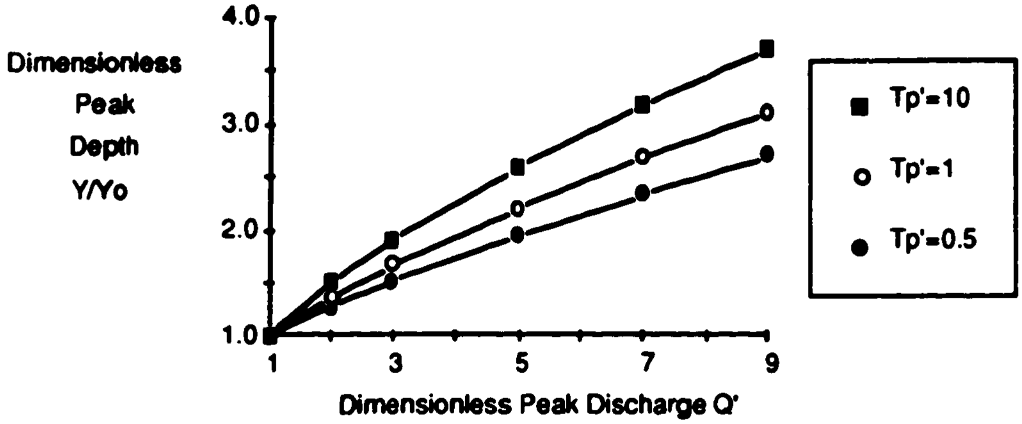

Fig. 3.4a Effect of Q'
on Peak Depth at x'=1,Tb'=2, Fo=0.3

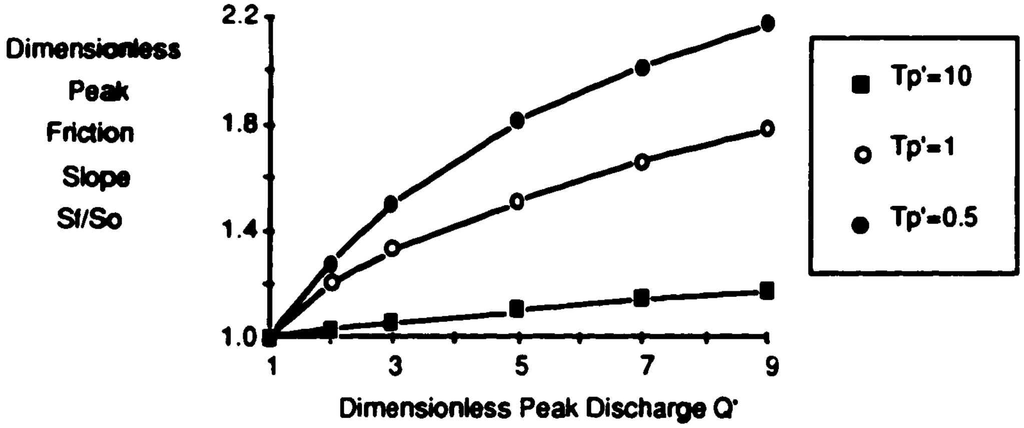

Fig. 3.4b Effect of Q'
on Peak Friction Slope at x'=1, Tb'=2, Fo=0.3

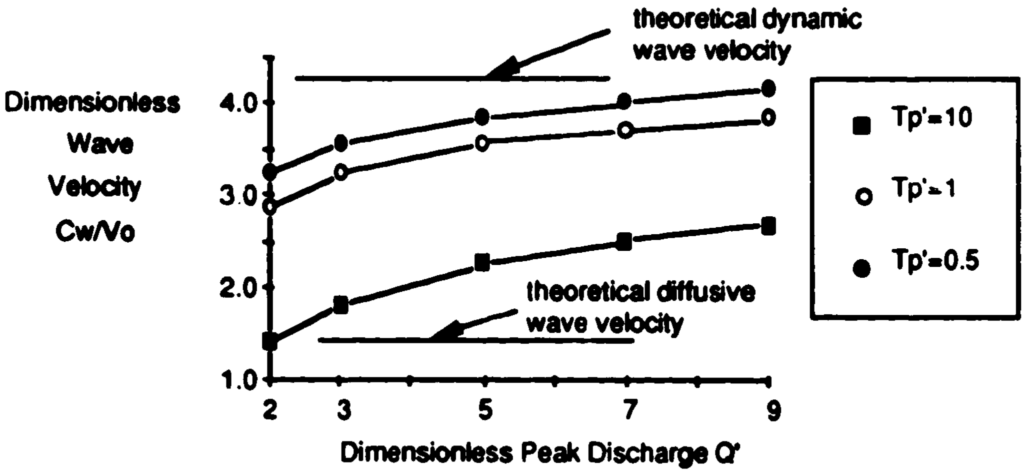

Fig. 3.4c Effect of Q'
on Wave Velocity at x'=1, Tb'=2, Fo=0.3

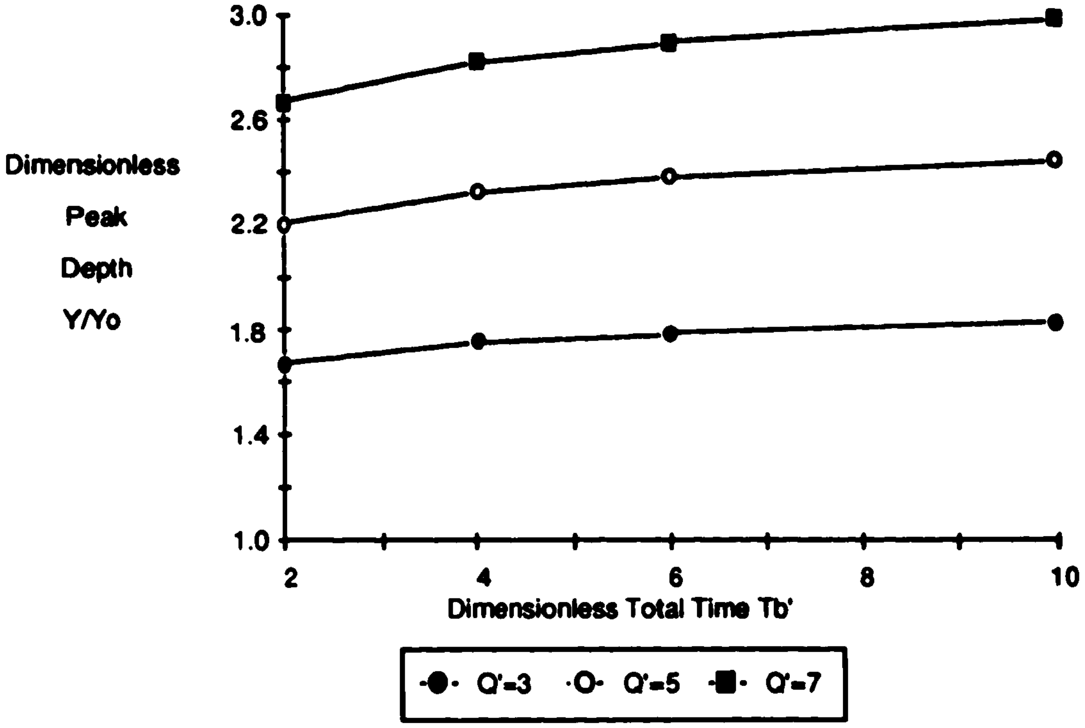

Fig. 3.5 Effect of Tb'
on Peak Depth at x'=1,Tp'=1, Fo=0.3

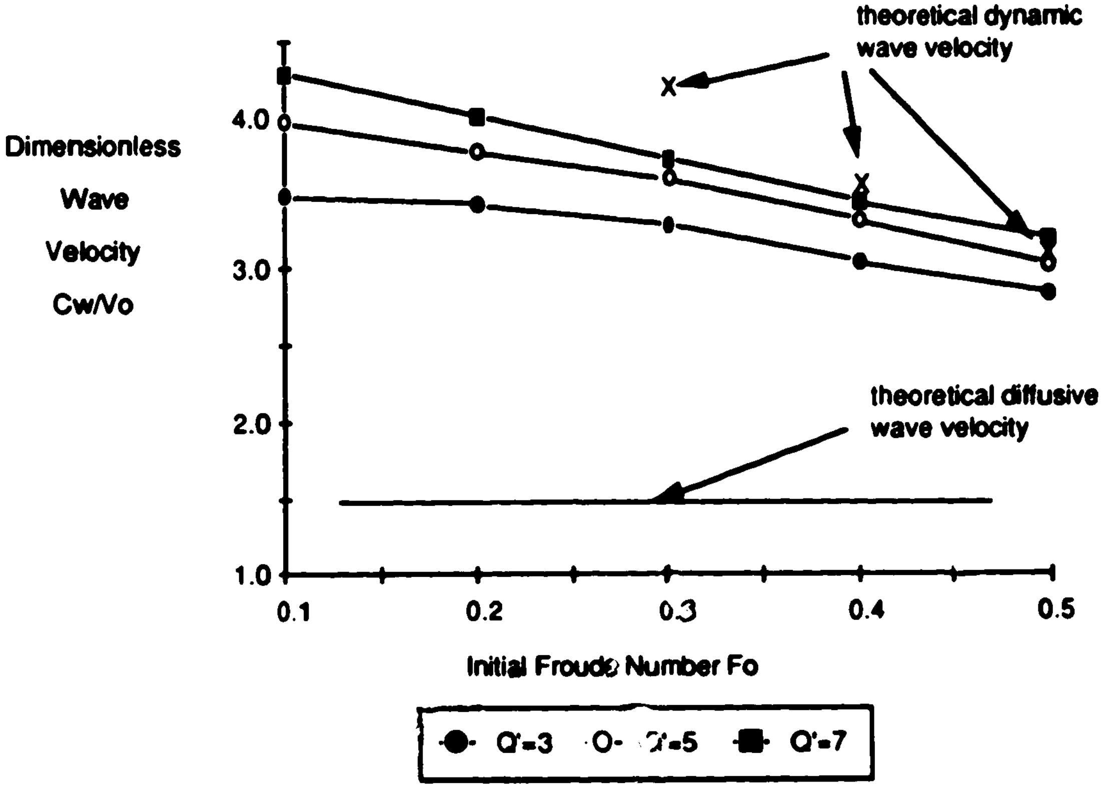

Fig. 3.6 Effect of Fo
on Wave Velocity at x'=1,Tp'=1, Tb'=2

velocity is observed as F_o increases. The effect of the Froude number decreases as distance increases. This shows that the dynamic terms of the governing equations are becoming less significant with distance. F_o also has a slight effect on the peak friction slope at short distances (≈1%), but very little effect is observed on the peak depth and discharge. The effect of the Froude number increases as T_p' becomes smaller.

Fig. 3.7 to Fig. 3.9 are the predictive plots. The data for these plots can be found in Appendix C. Plots of peak depth, peak discharge, peak energy gradient, and wave velocity against distance downstream are presented for a range of dimensionless parameters. It is evident that the parameters T_p' and Q' are important in predicting all four features. T_b' was found to be only significant in predicting peak depth and discharge, although its effect on the peak energy gradient and wave velocity becomes more apparent at long distances but not enough to be evident in the plots. The Froude number had only a small effect on the peak energy gradient and wave velocity, at short distances, but again not enough to have a major influence on the dimensionless plots, and had even less on the variation of Y and Q.

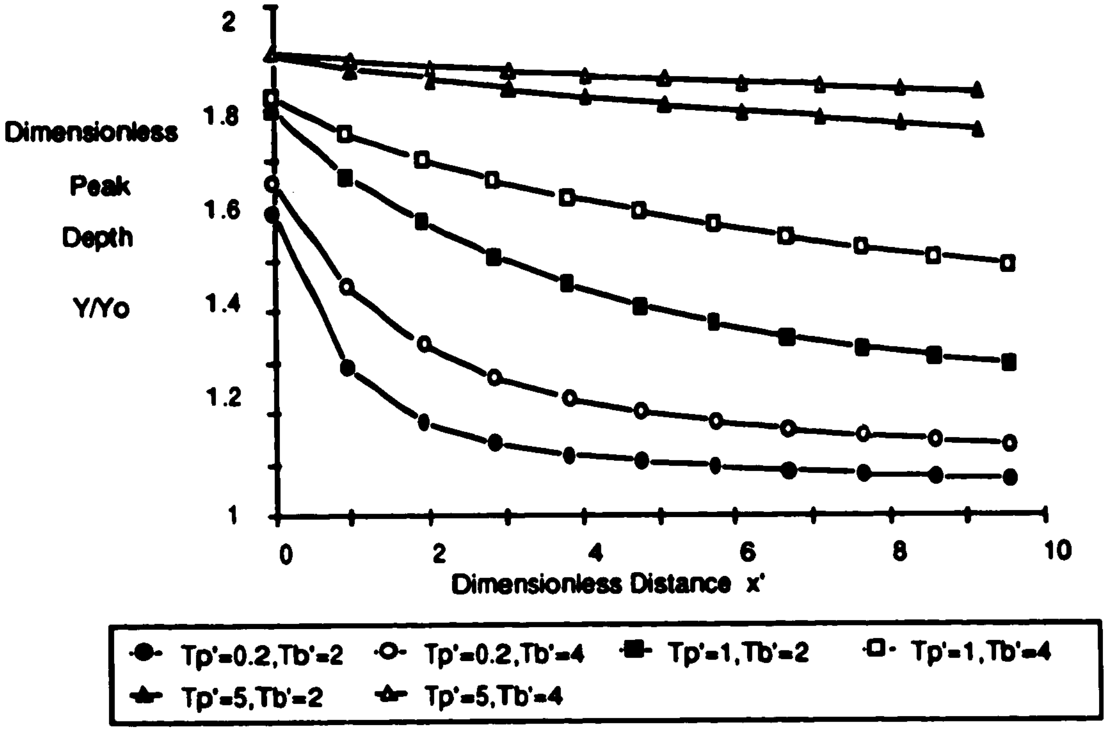

Fig. 3.7a Attenuation of Peak Depth for Q' = 3

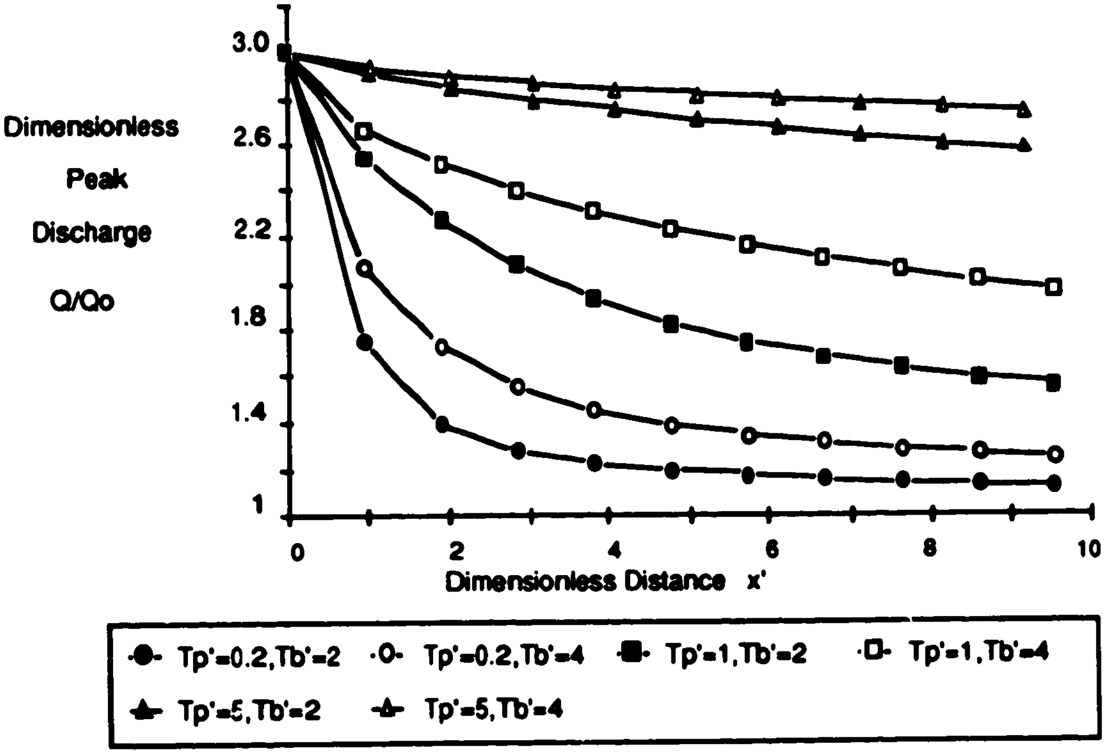

Fig. 3.7b Attenuation of Peak Discharge for Q' = 3

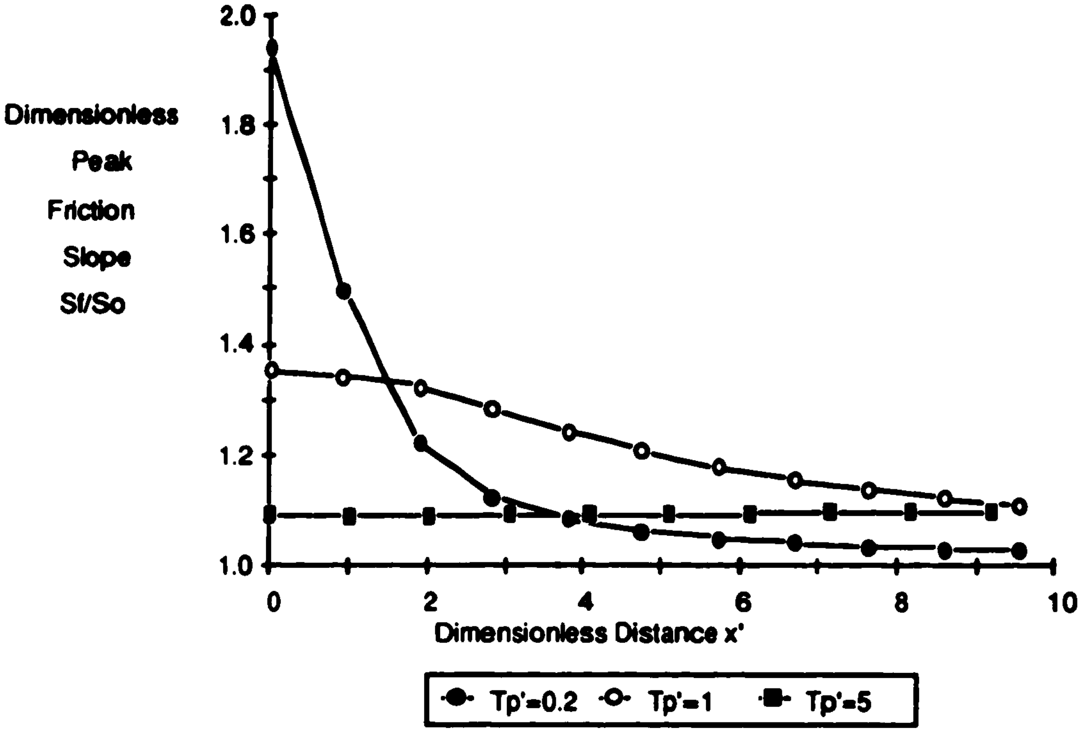

Fig. 3.7c Attenuation of Peak Friction Slope for Q' = 3

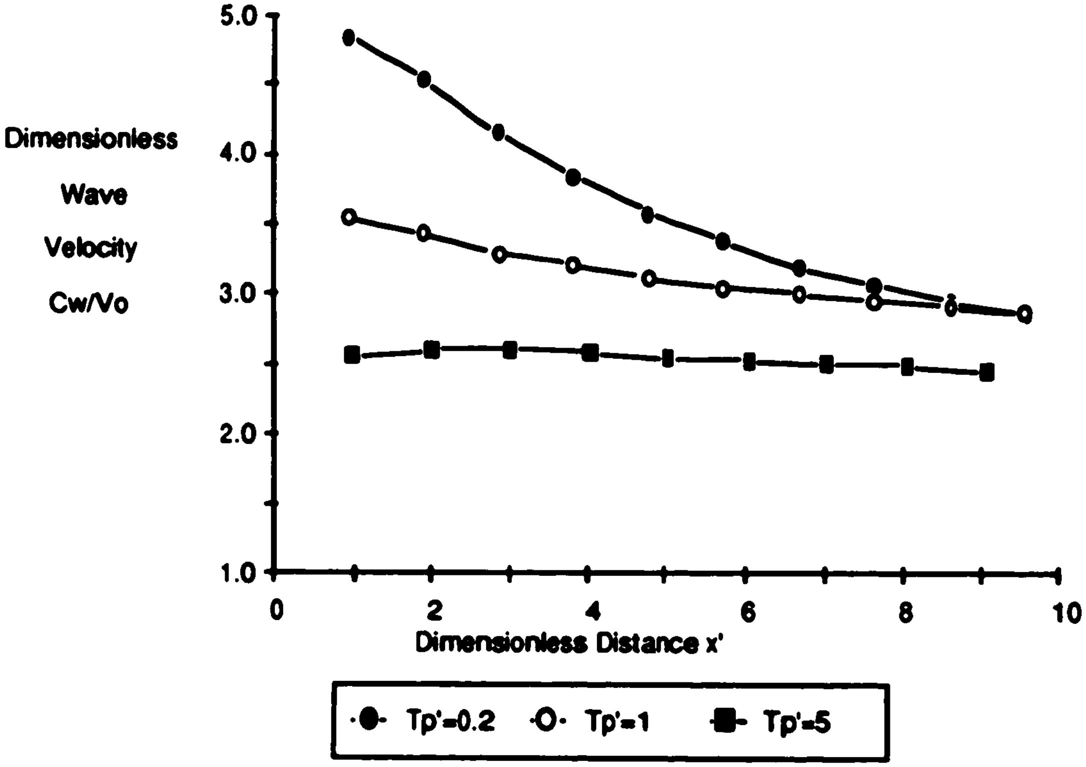

Fig. 3.7d Attenuation of Wave Velocity for Q' = 3

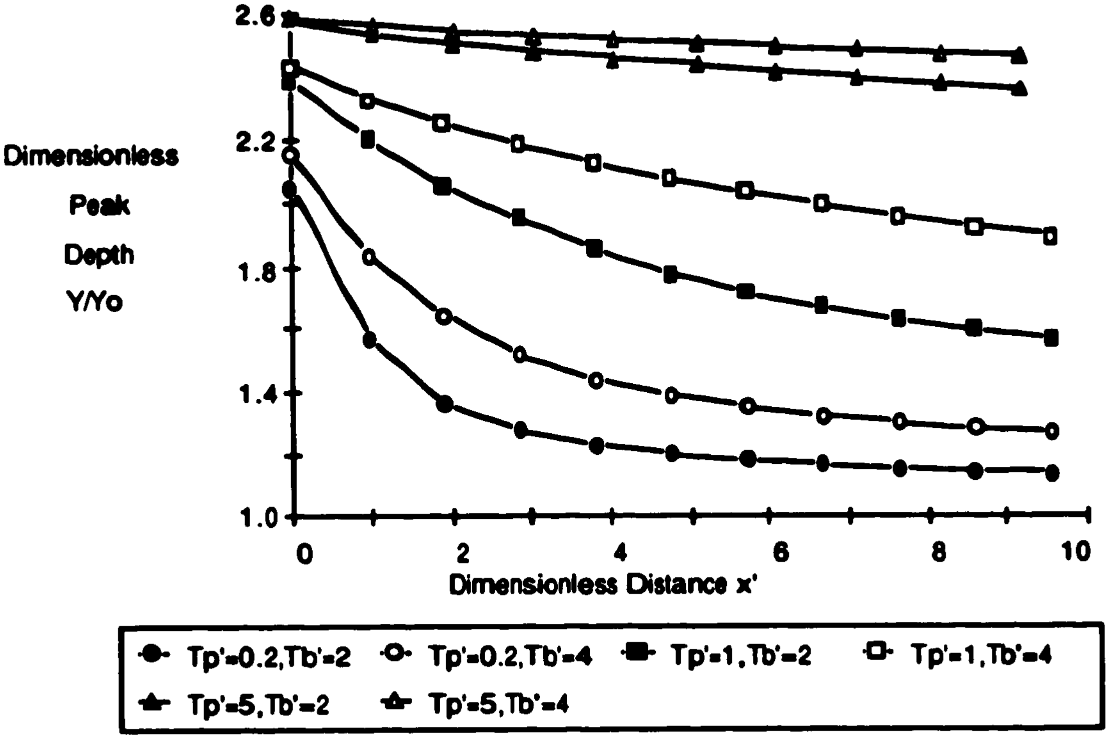

Fig. 3.8a Attenuation of Peak Depth for Q' = 5

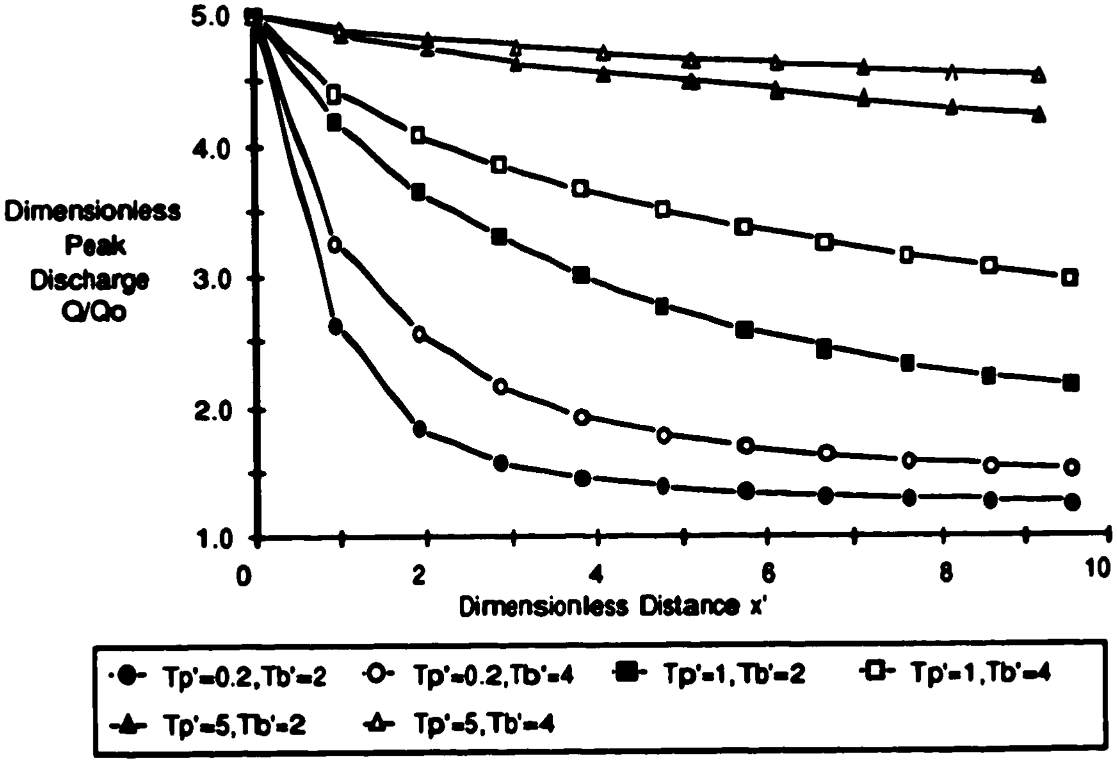

Fig. 3.8b Attenuation of Peak Discharge for Q' = 5

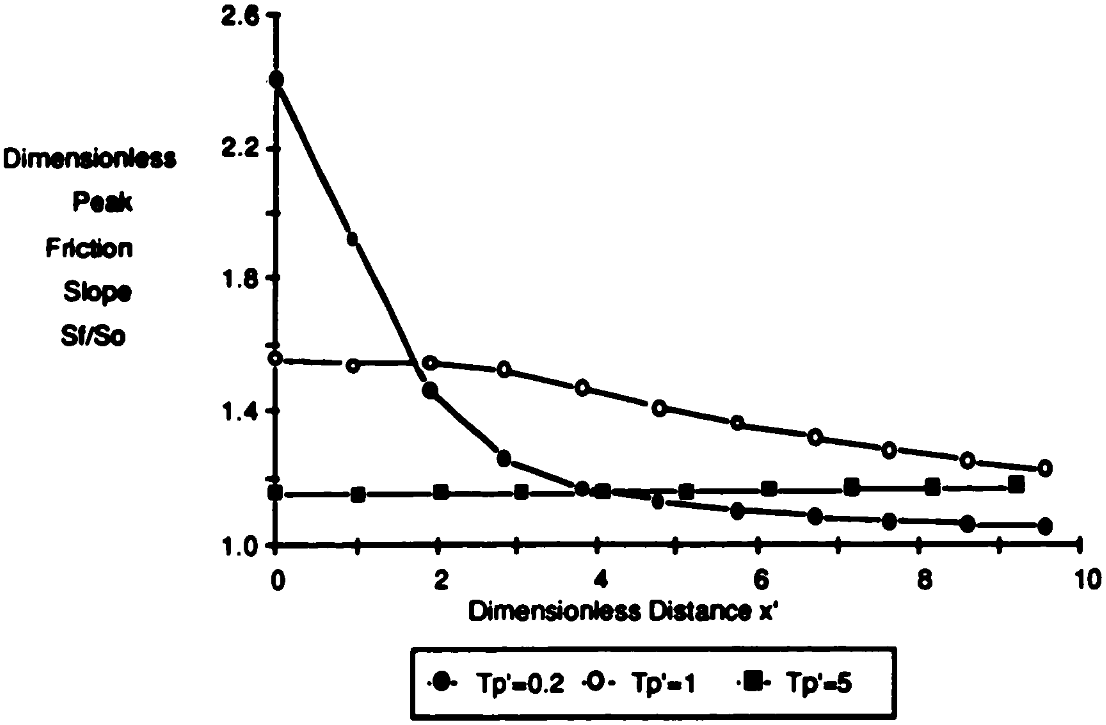

Fig. 3.8c Attenuation of Peak Friction Slope for Q' = 5

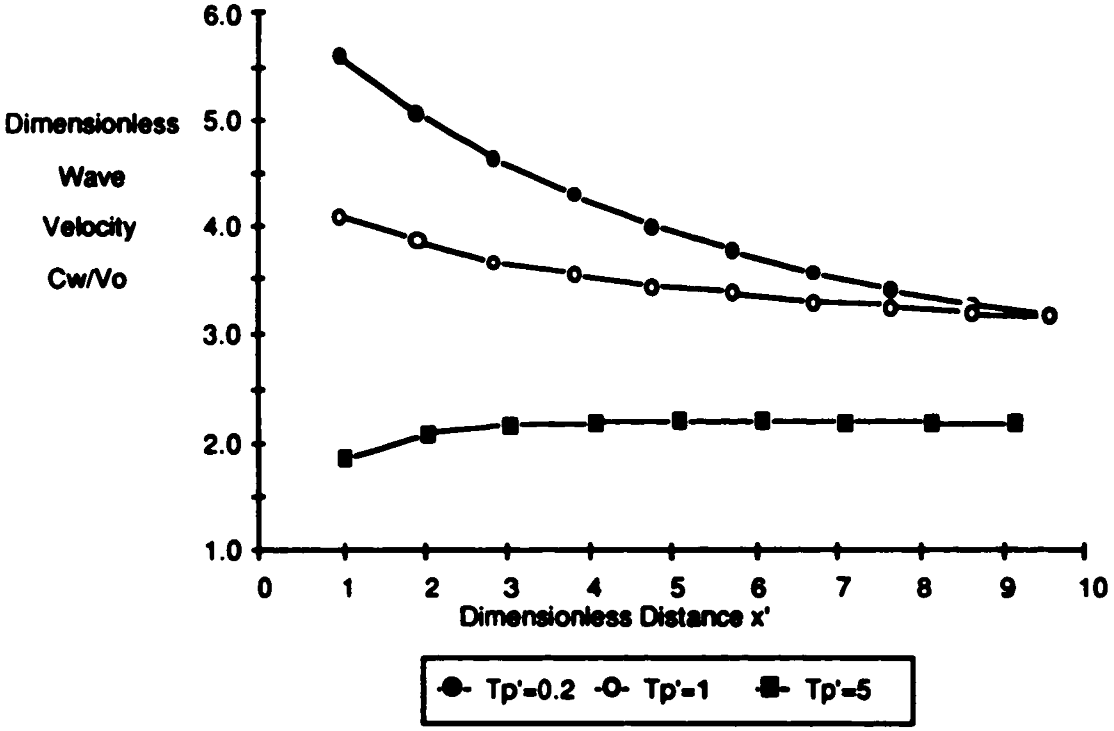

Fig. 3.8d Attenuation of Wave Velocity for Q' = 5

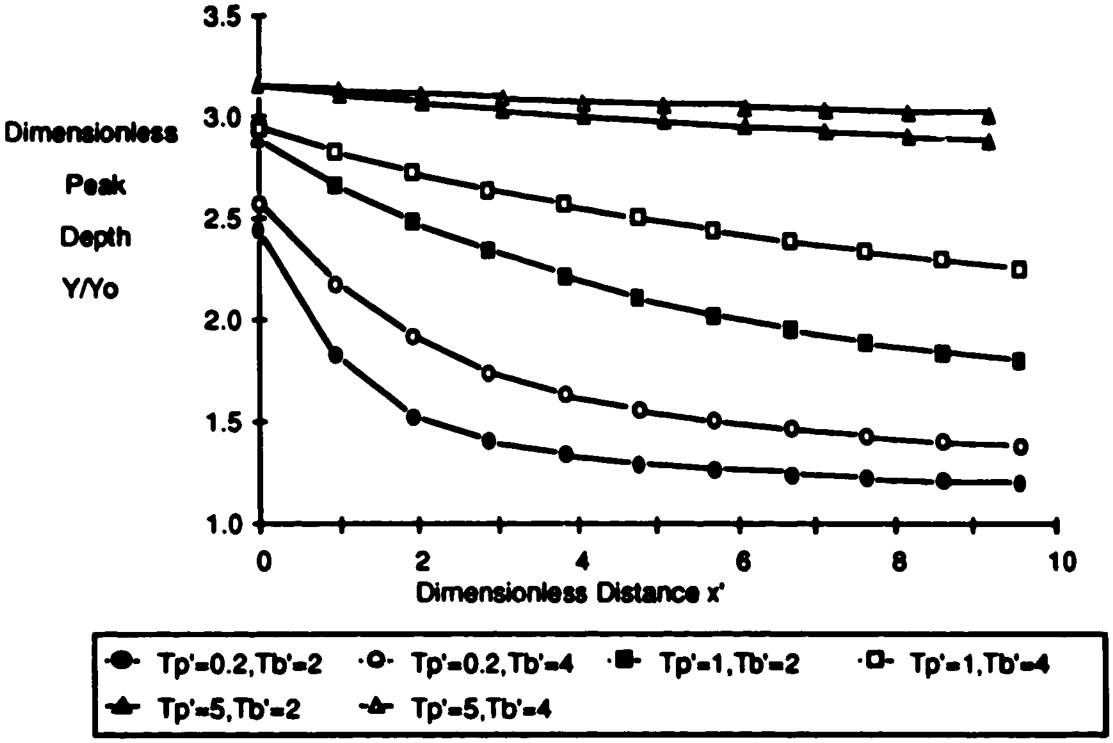

Fig. 3.9a Attenuation of Peak Depth for Q' = 7

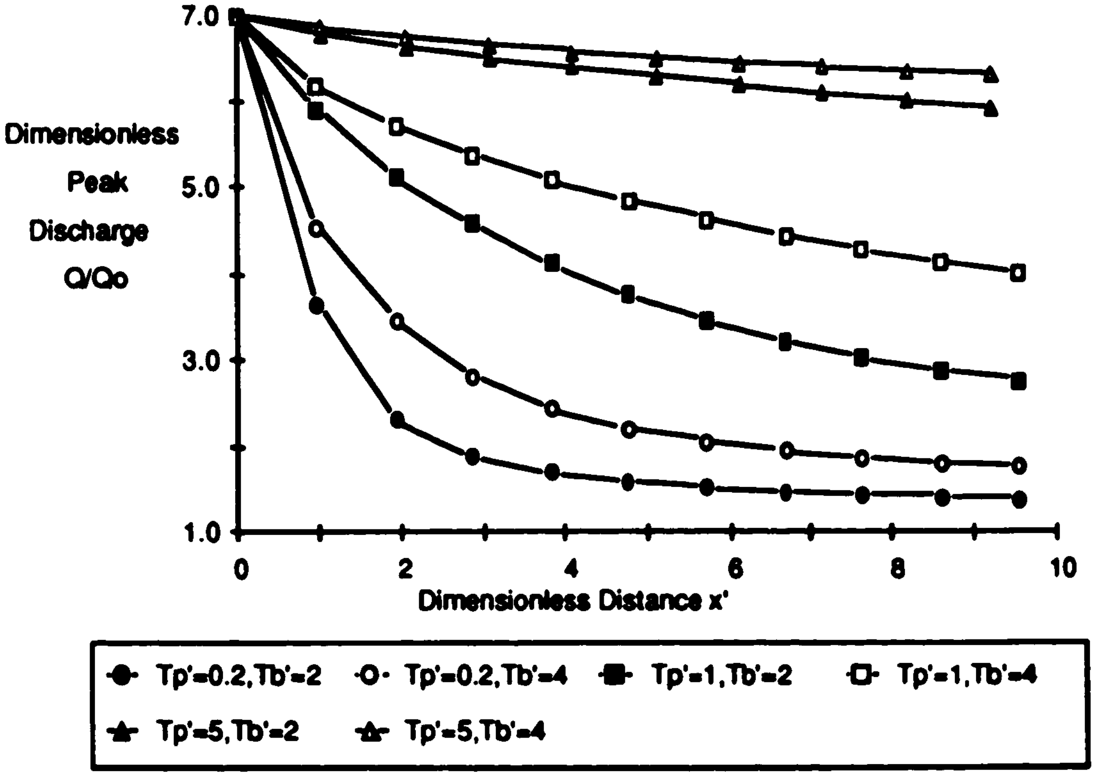

Fig. 3.9b Attenuation of Peak Discharge for Q' = 7

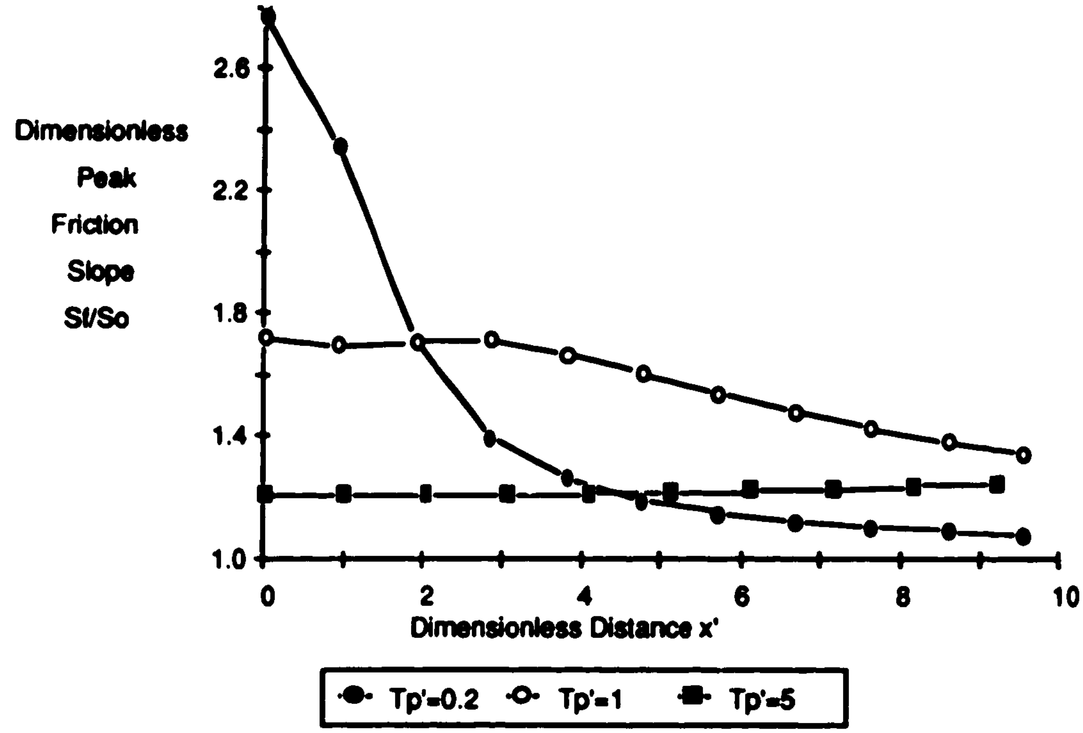

Fig. 3.9c Attenuation of Peak Friction Slope at Q' = 7

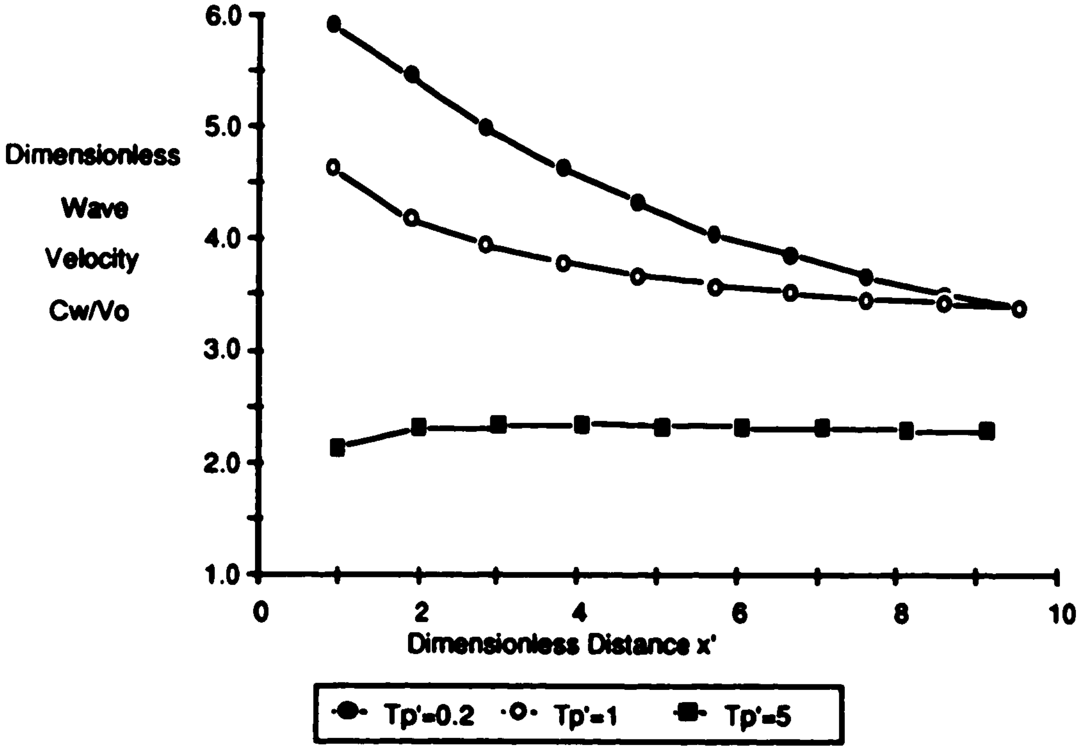

Fig. 3.9d Attenuation of Wave Velocity at Q' = 7

3.5 Application

In this section, the predictive plots are used to predict the amplitude and velocity of the river wave on the Connecticut River and the results are compared with the measured results of Ferrick et al.(1988) shown in Fig. 2.4a. The rectangular shaped hydrograph is approximated by using a large value for T_b. The initial conditions and the reach between the upstream end and station #1 are approximated as follows :

S_o = .00034
Y_o = 0.7 m
V_o = 0.7 m/s
Q_o = 65 m^3/s
x = 15 km
Q_p = 320 m^3/s
T_p = 1 hour
T_b = 6 hours

The resulting dimensionless parameters are :

$$Q' = \frac{Q_p}{Q_o} = \frac{320}{65} = 5$$

$$T_p' = \frac{V_o T_p S_o}{Y_o} = \frac{(0.7m/s * 1hr * 3600s/hr * .00034)}{0.7m} = 1.2$$

$$T_b' = \frac{T_b}{T_p} = \frac{6hr}{1hr} = 6$$

$$\frac{xS_o}{Y_o} = \frac{(15000m * .00034)}{0.7m} = 7.3$$

From Fig. 3.3a $\frac{Y}{Y_o} = 2.3$ and from Fig. 3.3d $\frac{C_w}{V_o} = 3.5$ for these values of the dimensionless parameters. Therefore :

$$Y = 2.3 * 0.7m = 1.6m$$

and the amplitude of the river wave is :

$$Y-Y_o = 1.6m - 0.7m = 0.9m.$$

This compares well with the observed result of 0.95m. Also :

$$C_w = 3.5 * 0.7 \text{ m/s} = 2.45 \text{ m/s}$$

so the time for the leading edge of the wave to reach station #1 is :

$$x = \frac{15000m}{2.45m/s} = 1.7 \text{ hr.}$$

This compares well with the time of arrival shown on Fig. 2.4a which lies between 1.5 and 2 hours.

This chapter has examined one type of unsteady flow that may trigger a dynamic breakup. Based on the simplified hydrograph of Fig. 3.1, a set of dimensionless parameters that describe the unsteady flow have been developed and used to generate a set of practical plots. These plots can be used to predict the nature of the resulting river wave at downstream locations. These plots have been applied to a case of unsteady flow on the Connecticut River with good results.

4 ICE JAM FAILURE

4.1 Introduction

Another cause of unsteady flow at breakup is the failure of an ice jam. Ice jams form when an ice run stalls. They are characterized by a large pack thickness and roughness. As a result, they can cause a large increase in water level and thereby store a lot of water in channel storage. If a jam fails suddenly, a large river wave will form which can cause high water levels downstream and may trigger further ice cover breakup downstream.

The characteristics of the wave formed by a sudden and complete release of an ice jam has been studied in several ways. Henderson and Gerard (1981) performed a preliminary theoretical study on both ice jam release and formation using the classical dam break solution. The effects of channel slope and friction were not considered. Beltaos and Krishnappan (1982) performed a numerical model study on ice jam release on the Athabasca River near Fort McMurray. Joliffe and Gerard (1982) also used a numerical model to analyse the release of a hypothetical ice jam at this location as well as performing some laboratory tests that indicated the ice in the jam has little effect on the hydraulics during a release. Wong et al. (1985) also performed some laboratory tests on ice jam releases and confirmed that the ice in the jam has little effect on the hydraulics. Parkinson and Holder (1988) used a computer model to study the wave released from an ice jam on the Mackenzie River N.W.T. and compared the results to some field observations.

Each of the above analyses has been for a specific case. In the present study, a wide range of characteristics and idealized ice jam profiles are considered with the aim of developing generalized plots that allow an assessment of the behaviour of a surge generated by ice jam failure.

Several approximations have been made in this analysis. As with the previous numerical studies on ice jam releases, the presence of the broken ice is assumed to have no effect on the hydraulics. Two possible reasons for the validity of this assumption are that the ice accelerates quickly to the flow velocity, thereby providing no resistance to flow, and that the wave moves ahead of the ice since wave celerity is greater than the flow velocity. Another approximation used in this analysis is the idealised profile used to model the water level profile through the ice jam prior to release. This profile is shown in Fig. 4.1. It consists of a sharp linear increase in depth, to represent that across the toe of a jam, followed by a length of constant depth to model the remainder of the jam. This simplified profile minimizes the number of variables required to define the jam profile

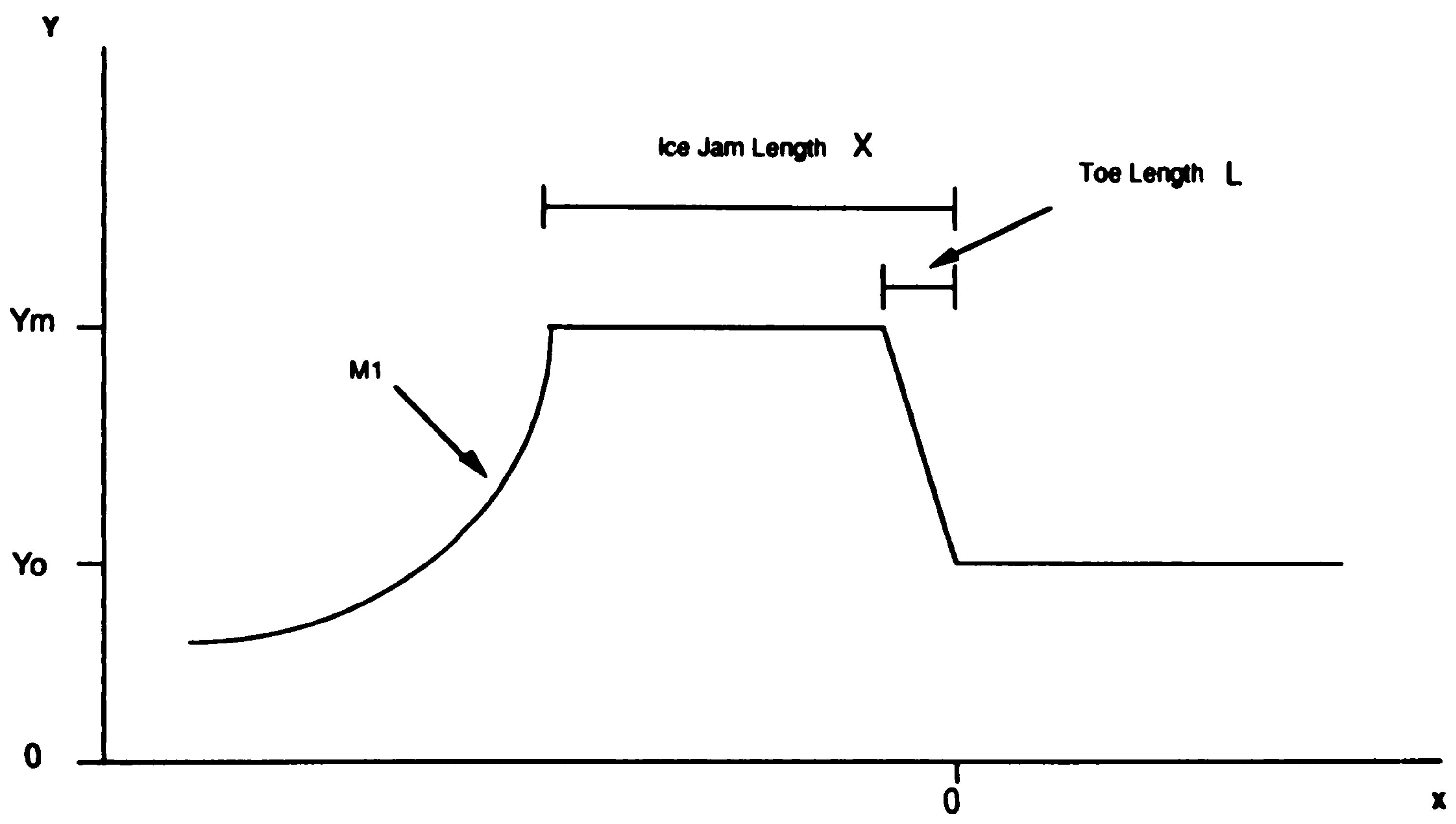
Y
Ym
Yo
0
Ice Jam Length X
Toe Length L
M1
0
x

Fig. 4.1 Schematic Describing Jam Profile at Failure

without being impractical. The depth rises sharply from the normal depth (Y_o) to the peak depth (Y_p) in a distance L. This represents the toe of the jam. The profile remains at depth Y_p for a total length of X. This is followed by an 'M1' type backwater curve as the depth decreases back to Y_o. Ice jam profiles presented by Gerard and Stanley (1988), Malcovish et al. (1988), and Beltaos (1988) show that this simplified profile is a good approximation of reality. The final major approximation is that all of the jam is released instantaneously. Although this is not always the case, it does represent an upper bound.

Because a wide range of ice jam profiles and channel geometries are used in this analysis, it is again necessary to use dimensionless parameters to present the results. These parameters are derived in a similar manner to those in the previous section. The results of interest in this case are the peak waterway depth (Y), the peak discharge (Q), the maximum energy gradient (S_f), and the wave velocity (C_w) as the wave moves downstream.

4.2 Parameter Definition

The waves resulting from the release of these jams are routed through a wide range of rectangular channels with uniform slopes. As with the hydrograph section, the channel geometry can be defined by the bed slope (S_o), the channel width (B), and the channel roughness (k). The use of the normal flow conditions (Y_o and V_o) as the initial flow conditions includes the effect of the channel width and roughness in the analysis.

4.3 Dimensional Analysis

As before, the only dimensionless parameter that results from the governing differential equations is the initial Froude number $F_o = \frac{V_o}{\sqrt{gY_o}}$. The remainder of the dimensionless parameters are provided by non-dimensionalizing the boundary conditions. The variables controlling the boundary conditions in this analysis are the toe length L, total jam length X, and depth of water through the jam Y_p.

Dividing the toe length L by the longitudinal distance scale yields :

$$\frac{L}{\frac{Y_o}{S_o}} = \frac{LS_o}{Y_o} = L'$$

Similarly, the total length of jam X can be non-dimensionalized by :

$$\frac{X}{\frac{Y_o}{S_o}} = \frac{XS_o}{Y_o} = X'$$

and the depth of water through the jam Y_p divided by the depth scale yields :

$$\frac{Y_p}{Y_o} = Y'$$

Therefore, any feature of the solution, say χ, will depend on :

$$\chi = f(F_o , L' , Y' , X' , x' , t')$$

4.4 Results

Fig. 4.2 shows the form of a wave generated by a complete ice jam release for a given set of conditions and the change in this wave as it moves downstream. As in the hydrograph routing case, the wave becomes broader and less peaked, but more dramatically. The following plots show the effect of certain parameters on the attenuation that results and quantify the changes in the river wave.

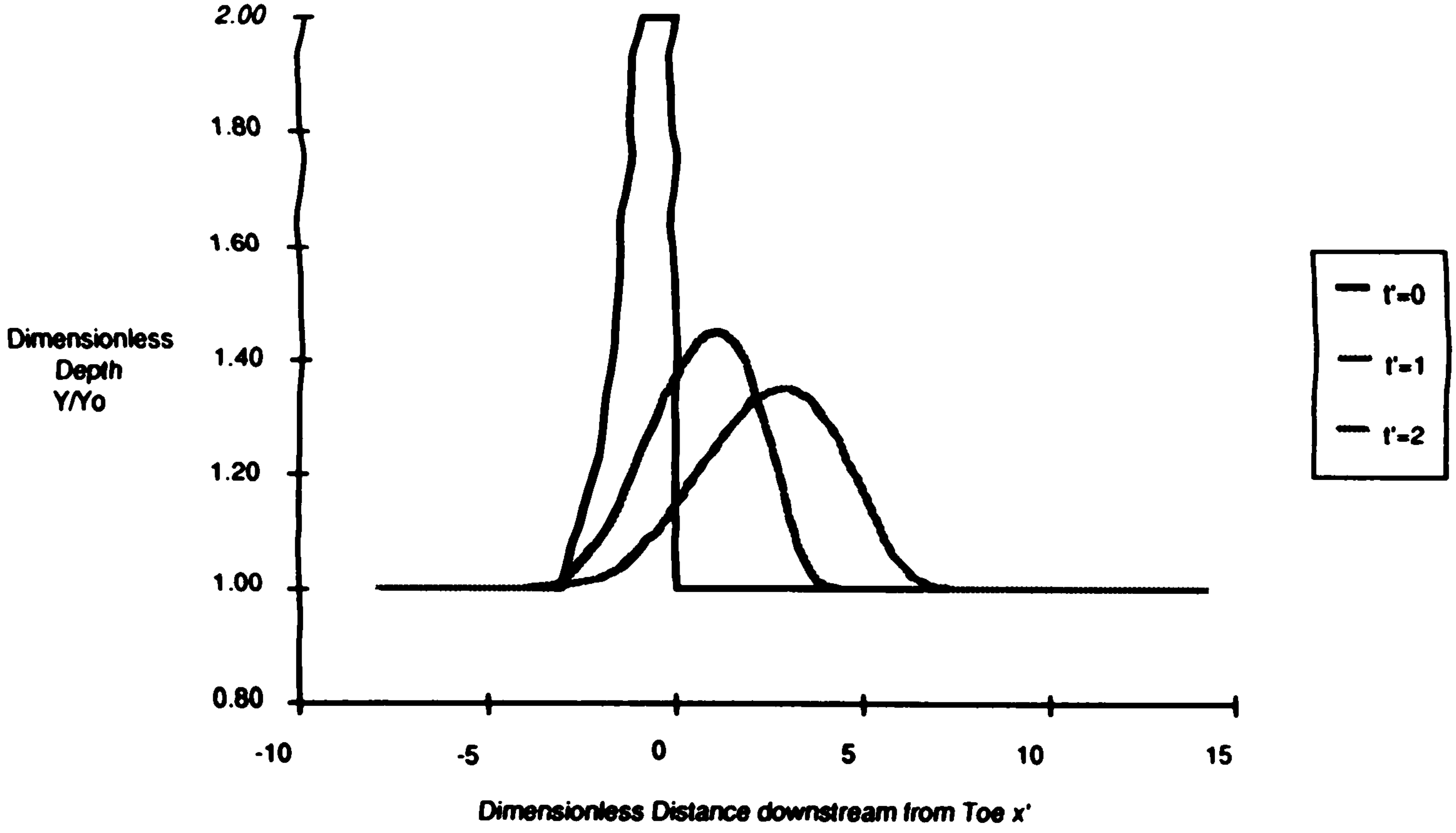

Fig. 4.2 Ice Jam Release - Fo=0.3, X'=1, Y'=2, L'=0.1

As before, the results of this chapter are presented in two parts: a set of 'diagnostic' plots and a set of 'predictive' plots. As with the hydrograph section, the plots are applicable to both open water and ice covered reaches.

Fig. 4.3 to Fig. 4.6 are the diagnostic plots. Selected data from these plots can be found in Table B.2. The effect of the X' parameter is investigated in Fig. 4.3. When X' is large, the peak depth approaches the steady state values but as X' decreases, significant attenuation is observed. X' also affects peak friction slope and wave velocity at large distances as the attenuation of the wave starts to affect these results. In the range of values shown in the predictive plots, the effect of X' is negligible on peak friction slope and its effect on wave celerity is less than 5% so the variation of these parameters with X' was not included.

The three plots of Fig. 4.4 isolate the effect of Y' on peak depth, peak friction slope, and wave velocity. All results show an almost linear increase as Y' increases, which justifies linear interpolation for this parameter when using the predictive plots. The effect of Y' is more noticeable on depth and friction slope than on wave velocity.

Fig. 4.5 together with the predictive plots show that, in contrast to the hydrograph case, the Froude number has a large effect on peak friction slope and wave velocity at short distances. At larger distances, the effect becomes

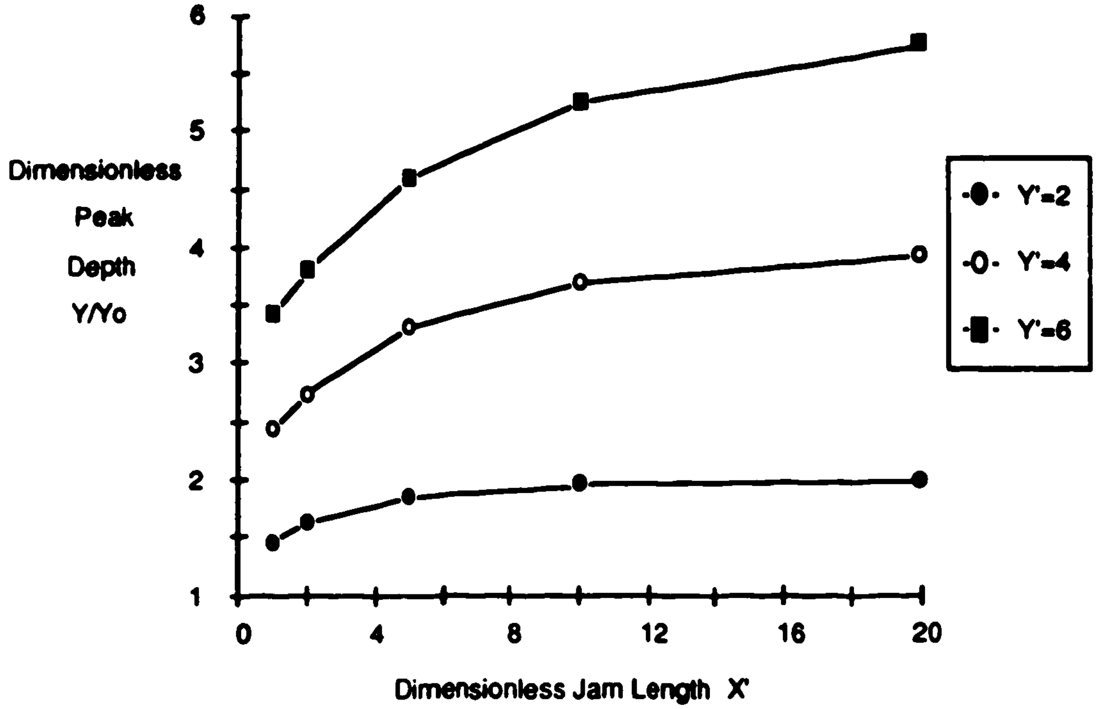

Fig. 4.3 Effect of X'
on Peak Depth at x'=1, Fo=0.3, L'=0.2

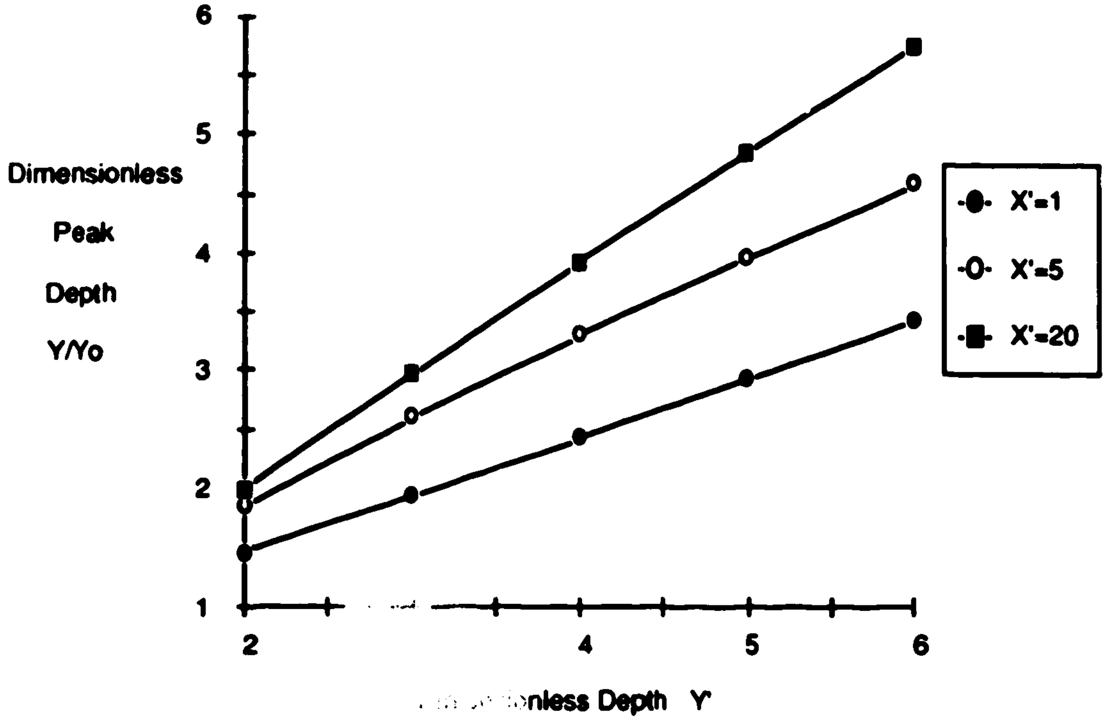

Fig. 4.4a Effect of Y'
on Peak Depth at x'=1, Fo=0.3, L'=0.2

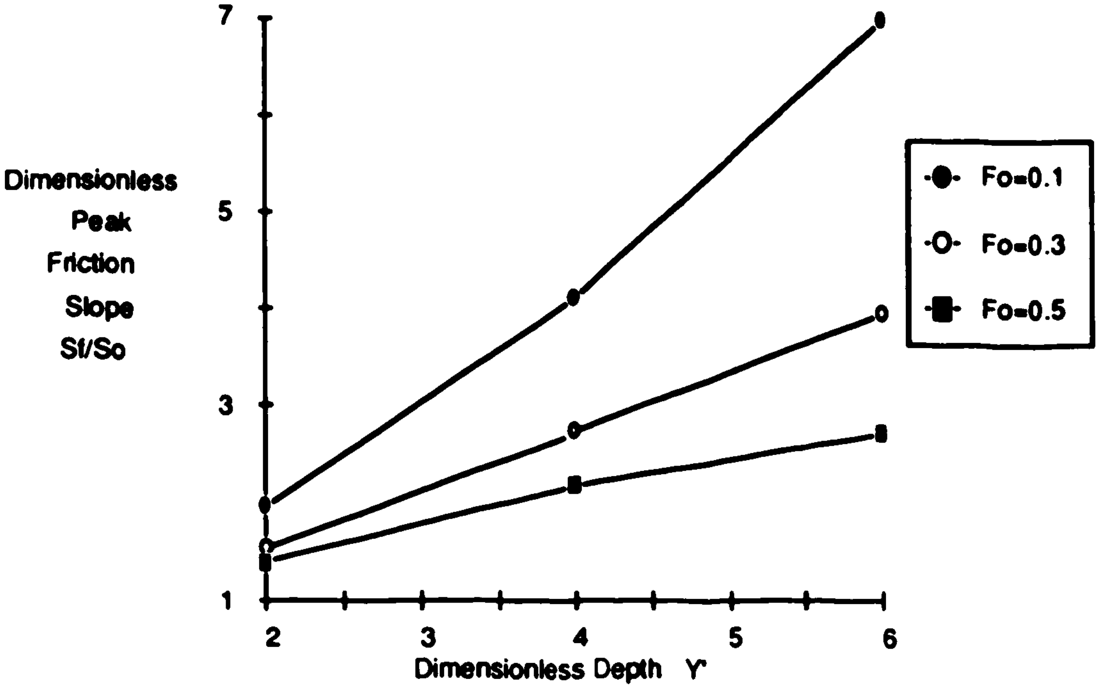

Fiq. 4.4b Effect of Y'
on Peak Friction Slope at x'=1, X'=5, L'=0.2

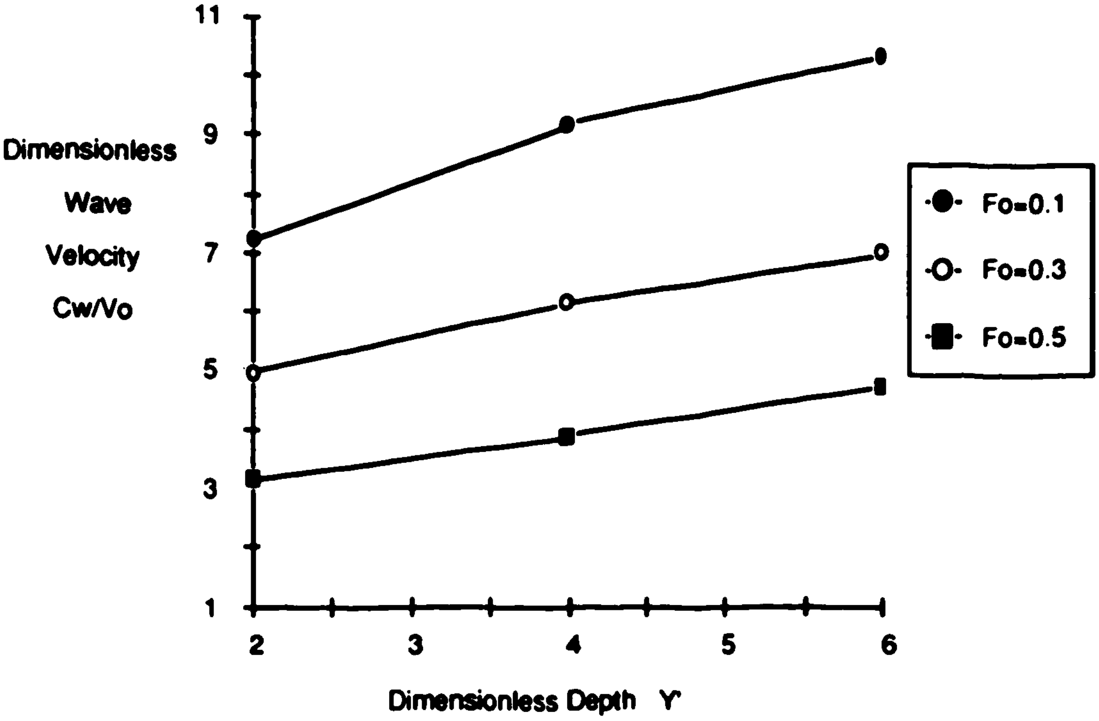

Fig. 4.4c Effect of Y'
on Wave Velocity at x'=1, X'=5, L'=0.2

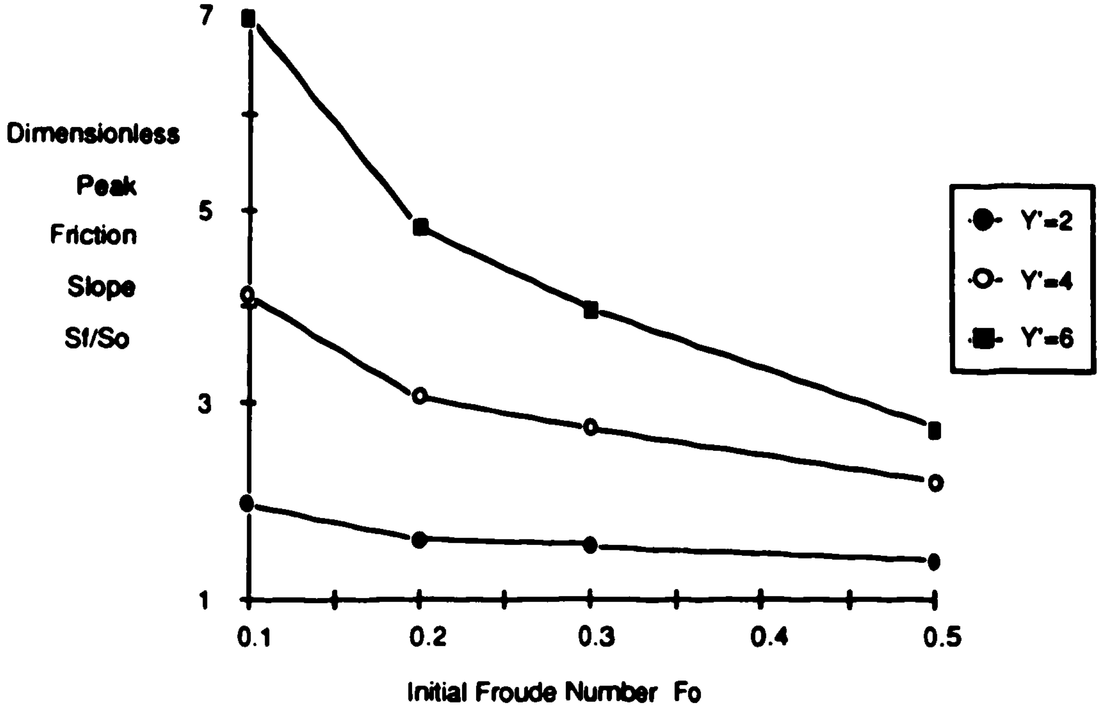

Fig. 4.5a Effect of Fo
on Peak Friction Slope at x'=1, X'=5, L'=0.2

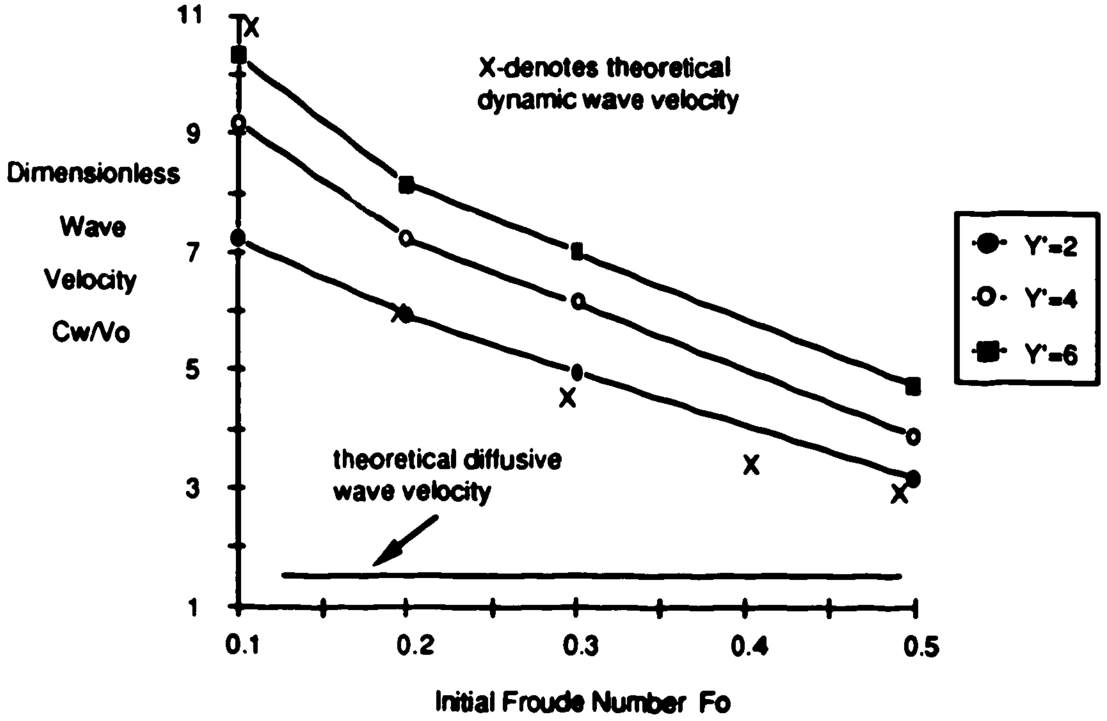

Fig. 4.5b Effect of Fo
on Wave Velocity at x'=1, X'=5, L'=0.2

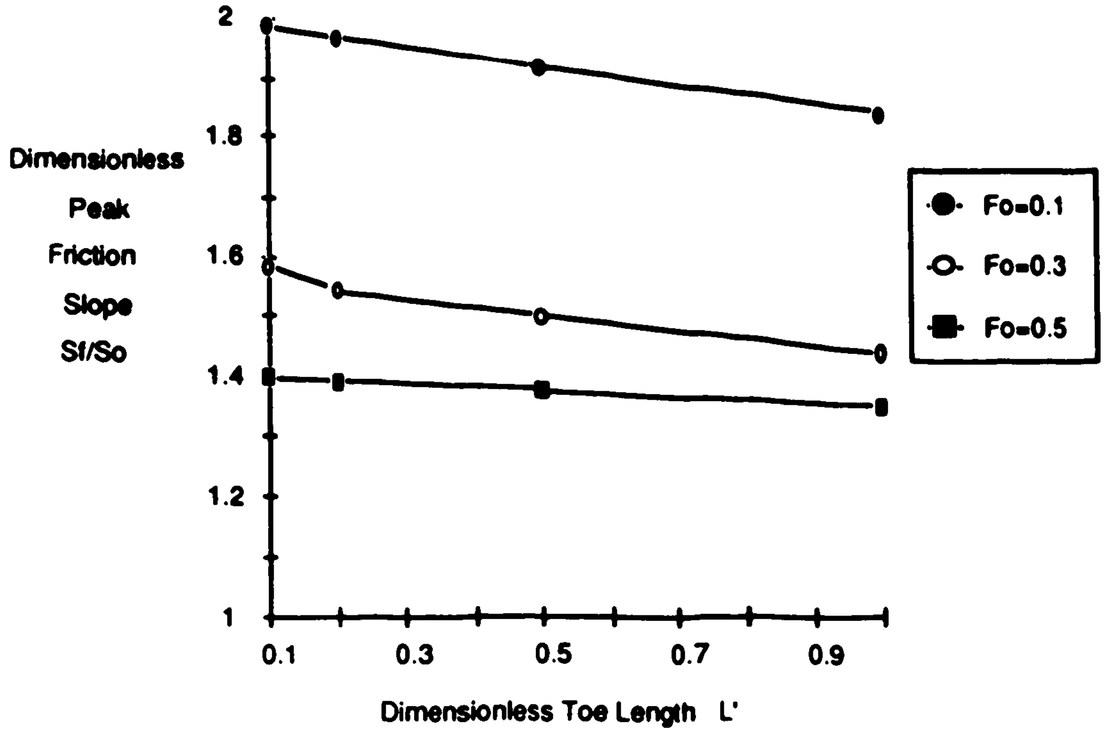

Fig. 4.6a Effect of L'
on Peak Friction Slope at x'=1, X'=5, Y'=2

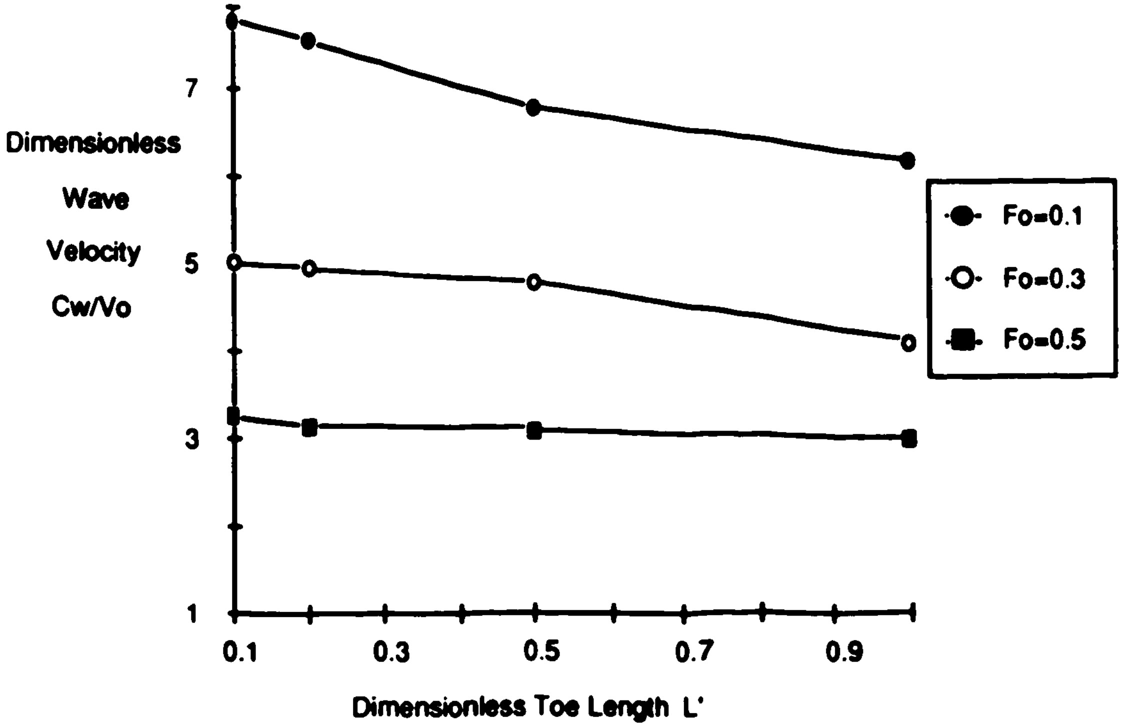

Fig. 4.6b Effect of L'
on Wave Velocity at x'=1, X'=5, Y'=2

negligible. The reason for the importance of the Froude number in the ice jam failure case is due to the more abrupt nature of the imposed change in flow compared to the change imposed by the inflow hydrograph of chapter 3. F_0 also affects the peak depth and discharge at short distances. Differences as high as 15-20% are caused by a change in Froude number at very short distances but the effect becomes negligible when x' increases beyond 1. Therefore, the F_0 was not included in the practical plots for depth and discharge.

Fig. 4.6a and b show the effect of L' on peak friction slope and wave velocity at a certain distance. These plots show an increase in peak friction slope and wave velocity as the toe profile steepens. The effect becomes more noticeable as F_0 becomes smaller. The effect of L' on peak friction slope is significant for values of x' less than 0.3, but negligible beyond this value. Differences in wave velocity on the order of 10% can also be attributed to L' at short distances but again the effect becomes negligible as x' increases. Large L' values will have a slight decreasing effect on the peak depth and discharge as the total volume of the jam is less. However, smaller L' values which more closely resemble the profile of real ice jams have no significant effect on peak depth and discharge.

Fig. 4.7 to Fig. 4.9 are the predictive plots. Data for these plots can be found in Table C.2. Plots of peak depth, peak discharge, peak energy gradient, and wave velocity against distance downstream are presented for a range of

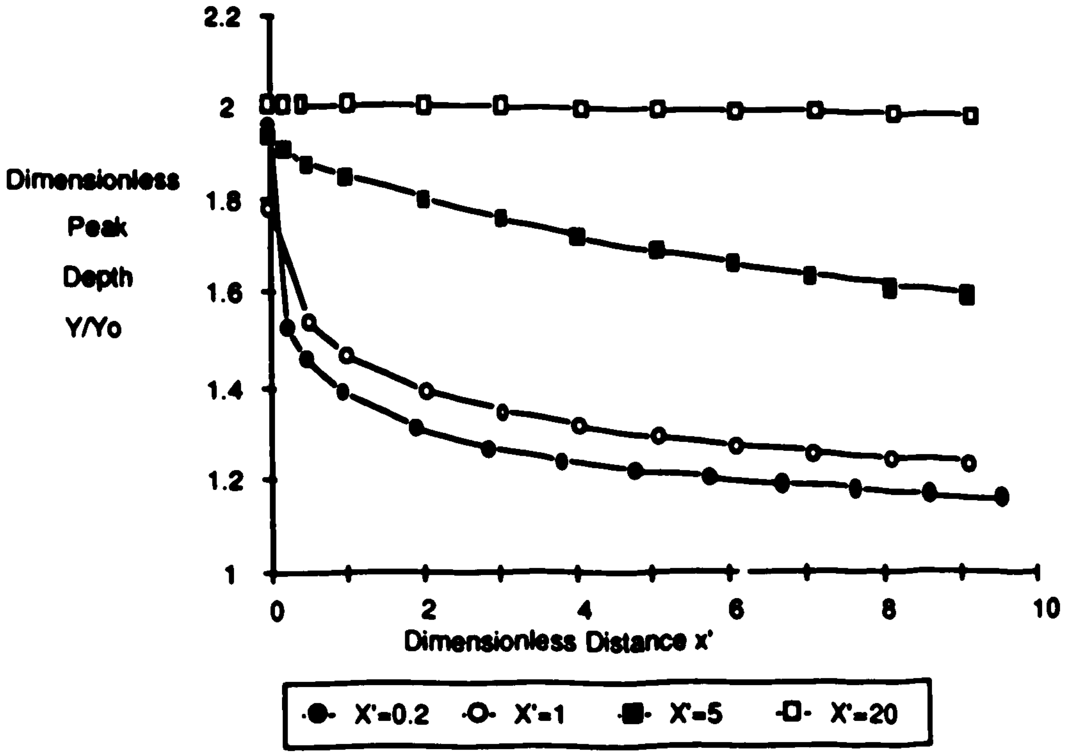

Fig. 4.7a Attenuation of Peak Depth for Y' = 2

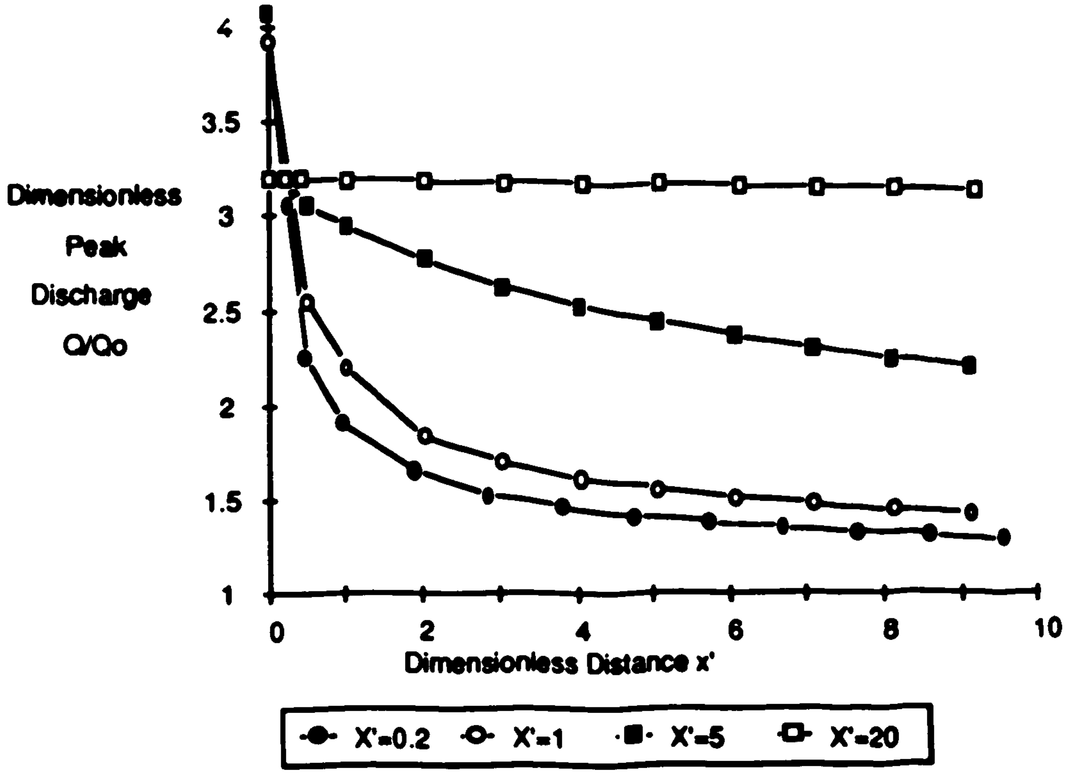

Fig. 4.7b Attenuation of Peak Discharge for Y' = 2

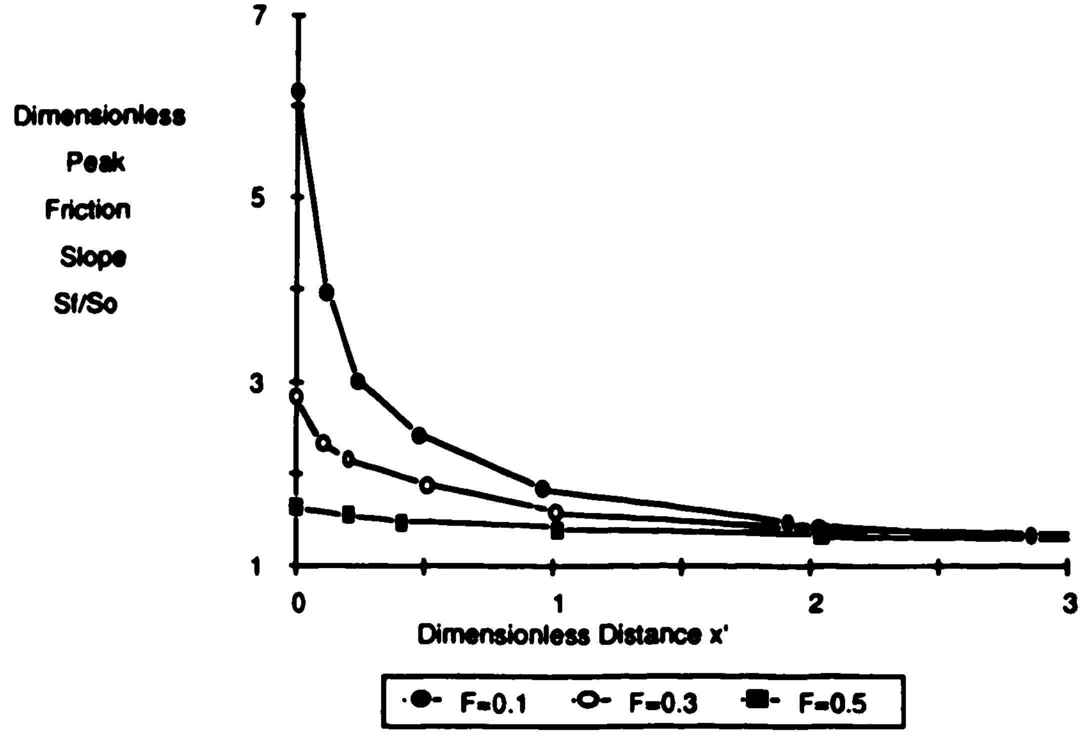

Fig. 4.7c Attenuation of Peak Friction Slope for Y' = 2

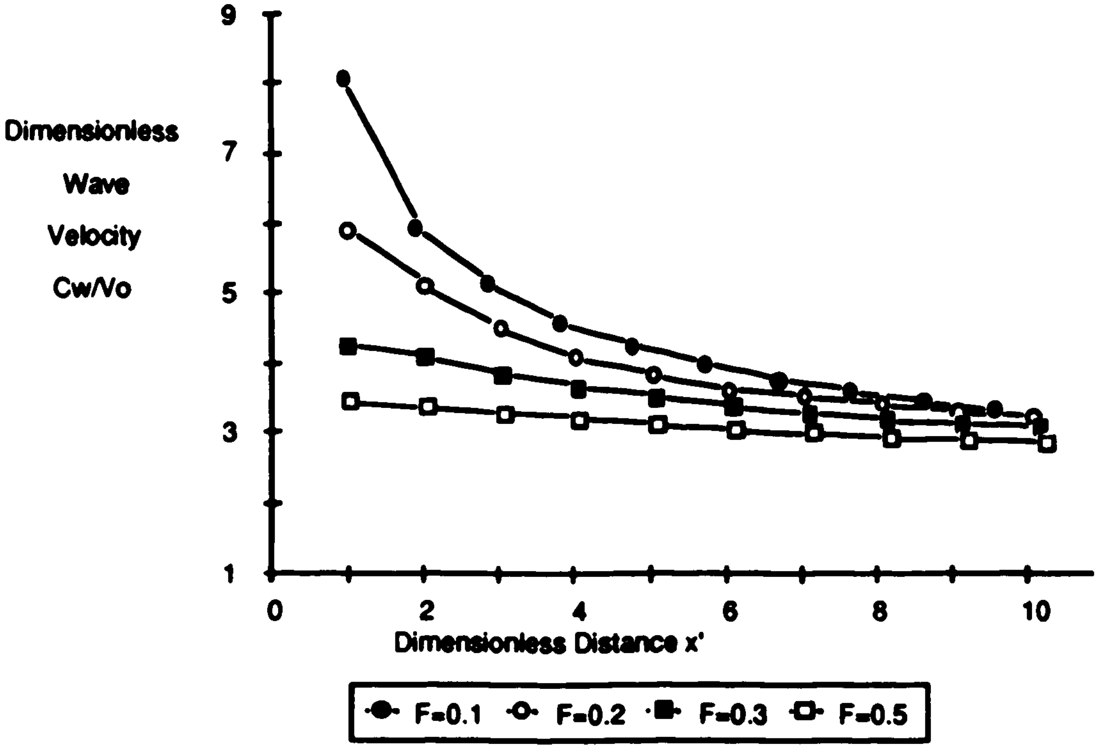

Fig. 4.7d Attenuation of Wave Velocity for Y' = 2

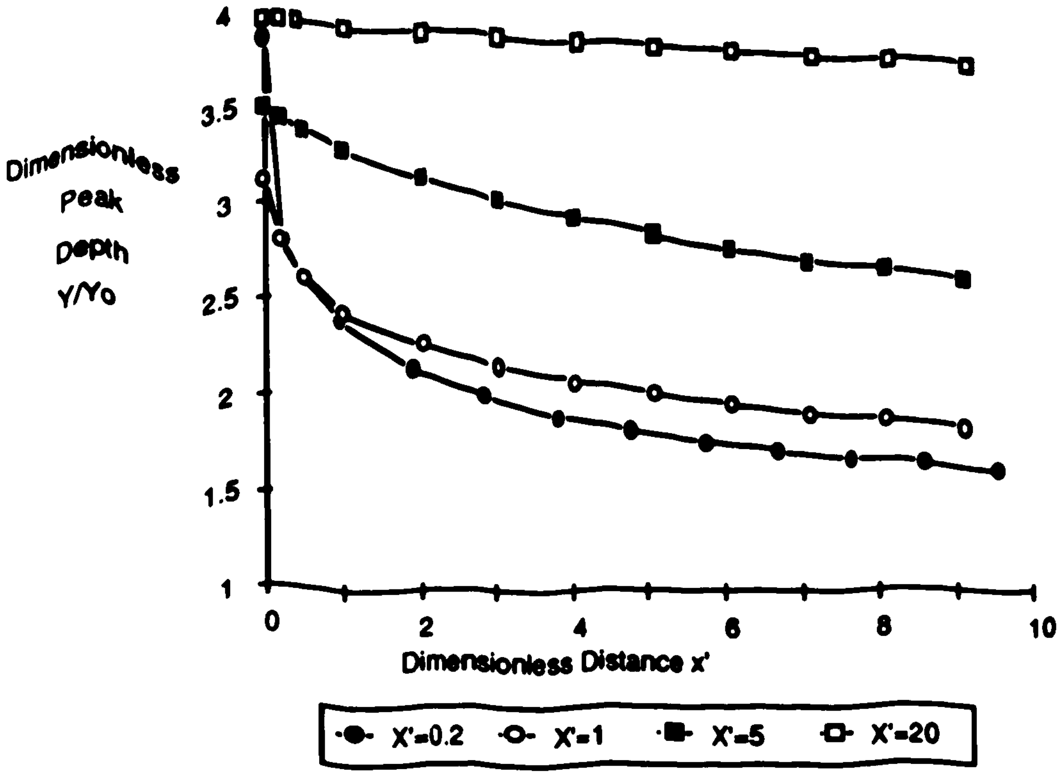

Fig. 4.8a Attenuation of Peak Depth for Y' = 4

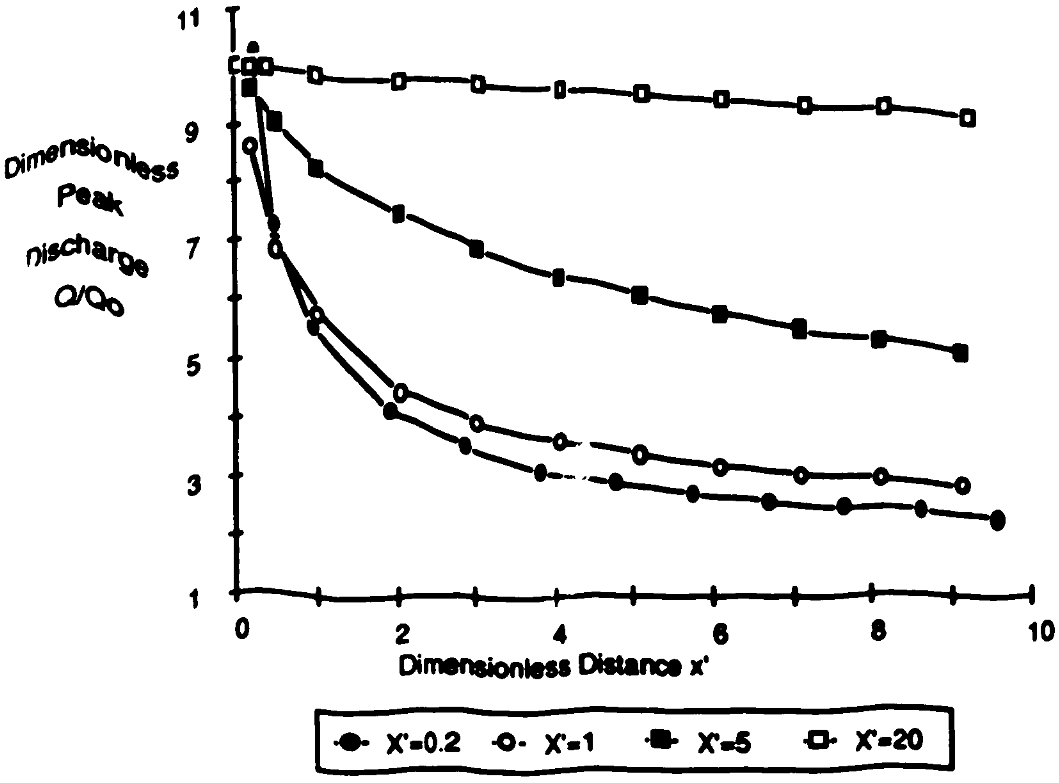

Fig. 4.8b Attenuation of Peak Discharge for Y' = 4

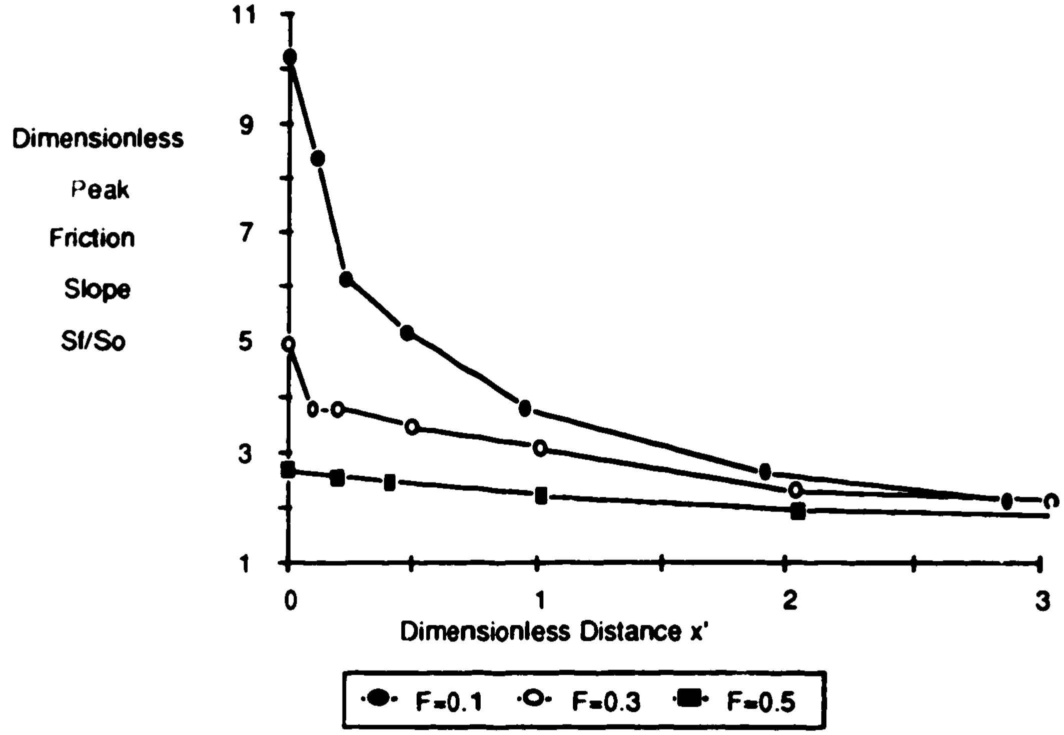

Fig. 4.8c Attenuation of Peak Friction Slope for Y' = 4

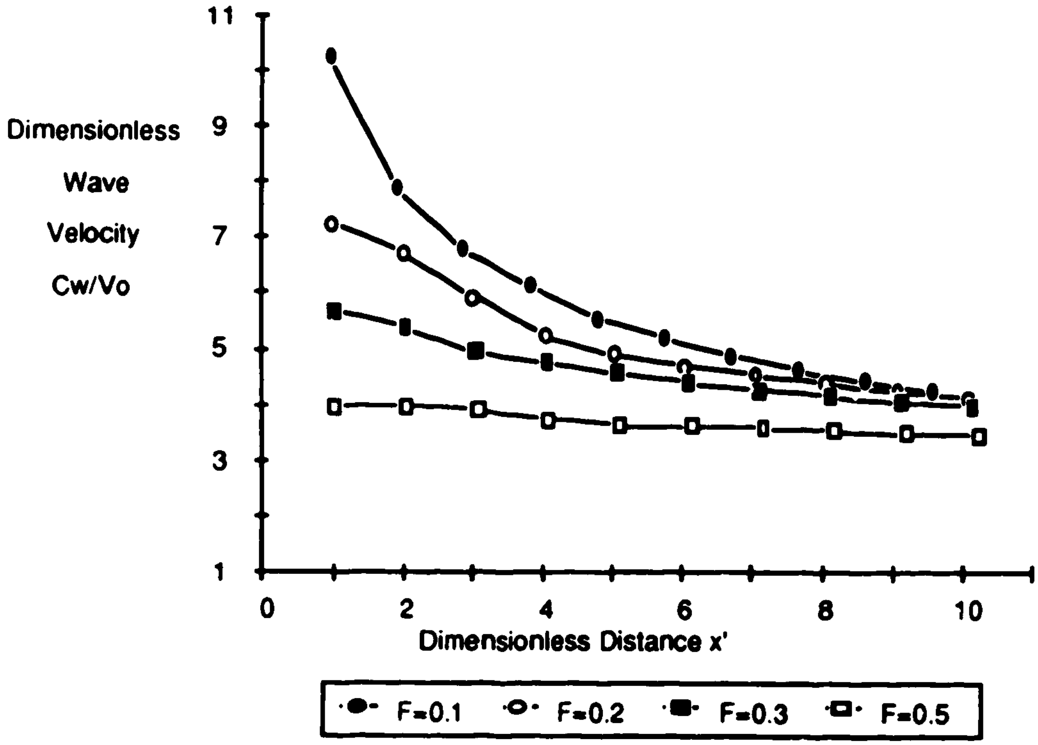

Fig. 4.8d Attenuation of Wave Velocity for Y' = 4

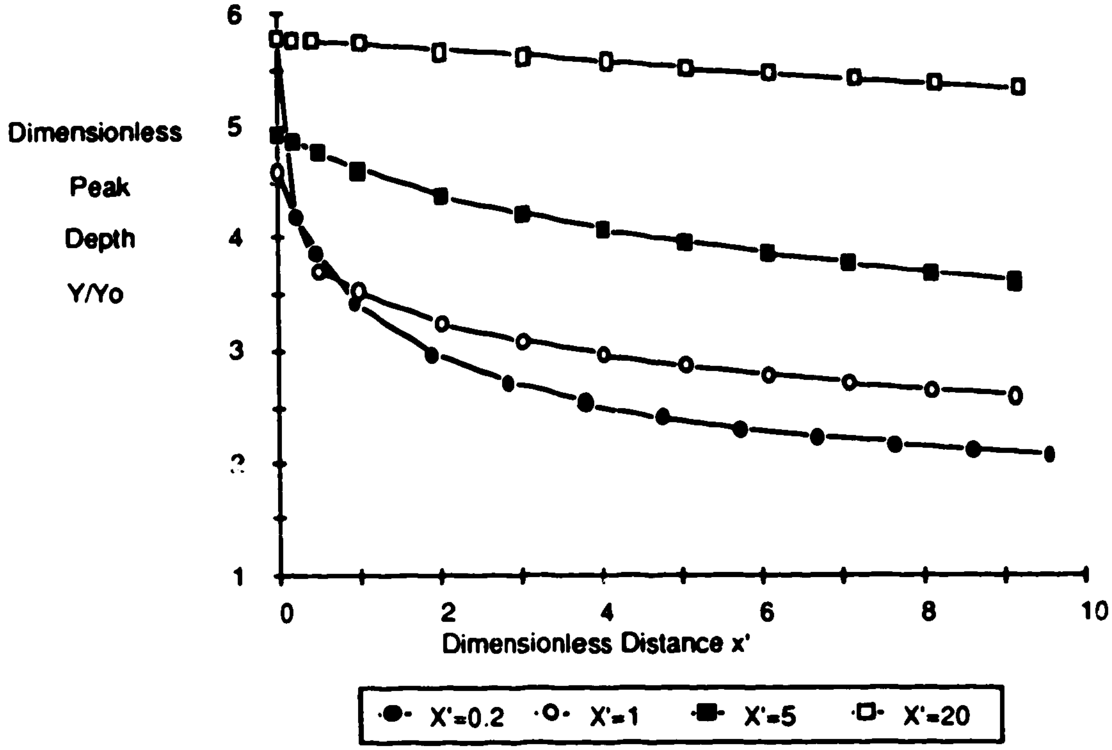

Fig. 4.9a Attenuation of Peak Depth for Y' = 6

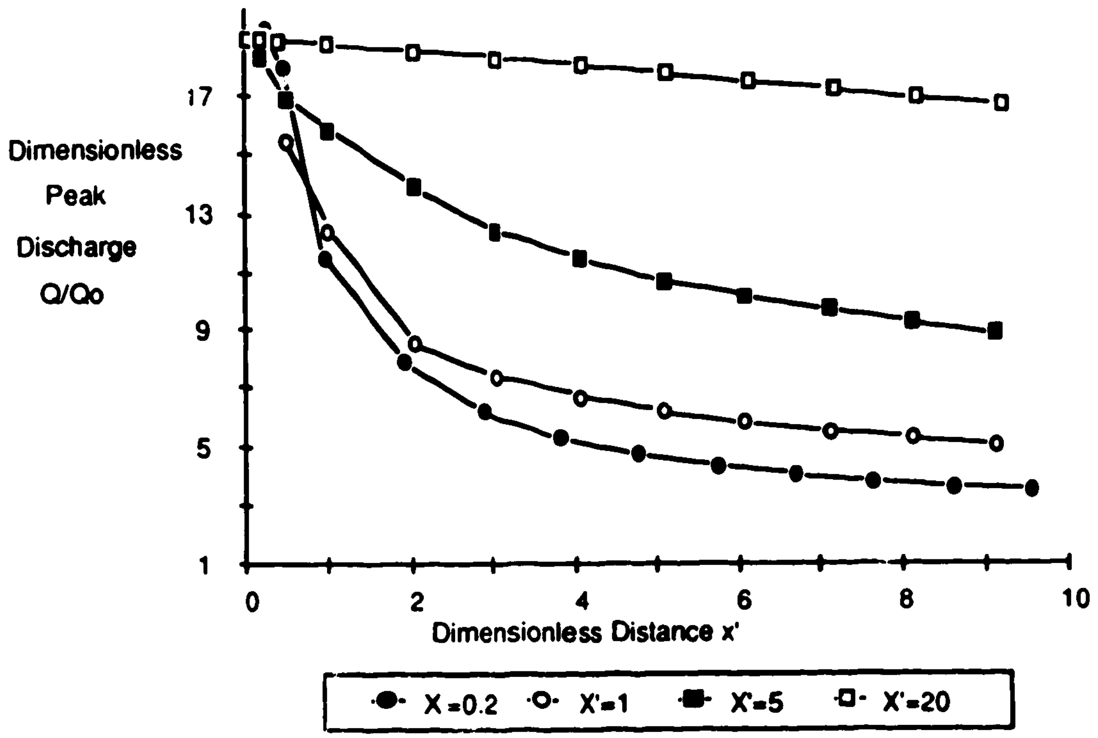

Fig. 4.9b Attenuation of Peak Discharge for Y' = 6

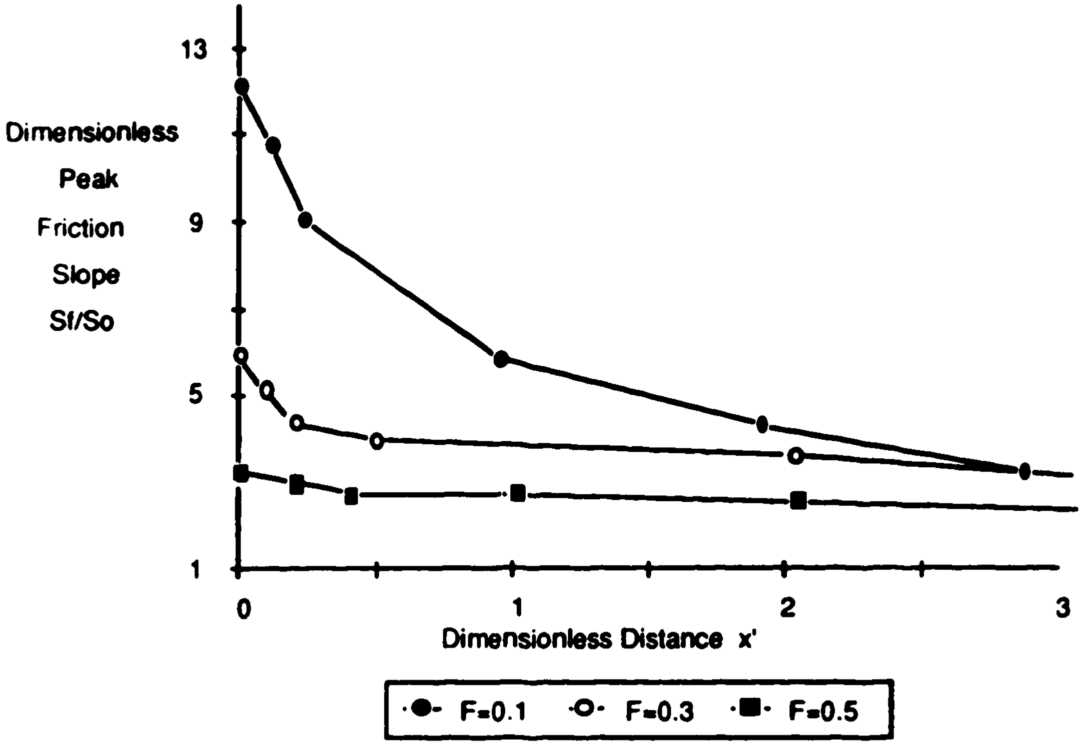

Fig. 4.9c Attenuation of Peak Friction Slope for Y' = 6

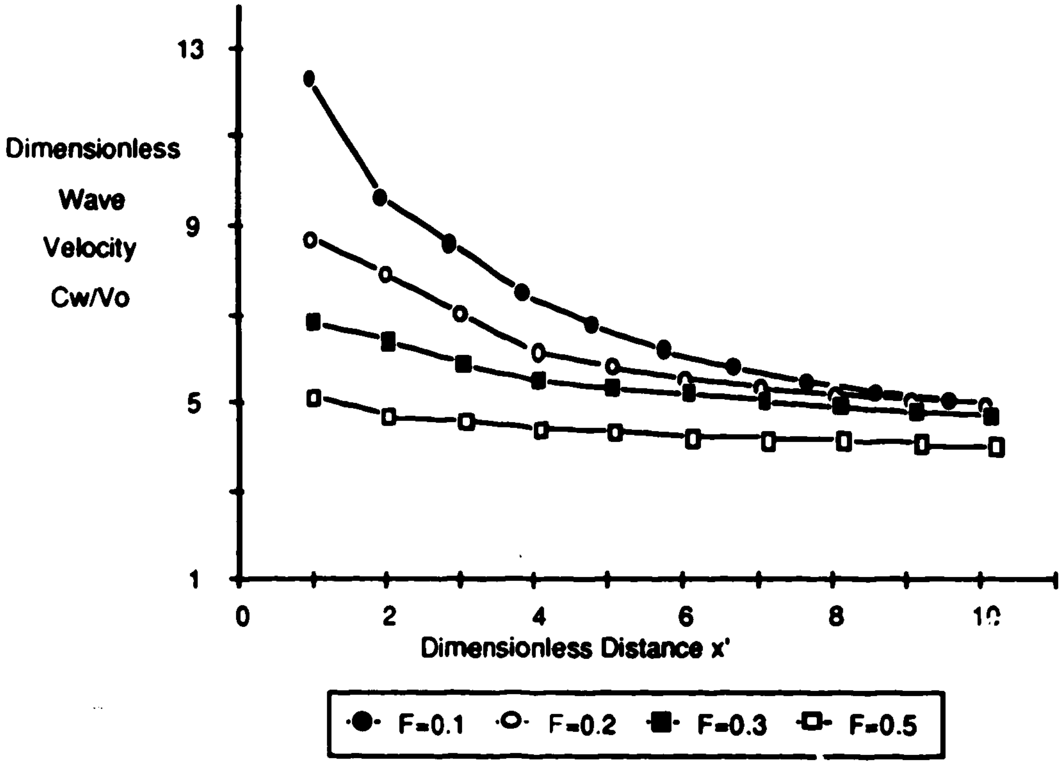

Fig. 4.9d Attenuation of Wave Velocity for Y' = 6

parameters. It is apparent that the parameters X' and Y' are important in predicting the peak depth and discharge results and F_o and Y' are significant in predicting peak friction slope and wave velocity. The L' parameter slightly affects the peak energy gradient and wave velocity but not enough to be included in the plots. The Froude number also affects the peak depth and discharge at short distances, but also not enough to be included in the dimensionless plots.

4.5 Application

In this section, the practical plots are used to predict the amplitude of the river wave on the Athabasca River near Fort McMurray following an ice jam failure documented by Malcovish et al. (1988). These results are then compared with the measured results and a more complete modelling of the situation presented in Fig. 4.9. The initial conditions and the characteristics of the ice jam and the reach downstream of the ice jam are approximately as follows :

S_o = 0.00016
Y_o = 1.45 m
x = 5 km and 10 km
Y_p = 6.4 m
L = 1000 m
X = 11000 m

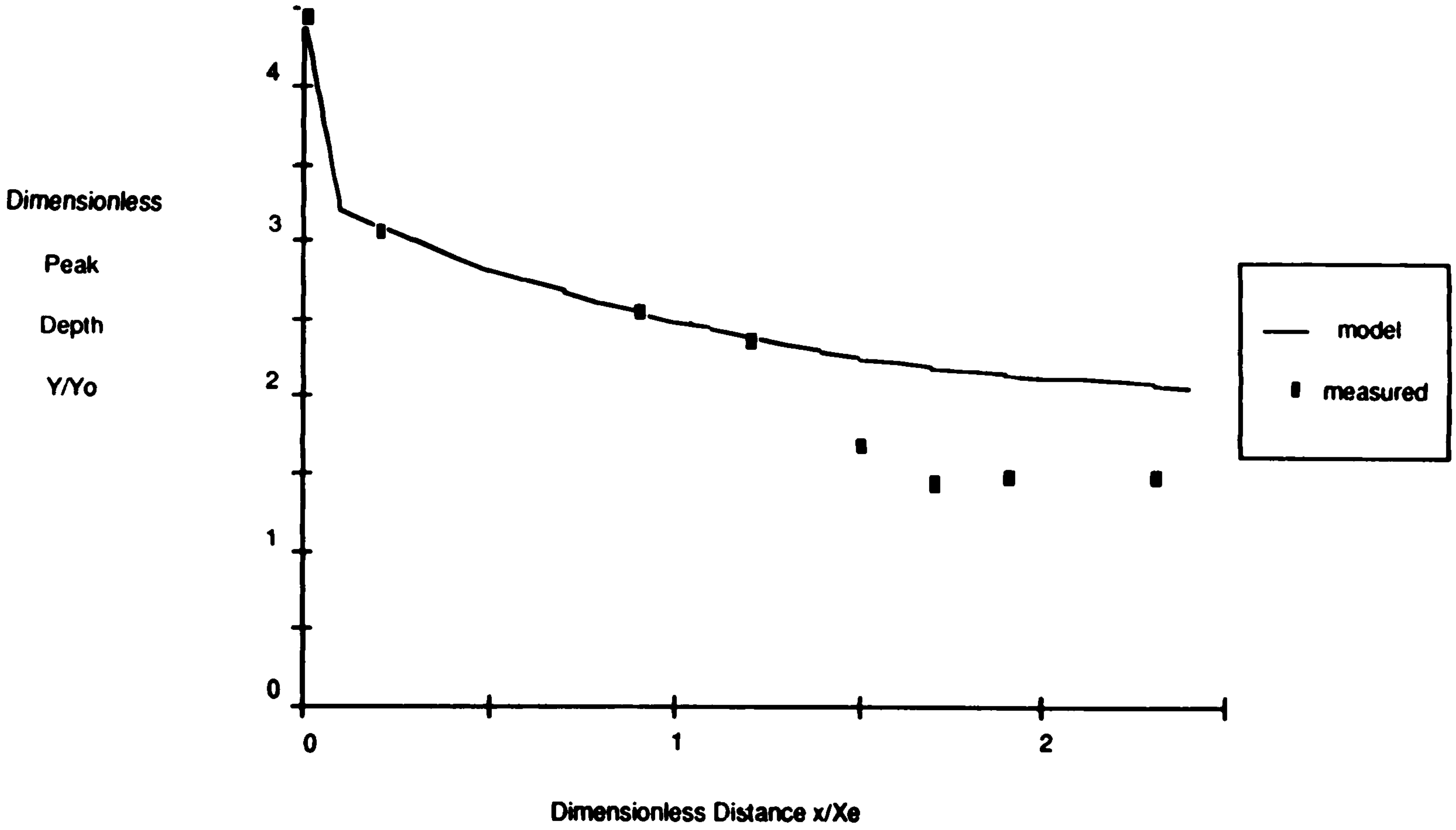

Fig. 4.10 Ice Jam Release
Athabasca River @ Fort McMurray

The variable Xe used in Fig. 4.9 to non-dimensionalize x is the length of the equilibrium portion of the jam which is equivalent to X-L. The distance variable x used in Fig. 4.9 is zero at the upstream end of the toe, a distance of -L in the coordinate system used in this chapter. The sharp kink in the plot is the toe of the jam. These differences were used to be consistent with the plot presented by Malcovish et al. (1988).

Two values of x were chosen. The resulting dimensionless parameters are :

$$Y' = \frac{Y_p}{Y_o} = \frac{6.4}{1.45} \approx 4.4$$

$$X' = \frac{LS_o}{Y_o} = \frac{(11000m * 0.00016)}{1.45m} \approx 1.26$$

$$\frac{xS_o}{Y_o} = \frac{(5000m * 0.00016)}{1.45m} = 0.57$$

and

$$\frac{xS_o}{Y_o} = \frac{(10000m * 0.00016)}{1.45m} = 1.15$$

From the plots, linearly interpolating for Y' yields :

$$\frac{Y}{Y_o} = 2.8 \text{ @ } 5 \text{ km}$$

$$\frac{Y}{Y_o} = 2.6 \text{ @ } 10 \text{ km}$$

Therefore :

Y = 2.8 * 1.45 m = 4.1 m @ 5 km

and

Y = 2.6 * 1.45 m = 3.8 m @ 10 km

From Fig. 4.9, the observed peak depths are :

Y = 4.05 m @ 5 km

and

Y = 3.65 m @ 10 km

The agreement between the predicted values and the observed values is very good. This shows that the prismatic channel assumption was not very limiting in this case.

The results of the more complete modelling of this specific case are also presented in Fig. 4.9. There is good agreement with the observed results for the first 12 km downstream of the start of the equilibrium portion of the jam. However, the observed values further downstream were significantly different from the model results. The reason for this disparity is not known. Attempts to model these values by using more precise geometry and different channel conditions were unsuccessful. One possible reason for the disparity could be that the jam did not completely release.

This chapter has examined another type of unsteady flow that may trigger a dynamic breakup. Using the initial profile of Fig. 4.1, a set of dimensionless parameters that describe the unsteady flow following the sudden failure of an ice jam have been developed and used to generate a set of practical plots. As with chapter 3, these plots can be used to predict the nature of the resulting river wave at downstream locations. These plots have been applied to a case of unsteady flow on the Athabasca River with good results.

5 BREAKUP

5.1 Introduction

The previous cases have been concerned with analysis of situations that can generate the change in discharge and stage that might trigger breakup. However, once breakup has begun, it generates its own suite of unsteady flow phenomena. The nature of this unsteady flow, and therefore the forces developed at the breaking front, depends on the manner of breakup. As mentioned in chapter 1, Ferrick and Mulherin (1989) have identified two distinct types of dynamic breakup: support-dominated breakup and strength-dominated breakup.

Support-dominated breakup is when the force applied to the cover exceeds the support strength of the cover near its banks. The result is a bank to bank release of the cover. As breakup progresses, the ice plates broken from the solid ice cover break into smaller blocks by colliding with other plates. As a result, the breaking front and the rubble front (the downstream end of the pack) are separated. The force applied at the breaking front causing breakup to continue is caused by the river wave that is responsible for the breakup event. Ferrick and Mulherin (1988) compute this as a force per unit length of channel :

$$f_h = BS_f\ (\gamma R + \gamma_i t_i)$$

where S_f is the flow energy gradient or friction slope, B the river width, γ and γ_i the specific weights of water and ice respectively, and t_i the ice thickness. This force must be balanced by the resistance of the ice cover at its supports for the cover not to fail. Ferrick and Mulherin (1988) report that the ice cover on the Connecticut River near Windsor, Vermont will fail when the stress applied to the points of support (hinge cracks near the banks) is in the order of 2 kPa. Since this type of breakup is related to the river wave, the ice run will stall when the wave moves ahead of the breaking front or when the wave attenuates significantly. When a support-dominated breakup stops, either breakup will continue as a strength-dominated breakup or the breakup will stall forming an ice jam.

A strength-dominated breakup is characterized by a pack pushing through the downstream ice cover (Gerard and Flato, 1988) (see Fig. 1.2). The rubble front and the breakup front are now coincident. The force applied to the solid ice cover at the breaking front can be calculated by integrating the shear stress applied to the pack over the length of the pack and subtracting the amount of force shed to the banks.

The shear force applied to a moving ice cover is calculated as :

$$\tau = \gamma R_i S_f \left(\frac{V-V_p}{V}\right)^2$$

where V is the velocity of water below the pack, V_p is the velocity of the pack (which is equal to the breaking front velocity C_b in this case), R_i is the distance from the underside of the ice cover to the point of maximum velocity of flow and can be calculated as :

$$R_i = \frac{Y}{2} \left(\frac{k_i}{k_c}\right)^p$$

5 Modelling Breakup

Daly and Ashton (1983) used a modified version of the DWOPER flood routing model to analyse the effect of breakup on the flow. They modelled the breakup process by assuming the ice cover instantaneously ceased to influence the hydraulics. They observed that the transient response to this change increased as the channel slope and length increased. Ferrick and Mulherin (1989) developed a model for the Connecticut River which treated breakup by removing the ice cover progressively downstream at a speed close to the observed speed of the breakup front. The assumption of complete removal of the ice cover is based on the assumption that the ice floes broken from the solid ice cover accelerate quickly to the surface velocity of the flow. This model is being used to predict the triggering and sustenance of dynamic breakup on the Connecticut River near Windsor, Vermont. Both model runs and measured data show that, as expected, water is released from storage due to breakup. This release feeds the river wave that triggered the breakup, reducing wave attenuation and prolonging the breakup event.

This study of dynamic ice cover breakup consists of two parts. The first part is a dimensionless study of the self-generated unsteady flow associated with a moving breakup. The second part uses a simplified version of the strength-dominated breakup model presented by Gerard and Flato to calculate the force applied to the breaking front during a strength-dominated breakup and to examine the effect of certain parameters on this force.

The two cases of unsteady flow analysed in the first part of this study are the complete removal of the ice cover, which is similar to the treatment of Ferrick and Mulherin (1989), and a progressive increase in ice cover roughness which models the breaking front of the model of Gerard and Flato (1988).

In the case of ice cover removal, the conditions at the node at the upstream end of the ice cover are changed from ice covered to open water at each time step. The result is the removal of the ice cover at a velocity equal to :

$$C_b = \frac{\Delta x}{\Delta t}$$

where Cb is the breaking front velocity, Δx is the spatial discretization, and Δt is the temporal discretization used in the numerical model. In the case of increased ice cover roughness, the ice cover roughness at the upstream end of the solid ice cover is changed to the broken ice roughness of the pack at each time step. The velocity of the breaking front is calculated in the same way. Dimensionless plots of depth, discharge, and shear stress against distance at certain times are presented for fixed values of certain dimensionless parameters. These plots show the nature of the unsteady flow associated with dynamic ice cover breakup.

In the second part of this study, these two cases of unsteady flow are combined to obtain a complete, albeit simplified model of a strength-dominated dynamic breakup. At each time step, the roughness of the upstream end of the solid ice cover is changed to the pack roughness and the flow condition at the upstream end of the pack is changes from ice covered to open water (see Fig. 1.2). The change in thickness of the pack is not considered at this time. The result is a fixed length of pack moving through a solid ice cover at the breaking front velocity. The force applied to the solid ice cover at the breaking front is calculated as described in the previous section. The amount of force shed to the banks is neglected as a first approximation and this is valid for pack lengths of about 5 channel widths. Dimensionless plots of force against breaking front velocity are presented for a range of parameters. It is presumed that this force is an important factor in the sustenance of a strength-dominated breakup. A range of breaking front velocities was obtained by changing Δt while holding Δx constant. Care was taken to make sure that Δt did not significantly exceed the values shown in Table 2.1.

5.3 Parameter Definition

The variables required to describe the situations are :

Y_i	normal waterway depth under solid ice cover
Y_p	normal waterway depth under pack of broken ice
Y_o	normal waterway depth for open water conditions
V_i	normal flow velocity under solid ice cover
τ_i	initial shear stress applied to solid ice cover
f_o	the initial shear force per unit width applied to a length L of solid ice cover
Q_o	initial discharge
S_o	channel slope
B	channel width
L	length of pack of broken ice

and

C_b	velocity of the two fronts.

The dependent variables considered are :

Y depth of flow

τ shear stress applied to cover

Q discharge.

and

f shear force per unit width applied to the pack of broken ice of length L

5.4 Dimensional Analysis

With Y_i and V_i being the initial conditions of the reach through which breakup will move, the initial Froude number becomes :

$$F_o = \frac{V_i}{\sqrt{gY_i}}$$

the dimensionless distance parameter :

$$x' = \frac{xS_o}{Y_i}$$

and the dimensionless pack length :

$$L' = \frac{LS_o}{Y_i}$$

The dimensionless depth parameter becomes :

$$Y' = \frac{Y_p}{Y_i}$$

for the roughness change study and the combined model study, and it is :

$$\frac{Y_i}{Y_o}$$

for the ice cover removal case. The dimensionless breakup front velocity is taken as :

$$\frac{C_b}{V_i}$$

The dimensionless versions of the dependent variables considered are :

$$\frac{Y}{Y_i}, \frac{V}{V_i}, \frac{Q}{Q_o}, \frac{\tau}{\tau_i}, \frac{f}{f_o}$$

5.5 Results - unsteady flow

The results of the first part of this study, the analysis of the unsteady flow associated with the two breakup components, are presented in Fig. 5.1 to Fig. 5.3.

Fig. 5.1 a and b show the change in flow depth in the vicinity of the breaking front for the ice cover removal case and the ice roughness increase respectively. In the ice cover removal case, water is being released from storage as the ice cover ceases to influence the hydraulics. As the velocity of the resulting wave is greater than the front velocity in this case, this released water moves downstream under the pack so that the distance downstream showing an increase in depth increases with time. The increase in depth at the front is rapid at first and then slows down, tending towards a constant (steady-state) value.

In the ice cover roughness increase case, water is taken from the flow and put into storage at the breaking front. This means that for a front velocity less than the wave velocity, a negative wave will propagate ahead of the breaking front resulting in a decrease in depth. Again, the change in depth at the front is rapid at first and then slows down as it approaches a steady state value.

The two plots of Fig. 5.2 show the change in discharge resulting in each case. The plot for ice cover removal shows an increase in discharge both upstream and downstream of the

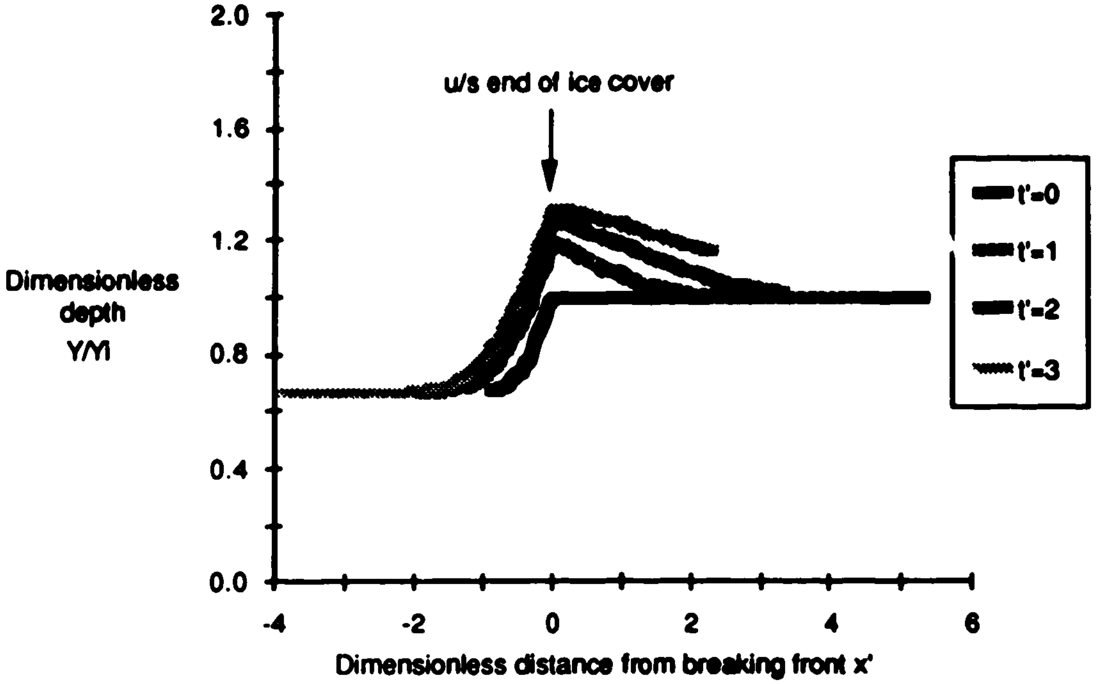

Fig. 5.1a Effect of Ice Cover Removal on Depth
Fo=0.3, Cb/Vi=1, Y'=1.5

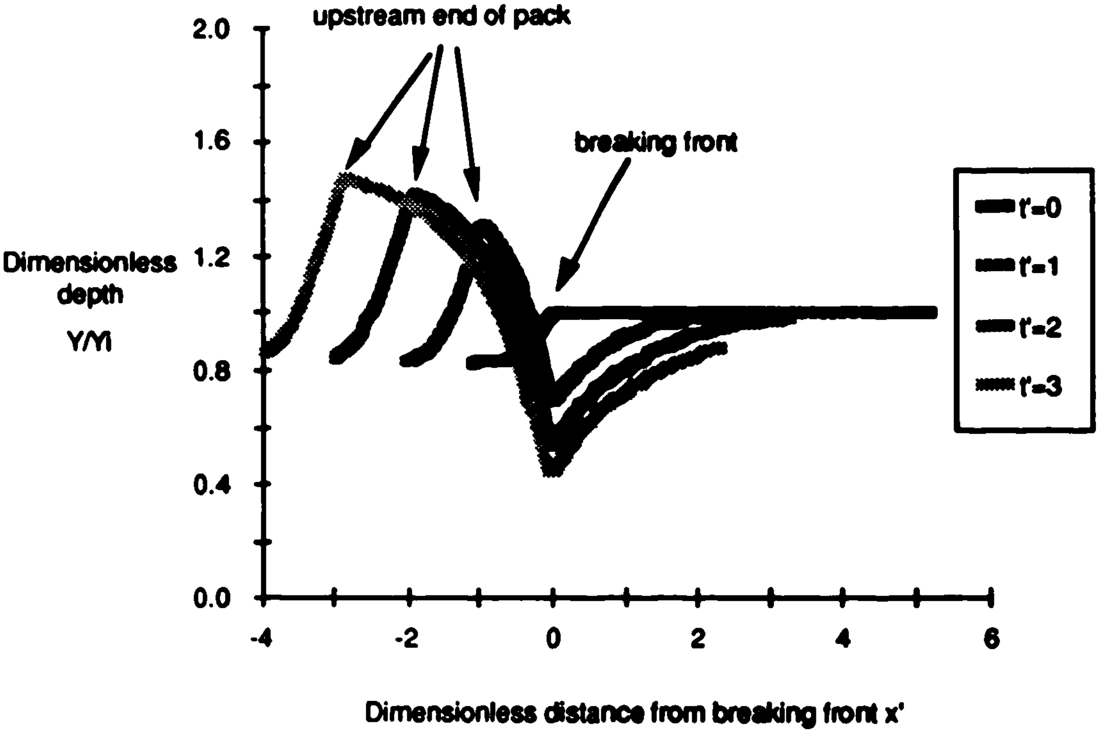

Fig. 5.1b Effect of Roughness Increase on Depth
Fo=0.3, Cb/Vi=1, Y'=1.5

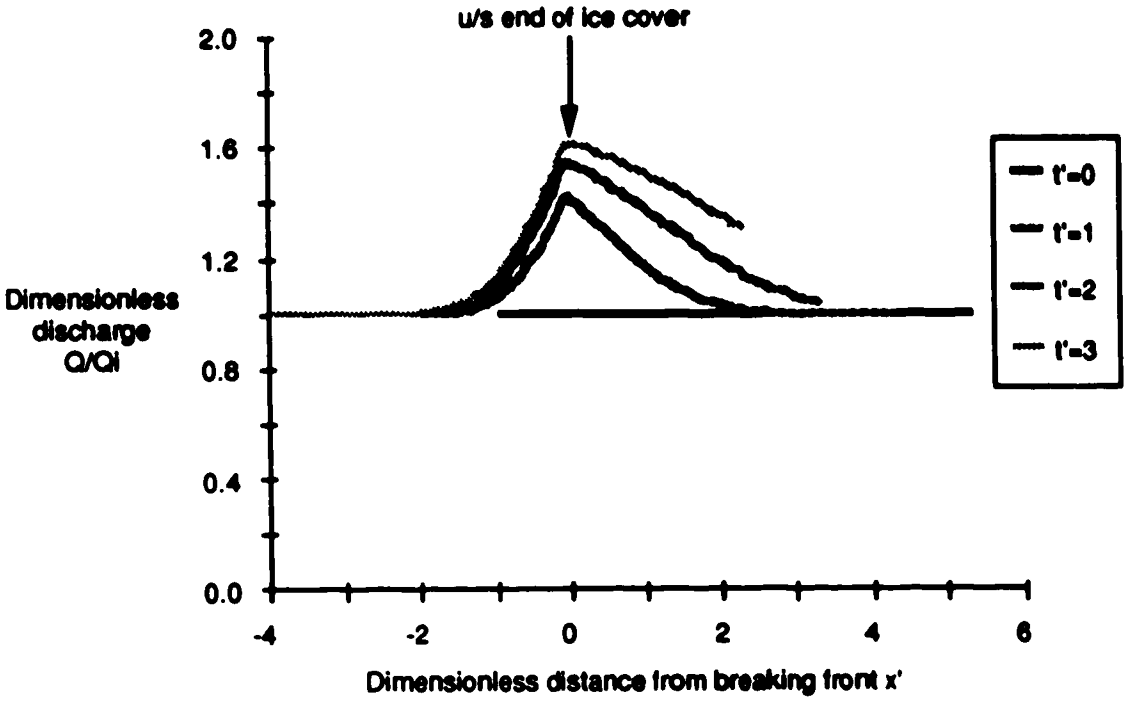

Fig. 5.2a Effect of Ice Cover Removal on Discharge
Fo=0.3, Cb/Vi=1, Y'=1.5

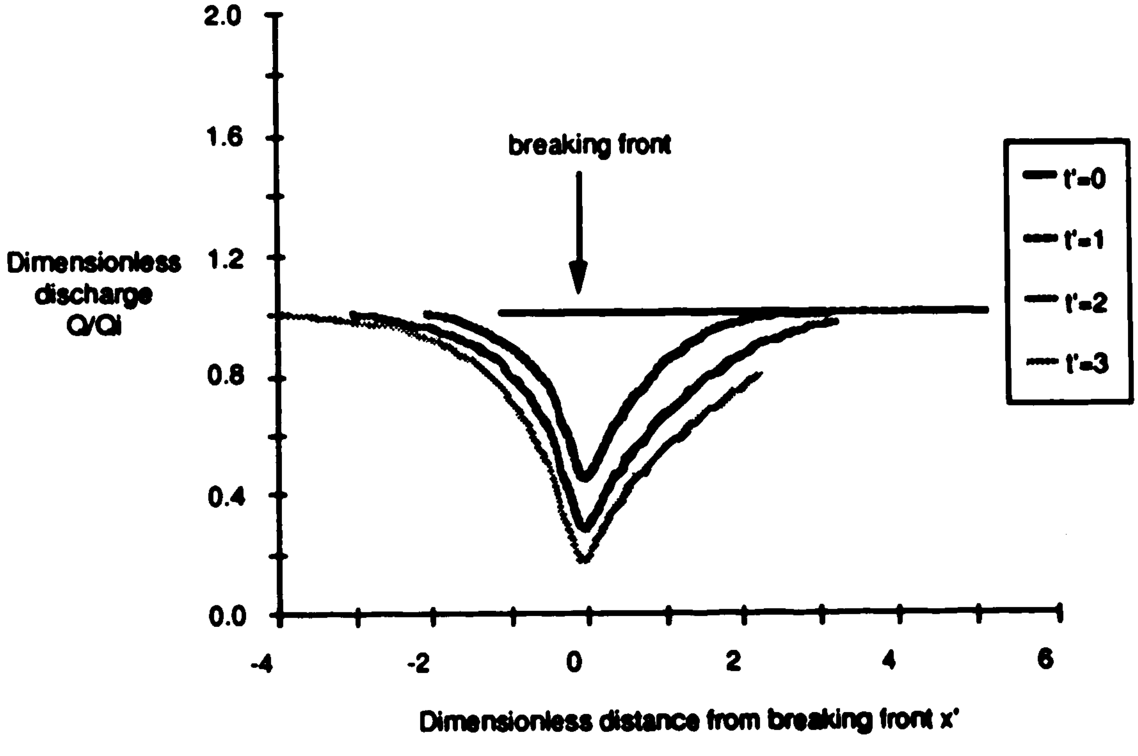

Fig. 5.2b Effect of Roughness Increase on Discharge
Fo=0.3, Cb/Vi=1, Y'=1.5

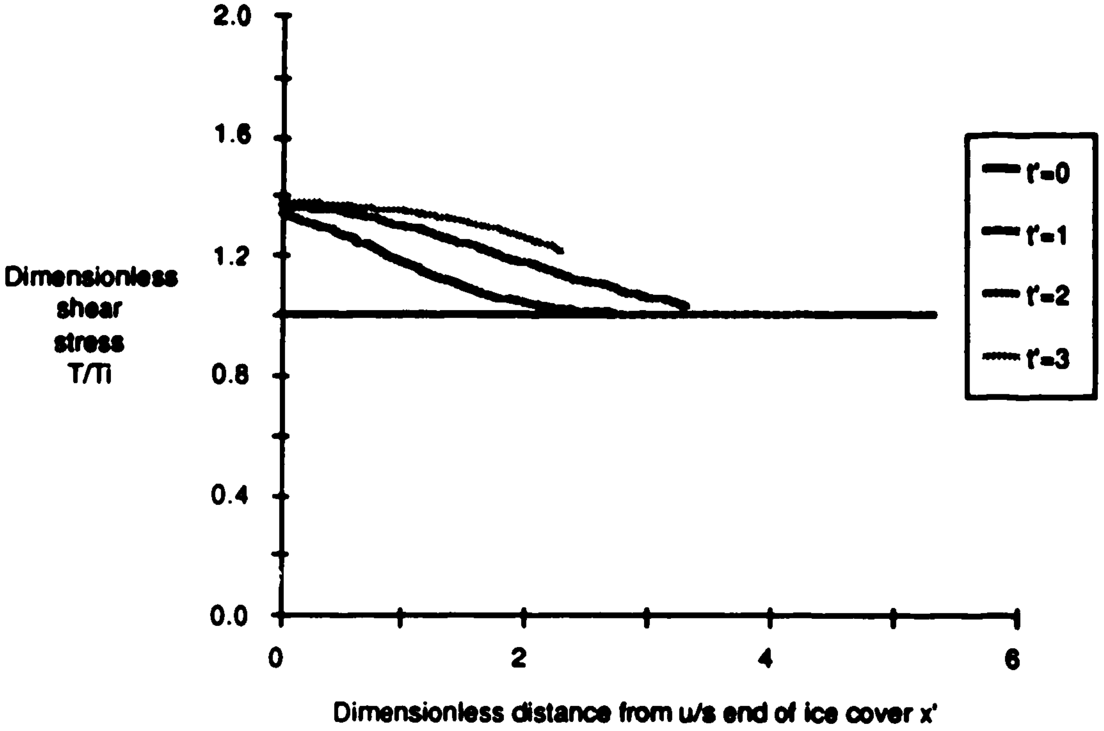

Fig. 5.3a Effect of Ice Cover Removal on Shear Stress
Fo=0.3, Cb/Vi=1, Y'=1.5

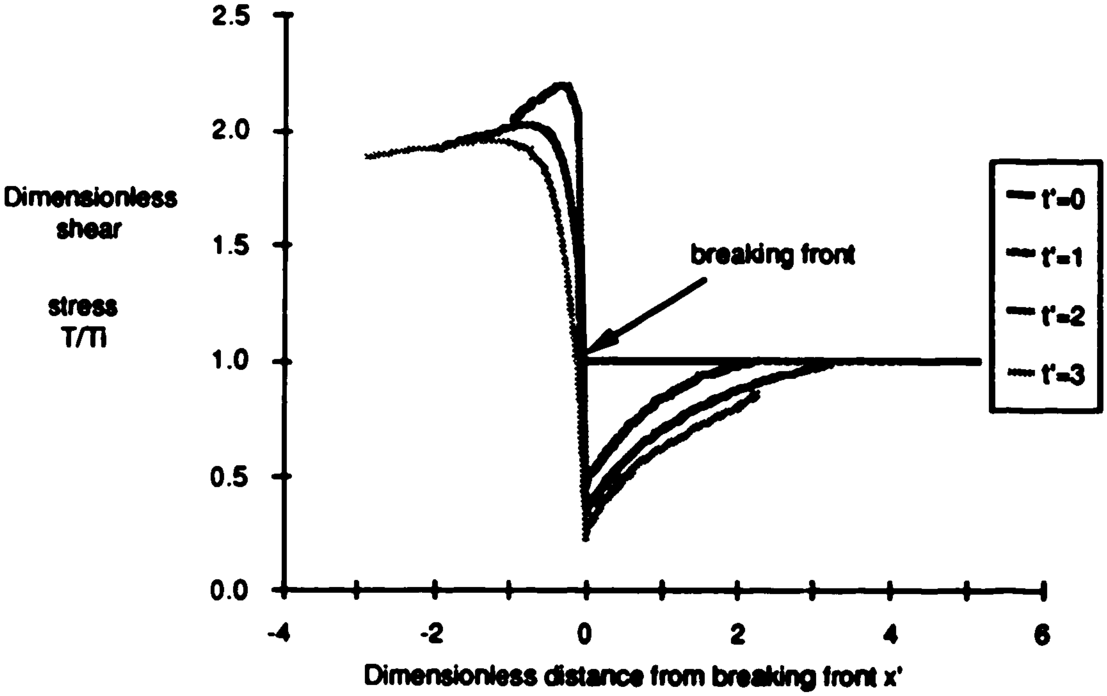

Fig. 5.3b Effect of Roughness Increase on Shear Stress
Fo=0.3, Cb/Vi=1, Y'=1.5

front, due to the release of water from storage. As with the depth, the increase in discharge at the front is rapid at first and then approaches a maximum and the influence downstream increases with time. A similar but opposite effect is shown for the roughness increase case since water is being put into storage.

The two plots of Fig. 5.3 show the changes in the shear stress applied to the ice cover in the two cases. For the ice cover removal case, which is similar to previous models of a support-dominated breakup, the shear applied to the ice cover downstream of the breaking front is shown to increase. It is this increase in shear, together with that of the wave that triggered breakup, that is responsible for continued breaking of the ice cover. This increase reaches further downstream of the front with time. This additional shear will compress the solid ice cover, providing room for the broken ice to move into, thus satisfying continuity. The plot for roughness increase shows an increase in shear behind the breaking front and a decrease in shear ahead of the breaking front. The decrease ahead of the breaking front is due to the reduction in discharge downstream described earlier. The increase upstream of the front is due largely to the increased roughness of the cover. It can be seen that the stress applied to the pack decreases slightly with time. This is caused by the decreasing discharges as more water is taken from the flow and is stored.

5.6 Results - Model of strength-dominated breakup

When these two unsteady flow generating processes are combined (ice cover roughness increase followed at a fixed distance by ice cover removal), the current model of a strength-dominated breakup is formed. The results presented in Fig. 5.4 to 5.6 are the force applied at the breaking front (calculated as outlined in section 5.1) non-dimensionalized by the force applied initially to a length of smooth ice cover of equal length to the pack. These results are presented as a function of the dimensionless breaking front velocity for various pack lengths, initial Froude numbers, and pack roughnesses. The forces were calculated after a long period of time and the solution was at a steady state.

Although the magnitude of the self-generated unsteady flow increases as dimensionless breaking front velocity increases, all three plots show a sharp decrease in the magnitude of force applied to the pack as C_b/V_i increases. This is because the most dominant factor in the evaluation of this force is the relative velocity between the pack and the flow. As C_b/V_i increases, the pack velocity increases and the shear applied to the pack by the flow decreases. An interesting result of this study is therefore that large

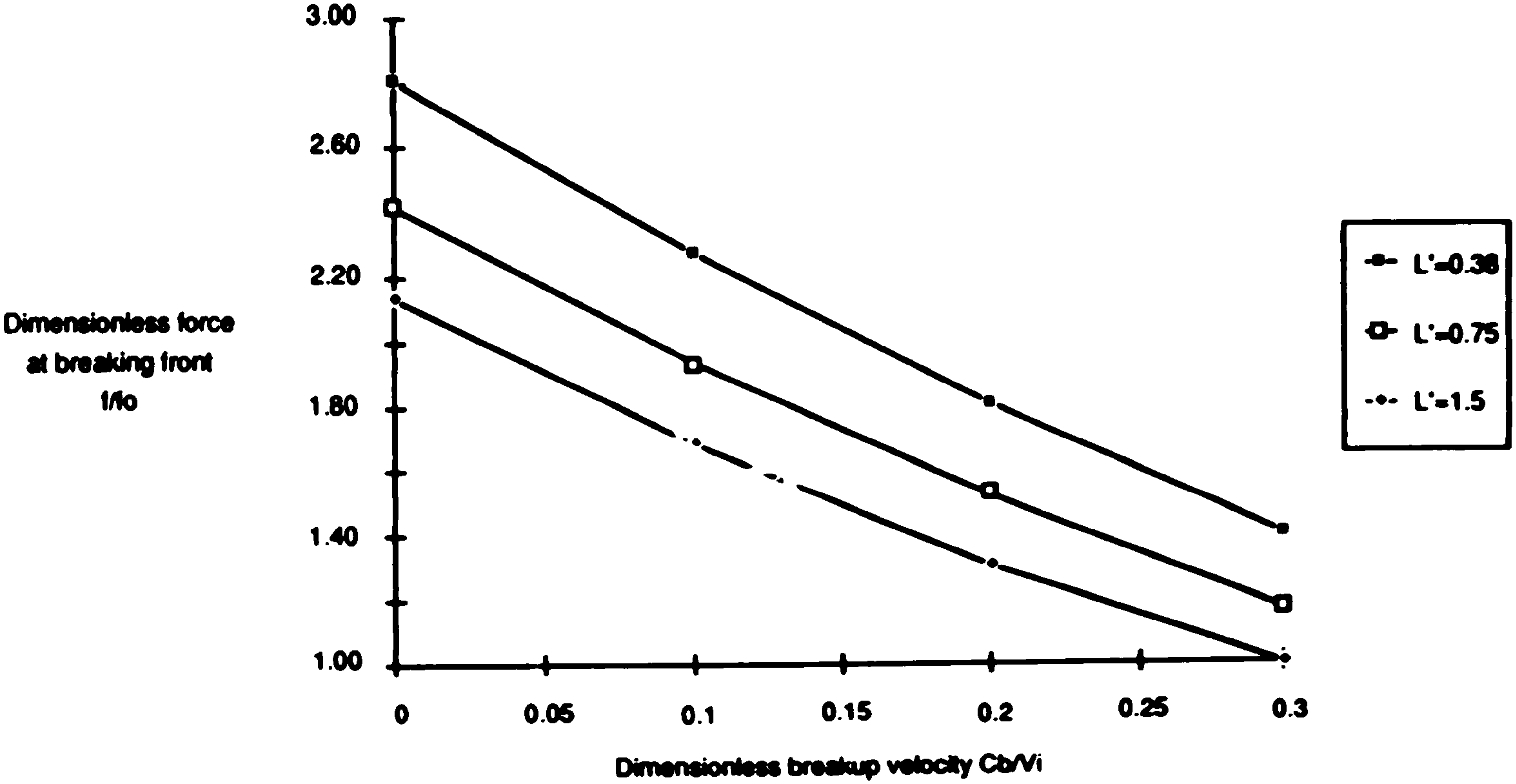

Fig. 5.4 Effect of Pack Length and Breakup Velocity on Force Applied at Breaking Front
Fo=0.3,Y'=1.5

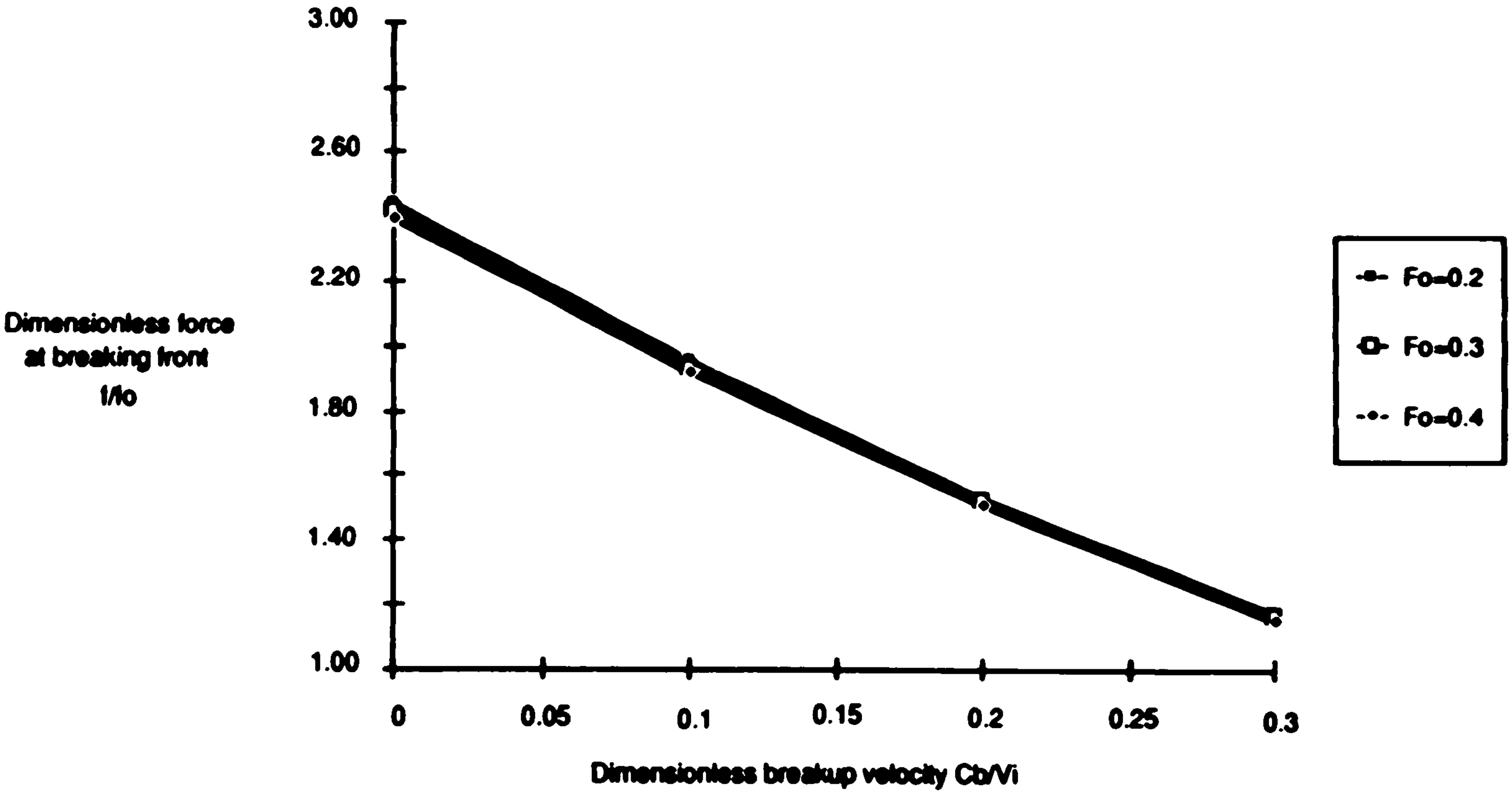

Fig. 5.5 Effect of Initial Froude number and Breakup Velocity on Force Applied at Breaking Front

L'=0.75, Y'=1.5

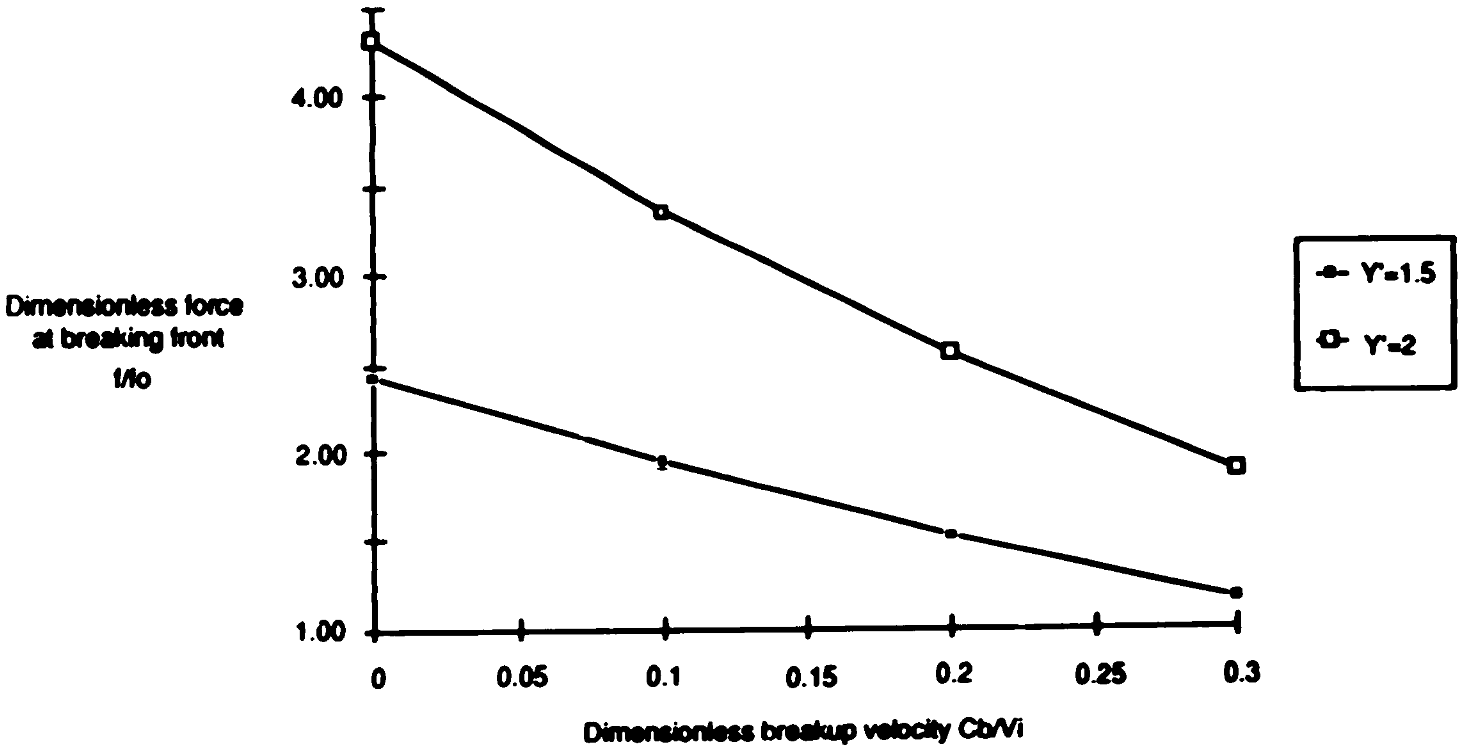

Fig. 5.6 Effect of Pack Roughness and Breakup Velocity on Force Applied at Breaking Front
Fo=0.3, L'=0.75

forces at the breaking front result only when the breaking front velocity is considerably less than the flow velocity. The unsteady flow component of the resulting force at these low breaking front velocities is small.

Fig. 5.4 through 5.6 also show the effect of the other dimensionless parameters on the force applied at the breaking front. Fig. 5.4 shows that shorter pack lengths result in slightly higher values of f/f_o. Of course, the magnitude of the force applied at the breaking front will increase as the length of the pack increases since f_o will also increase with L. This result shows that f_o, however, will not increase linearly with the length of pack. even when the amount of force shed to the banks is neglected. Fig. 5.5 shows that the initial Froude number has a negligible effect on the results if the other parameters remain constant. Fig. 5.6 shows that the increase in roughness of the broken ice, which is represented in this analysis by the Y' parameter, has a very significant effect on the magnitude of force applied at the breaking front. For slow moving breakups and $Y'=2$ (which corresponds to a pack roughness approximately 5 times that of the solid ice cover), the force applied at the breaking front increases by 3 to 4 times.

5.7 Discussion

It is of interest to see if the increase in force shown in these plots could be solely responsible for the breakup of a solid ice cover. For a hypothetical river with the following characteristics :

$B = 400m$

$S_o = 0.001$

$n_b = 0.025$

$n_i = 0.025$

$Q = 800\ m^3/s$

$Y = 1.74m$

the initial shear stress applied to the ice cover is 8.6 N/m^2. Choosing L as 2000m so that the shedding of force to the banks can be neglected, the initial force per unit width (f_o) applied to an ice cover of length L is :

$$f_o = 8.6*2000 = 17.2\ kN/m$$

For a Manning coefficient of broken ice of 0.1, $Y' = 2$. Therefore, from Fig. 5.6 assuming $C_b/V_i = 0.1$, $f/f_o = 3.4$. The force applied at the breaking front is :

$$f = 17.2\ kN/m * 3.4 = 58.5\ kN/m$$

Sanderson (1988) indicates that an average stress in the order of 100 kN/m over a wide front is sufficient to break a competent ice cover. Therefore, allowing for local forces exceeding the average value and noting that deterioration of the ice cover is often coincident with this type of breakup, it does seem feasible that enough force can be generated by this process alone to sustain a breakup. Possible reasons for the stall of a strength-dominated breakup include: the pack becoming too long for the water released at the upstream end to reach the breaking front, and a local increase in the strength of the ice cover.

A more detailed modelling of a strength-dominated breakup could be performed by allowing the velocity of the two fronts to be different, meaning the length of the pack can vary, and to take into account the change in thickness of the pack. The latter will involve consideration of ice continuity and an interaction between shear stress applied and the ice thickness. Such a model would allow a more complete analysis of the various phases of a dynamic strength-dominated breakup.

6 CONCLUSION

The dynamic breakup of a solid ice cover on a river is associated with unsteady flow. A finite difference numerical model was developed to solve the unsteady flow equations for typical breakup situations. The first concern was with situations that may trigger breakup. Two situations were considered: an abrupt change in discharge and a sharp increase in stage.

The change in discharge is a simplified hydrograph which models flows such as hydropower plant or dam releases and natural flood waves. The increase in stage models the sudden failure of an ice jam. For both cases, dimensional analysis has been used to derive the parameters necessary to describe the solution in as concise a manner as possible. The intent was to develop a series of dimensionless curves that would allow an assessment of the influence of the various parameters on the character of the river waves released by these phenomena. These curves were also intended to provide the means for making preliminary estimates in real situations, such as has traditionally been done in the related field of waterhammer. Comparison of the plots with measured field data shows these plots to indeed be useful.

The change in discharge was modelled by a triangular hydrograph. A wide range of these hydrographs were routed through a range of prismatic channels and the characteristics of the resulting river wave were presented in a set of dimensionless plots. Characteristics of interest were the peak waterway depth, peak discharge, peak friction slope, and wave velocity. These plots are presented in the form of a set of 'diagnostic' plots which isolates the effect of each parameter on the results, and a set of 'predictive' plots that can be used in practice to quickly estimate the salient features of a river wave resulting from a given discharge change. The plots are applicable to both ice-covered and open water channels. Published results of a field study were used to test the usefulness of these plots and the results were good. The effect of each of the dimensionless parameters developed from the governing unsteady flow equations and boundary conditions is presented. The most important parameters influencing the evolution of the river wave were found to be the peak discharge and the time to peak discharge.

The change in stage was modelled by supplying an idealized ice jam profile as the initial conditions. The effect of the ice in the jam on the hydraulics was neglected. Again, a general analysis using a wide range of initial profiles and prismatic channels was performed and sets of both diagnostic and predictive dimensionless plots developed. The latter are intended to allow quick assessment of the characteristics of a river wave that will result should an upstream ice jam fail. Again, the plots are valid for both ice covered and open water reaches. A comparison with published field data was made and the results were good. The results of this study showed more dependence on the Froude number than those of the hydrograph routing study. This was due to the much more abrupt imposed change on the flow. The parameters of major significance were the depth of water at the jam, the length of the jam, and the Froude number.

The final situation considered was a preliminary study of the unsteady flow associated with a breakup and ice run. This study consisted of two parts. The first was an investigation of the unsteady flow associated with the change in ice cover conditions during breakup. The second was a preliminary modelling of a somewhat simplified and idealised strength-dominated breakup with the intention of calculating the force applied to the upstream end of the ice cover.

The two ice cover chang associated with breakup are an increase in roughness of the ice cover as it is broken, and a removal of the ice cover as it ceases to affect the hydraulics either because it is no longer present or because it is travelling at the flow velocity. The results presented in this part of the study were dimensionless plots showing profiles of depth, discharge, and shear stress applied to the ice cover for a given set of conditions. These results provide insight into the nature of the unsteady flow that results from these changes in ice cover.

The modelling of a strength-dominated breakup was achieved by combining both of these changes, with the removal of ice cover following the ice cover roughness increase at a fixed distance. The shear stress applied to the pack of rough ice was integrated over the length of the pack to calculate the increase in force applied to the solid ice cover at the breaking front. It is presumed that this force is an important factor in the sustenance of a strength-dominated breakup. The effect of certain dimensionless parameters on this increase in force is presented in the form of dimensionless plots. For a significant increase in force to result, the velocity of the breaking front must be small compared to the flow velocity, and the increase in roughness of the broken ice of the pack must be significant. The major simplifications used in this model were that the shear stress-pack thickness relationship was not considered, and the velocity of the two fronts which make up the model were equal, not allowing a variation in the length of the pack. Despite these simplifications, the analysis confirmed that it is indeed feasible for a strength-dominated breakup to be sustained by the unsteady flow generated by motion of the breakup front.

LIST OF REFERENCES

Amein, M., 1968, ' An implicit method for natural flood routing ', Water Resources Research, Vol.4, No.4, pp. 719-726.

Beltaos, S., and Krishnappan, B.G., 1982, ' Surges from ice jam releases ; a case study ', Can. J. Civ. Eng., Vol.9, pp. 276-284.

Beltaos, S., 1984, ' A conceptual model of river ice breakup ', Can. J. Civ. Eng., Vol.11, pp. 516-529.

Beltaos, S., 1988, ' Configuration and properties of a breakup jam ', Can. J. Civ. Eng., Vol.15, pp. 685-697.

Billfalk, L., 1982, ' Breakup of solid ice covers due to rapid water level variations ', CRREL Report 82-3, U.S. Army Cold Regions Research and Engineering Laboratory, Hanover, NH.

Chaudry, Y.M., and Contractor, D.N., 1973, ' Application of the implicit method to surges in open channels ', Water Resources Research, Vol.9, No.6, pp. 1605-1612.

Daly, S.F., and Ashton, G.D., 1983, ' Using the DWOPER routing model to simulate river flows with ice ', CRREL Special Report 83-1, U.S. Army Cold Regions Research and Engineering Laboratory, Hanover, NH.

Doyle, P.F., and Andres, D.D., 1979, ' Spring breakup and ice jamming on the Athabasca River near Fort McMurray ', Report SWE-79-05, Transportation and Surface Water Engineering Division, Alberta Research Council, Edmonton.

Ferrick, M.G., 1985, ' Analysis of river wave types ', CRREL Report 85-12, U.S. Army Cold Regions Research and Engineering Laboratory, Hanover, NH.

Ferrick, M., Lemieux, G., Mulherin, N., Demont, W., 1986, ' Controlled river ice breakup ', Proceedings of the IAHR Symposium on Ice 1986, Iowa City, Iowa.

Ferrick, M.G., Lemieux, G.E., Weyrick, P.B., and Demont, W., 1988,' Options for management of dynamic ice breakup on the Connecticut River near Windsor, Vermont ', CRREL U.S. Army Cold Regions Research and Engineering Laboratory, Hanover, NH.

Ferrick, M.G., and Mulherin, N.D., 1989, ' Framework for control of dynamic ice breakup by river regulation ', CRREL Report 89-12, U.S. Army Cold Regions Research and Engineering Laboratory, Hanover, NH.

Fread, D.L., 1984, ' DAMBRK : the NWS dam-break flood forecasting model ', Office of Hydrology, National Weather Service (NWS), Silver Spring, Maryland.

Gerard, R., and Andres, D., 1982, ' Hydraulic roughness of freeze-up ice accumulations: North Saskatchewan River through Edmonton ', Proceedings, Workshop on the Hydraulics of Ice-covered Rivers, National Research Council of Canada, Edmonton, Alberta, pp. 62-87.

Gerard, R., Kent, T.D., Janowicz, R., and Lyons, R.D., 1984, ' Ice regime reconnaissance, Yukon River, Yukon ', Proceedings, Cold Regions Specialty Conference, Canadian Society for Civil Engineering, Edmonton, Alberta, pp. 1059-1073.

Gerard, R., and Flato, G., 1988, ' Some thoughts on break-up and ice jams ', Proceedings of the 5th Workshop on Hydraulics of River Ice / Ice Jams ', Winnipeg, Manitoba, pp. 225-236.

Gerard, R., and Stanley, S., 1988, ' Ice jams and flood forecasting, Hay River, N.W.T. ', Water Resource Engineering Report 88-6, Department of Civil Engineering, University of Alberta, Edmonton.

Henderson, F.M., and Gerard, R., 1981, ' Flood waves caused by ice jam formation and failure ', Proceedings of the IAHR Symposium on Ice, Quebec City, Quebec, pp. 209-219.

Joliffe, I., 1982, ' Comparison of implicit finite difference methods to solve the unsteady open channel flow equations ', Report WRE 82-1, Water Resources Engineering Group, Department of Civil Engineering, University of Alberta, Edmonton.

Joliffe, I., and Gerard, R., 1982, ' Surges released by ice jams ', Proceedings, Workshop on the Hydraulics of Ice-covered Rivers, National Research Council of Canada, Edmonton, Alberta, pp. 253-259.

Kabir,N., and Orsborn, J.F., 1984, 'Numerical flood routing for natural channels ', Proceedings of the Conference, Water for Resource Development, Hydraulic Division of ASCE, Coeur d'Alene, Idaho, pp. 148-152.

Liland, D.M., 1971, ' Surges in ice covered channels ', M.Sc. thesis presented to the Department of Civil Engineering, University of Alberta, Edmonton.

Malcovish, C.D., Andres, D.D., and Mostert, P., 1988, ' Observations of breakup on the Athabasca River near Fort McMurray, 1986 and 1987 ', Report No. SWE-88/12, Resource Technologies Department, Alberta Research Council, Edmonton.

Parkinson, F.E., 1982, ' Water temperature observations during breakup on the Liard-Mackenzie River system ', Proceedings, Workshop on the Hydraulics of Ice-covered Rivers, National Research Council of Canada, Edmonton, Alberta, pp. 261-295.

Parkinson, F.E., and Holder, G.K., 1988, ' Ice jam development, release, and surge wave propagation, Mackenzie River at Norman Wells ', Proceedings of the 5th Workshop on Hydraulics of River Ice / Ice Jams, Winnipeg, Manitoba, pp. 209-218.

Prowse, T.D., 1986, ' Ice jam characteristics, Liard-Mackenzie rivers confluence ', Can. J. Civ, Eng., Vol. 13, pp. 653-665.

Prowse, T.D., Anderson, J.C., and Smith, R.L., 1986, ' Discharge measurement during river ice breakup ', Proceedings of the 43rd Eastern Snow Conference, Hanover, NH., pp. 55-69.

Sanderson, T.J.O., 1988, Ice mechanics: risks to offshore structures, Graham and Trotman, Boston, p. 253.

Shulyakovskii, L.G. (editor), 1963, Manual of forecasting ice-formation for rivers and inland lakes, Translated from Russian, Israel Program for Scientific Translations, Jerusalem, 1966.

Wong, J., Beltaos, S., and Krishnappan, B.G., 1985, ' Laboratory tests on surges created by ice jam releases ', Can. J. Civ. Eng., Vol. 12, pp. 930-933.

Zienkiewicz, O.C., 1977, The Finite Element Method, 3rd Ed., Mcgraw-Hill (UK), London, p. 787.

APPENDIX A: DETAILS OF COMPUTER PROGRAM

A.1 Numerical Solution Technique

As mentioned in chapter 2, applying the finite difference scheme to the governing equations yields a set of 2N non-linear algebraic equations, where N is the number of nodes in the reach. These equations are of the form :

$$
\begin{array}{ll}
U\ (Y_1, V_1) & = -r_1 \\
C_1\ (Y_1, V_1, Y_2, V_2) & = -r_2 \\
M_1\ (Y_1, V_1, Y_2, V_2) & = -r_3 \\
\cdot & \\
\cdot & \\
\cdot & \\
C_i\ (Y_i, V_i, Y_{i+1}, V_{i+1}) & = -r_{2i} \\
M_i\ (Y_i, V_i, Y_{i+1}, V_{i+1}) & = -r_{2i+1} \\
\cdot & \\
\cdot & \\
\cdot & \\
D\ (Y_N, V_N) & = -r_{2N}
\end{array}
$$

where U and D represent the upstream and downstream boundary conditions, C is the continuity equation, M is the momentum equation, and R is the residual calculated when the trial values of the depth Y and velocity V are substituted into these equations.

Using the Newton Raphson solution procedure, these equations become :

$$\frac{\partial U}{\partial Y_1} dY_1 + \frac{\partial U}{\partial V_1} dV_1 = -R_1$$

.

.

.

$$\frac{\partial C_i}{\partial Y_i} dY_i + \frac{\partial C_i}{\partial V_i} dV_i + \frac{\partial C_i}{\partial Y_{i+1}} dY_{i+1} + \frac{\partial C_i}{\partial V_{i+1}} dV_{i+1} = -R_{2i}$$

$$\frac{\partial M_i}{\partial Y_i} dY_i + \frac{\partial M_i}{\partial V_i} dV_i + \frac{\partial M_i}{\partial Y_{i+1}} dY_{i+1} + \frac{\partial M_i}{\partial V_{i+1}} dV_{i+1} = -R_{2i+1}$$

.

.

.

$$\frac{\partial D}{\partial Y_N} dY_N + \frac{\partial D}{\partial V_N} dV_N = -R_{2N}$$

These derivatives and residuals are calculated as described in chapter 2, and stored in a banded matrix and the corrections dY_i and dV_i are solved for. The new trial values for depth and velocity are calculated by :

$$Y_i^n = Y_i^o + dY_i \text{ and}$$

$$V_i^n = V_i^o + dV_i$$

where the superscript n denotes the new trial value and the superscript o denotes the previous trial value. This procedure is repeated until a specified tolerance is met by all equations.

A.2 Program Structure

The program consists of the main program and 8 subroutines. The main program reads the input data, performs some preliminary calculations, calculates the matrix to be solved at each iteration, and stores hydrographs and maximum values.

The subroutines are :

DERIV - calculates the derivatives $\frac{\partial A}{\partial Y}$, $\frac{\partial B}{\partial Y}$, and $\frac{\partial R}{\partial Y}$ for a given section and depth.

PROP - calculates area A, hydraulic radius R, and topwidth B for a given section and depth.

INIT - calculates uniform flow profile for use as initial conditions based on channel data and boundary conditions using the standard step gradually varied flow algorithm.

UACTL - solves matrix for corrections in depth Y, and velocity V at each iteration of each time step (Zienkiewicz, 1977).

ROUGH - calculates composite roughness of an ice covered channel. The current combined roughness equation used in the model assumes that $\frac{R}{k}$ is in the range such that $C_* \alpha (\frac{R}{k})^{(1/4)}$.

OUTPUT - writes profiles to output file at specified times.

MAXPUT - writes maximum conditions calculated for each section to the output file at the end of the simulation.

HYDPUT - writes the stored hydrographs to the output file at the end of the simulation.

A.3 Data Requirements

The first line of the input data file consists of 7 integer variables which define the size of certain arrays used in the program. These variables are :

NXS - Number of cross sections

NIO - Number of points in upstream boundary condition table

NOO - Number of points in downstream boundary condition table

MAXIT - Total number of time increments

NTP - Number of profile printouts

NHYD - Number of hydrographs to be printed

NHT - Number of time increments between hydrograph points

The second line is made up of 6 integers which control certain options available in the program. These are :

NUBC - Integer to control upstream boundary condition option

NUBC = 1 - inflow discharge hydrograph

NUBC = 2 - inflow depth hydrograph

NDBC - Integer to control downstream boundary condition option

NDBC = 1 - channel control

NDBC = 2 - critical flow

NDBC = 3 - given depth table

NDBC = 4 - given discharge table

NDBG - Integer to control output to screen

NDBG = 0 - no output

NDBG = 1 - output time, discharge, and iteration #

NRF - Integer to control type of roughness
NRF = 1 - roughness height (m)
NRF = 2 - Manning roughness coefficient

NTXS - Integer to control type of cross section
NTXS = 1 - irregular cross section
NTXS = 2 - trapezoidal cross section

NINIT - Integer to control ini[illegible] profile calculations
NINIT = 0 - initial profile calculated from input
NINIT = 1 - steady flow computations performed

The third line has 6 real constants. These are :

DT - Time increment (hours)

SOD - Downstream slope used in initial profile computations

TH - Weighting factor in finite difference algorithm

G - Acceleration due to gravity, which is also used to select the system of units
$G < 30$ - metric
$G > 30$ - imperial

DER - Range used to calculate derivatives

TOL - Tolerance for convergence criteria

The next NIO lines define a table of input values for the upstream boundary condition. This table can be either discharge or depth versus time, depending on the NUBC parameter. Each line consists of a value VLI(I) (discharge or depth) and the associated time TI(I). The program will linearly interpolate between the points in this table.

The next NOO lines define a table of values for the downstream boundary condition. This is used when NDBC = 3 or 4. The depth or discharge value is read into the array VLO and the associated time is read into the array TO.

The next NTP lines are read into the TP array and define the times at which profiles will be written to the output file.

The next NHYD lines are read into the NH array which defines at which sections hydrographs will be stored. The section is identified by an integer indicating its position in the reach (i.e. 1 for the first section in the data file, 2 for the second, etc.).

The remainder of the input file defines the channel geometry and initial conditions. This data can be read in two ways, depending on the NTXS variable.

If NTXS =1, data is read in for an irregular channel. Each section requires one line to describe the section plus a table of cross section data points. The first line consists of :

XX - Longitudinal distance of cross section

YO - initial depth of flow
Q1 - initial discharge
TCK - ice thickness
RKB - bed roughness or roughness coefficient
RKI - ice roughness or roughness coefficient
NPTS - number of points in cross section table

The table of cross section data points consists of NPTS(I) lines. Each line has the variables :

X(I,J) - Horizontal distance from left bank
EL(I,J) - Elevation of point
where I is the cross section number and J is the point number.

If NTXS = 2, the channel is regular, having a constant trapezoidal shape and constant slope. The first line of the cross section data will contain :

B - Channel bottom width
RM - Side slope ratio (horiz./vert.)
BEL - Elevation of thalweg at upstream section
SC - Slope of channel

This is followed by NXS lines containing :

XX - Longitudinal distance of cross section

YO - initial depth of flow

Q1 - initial discharge

TCK - ice thickness

RKB - bed roughness or roughness coefficient

RKI - ice roughness or roughness coefficient

A.4 Running the Program

To run the program, type :

```
PROG  datafile echofile outfile
```

where PROG is the name of the program, datafile is the input data file, echofile is the name of an output file which echoes some of the input parameters, and outfile is the name of the output file where the results are written. The following are examples of these files for the hydrograph routing analysis.

DATAFILE

```
51,4,0,40,1,1,1,
1,1,1,2,2,1,
.05,0.,.6,9.806,.001,.001,
600.,0.,
4200.,.5,
600.,1.,
600.,50.,
1.,
13,
400.,0.,500.,.0007,
0.,1.379,600.,0.,.03,.03,
500.,1.379,600.,0.,.03,.03,
1000.,1.379,600.,0.,.03,.03,
1500.,1.379,600.,0.,.03,.03,
2000.,1.379,600.,0.,.03,.03,
2500.,1.379,600.,0.,.03,.03,
3000.,1.379,600.,0.,.03,.03,
3500.,1.379,600.,0.,.03,.03,
4000.,1.379,600.,0.,.03,.03,
4500.,1.379,600.,0.,.03,.03,
5000.,1.379,600.,0.,.03,.03,
5500.,1.379,600.,0.,.03,.03,
6000.,1.379,600.,0.,.03,.03,
6500.,1.379,600.,0.,.03,.03,
7000.,1.379,600.,0.,.03,.03,
7500.,1.379,600.,0.,.03,.03,
8000.,1.379,600.,0.,.03,.03,
8500.,1.379,600.,0.,.03,.03,
9000.,1.379,600.,0.,.03,.03,
9500.,1.379,600.,0.,.03,.03,
10000.,1.379,600.,0.,.03,.03,
10500.,1.379,600.,0.,.03,.03,
11000.,1.379,600.,0.,.03,.03,
11500.,1.379,600.,0.,.03,.03,
12000.,1.379,600.,0.,.03,.03,
12500.,1.379,600.,0.,.03,.03,
13000.,1.379,600.,0.,.03,.03,
13500.,1.379,600.,0.,.03,.03,
14000.,1.379,600.,0.,.03,.03,
14500.,1.379,600.,0.,.03,.03,
15000.,1.379,600.,0.,.03,.03,
15500.,1.379,600.,0.,.03,.03,
16000.,1.379,600.,0.,.03,.03,
16500.,1.379,600.,0.,.03,.03,
17000.,1.379,600.,0.,.03,.03,
17500.,1.379,600.,0.,.03,.03,
18000.,1.379,600.,0.,.03,.03,
18500.,1.379,600.,0.,.03,.03,
19000.,1.379,600.,0.,.03,.03,
19500.,1.379,600.,0.,.03,.03,
20000.,1.379,600.,0.,.03,.03,
20500.,1.379,600.,0.,.03,.03,
21000.,1.379,600.,0.,.03,.03,
21500.,1.379,600.,0.,.03,.03,
22000.,1.379,600.,0.,.03,.03,
22500.,1.379,600.,0.,.03,.03,
23000.,1.379,600.,0.,.03,.03,
23500.,1.379,600.,0.,.03,.03,
24000.,1.379,600.,0.,.03,.03,
24500.,1.379,600.,0.,.03,.03,
25000.,1.379,600.,0.,.03,.03,
```

ECHOFILE

```
      NXS    =              51
      NIO    =               4
      NOO    =               0
      MAXIT  =              40
      NTP    =               1
      NHYD   =               1
      NHT    =               1

      NUBC   =               1
      NDBC   =               1
      NDBG   =               1
      NRF    =               2
      NTXS   =               2
      NINIT  =               1

      DT    =       .0500
      SOD   =   .0000000
      TH    =     .60000
      G     =    9.80600
      DER   =     .00100
      TOL   =     .00100

 I    =     1    VLI(I) =    600.000     TI(I) =        .000

 I    =     2    VLI(I) =   4200.000     TI(I) =        .500

 I    =     3    VLI(I) =    600.000     TI(I) =       1.000

 I    =     4    VLI(I) =    600.000     TI(I) =      50.000
```

OUTFILE

```
     AFTER        .000 HOURS, CONDITIONS ARE :

DISTANCE WAT.SURF THALWEG    DEPTH     VELOCITY  DISCHARGE  FRIC. SLOPE

    0.    501.379   500.000    1.379      1.088      600.0     .00070000
  500.    501.029   499.650    1.379      1.088      600.0     .00070000
 1000.    500.679   499.300    1.379      1.088      600.0     .00070000
 1500.    500.329   498.950    1.379      1.088      600.0     .00070000
 2000.    499.979   498.600    1.379      1.088      600.0     .00070000
 2500.    499.629   498.250    1.379      1.088      600.0     .00070000
 3000.    499.279   497.900    1.379      1.088      600.0     .00070000
 3500.    498.929   497.550    1.379      1.088      600.0     .00070000
 4000.    498.579   497.200    1.379      1.088      600.0     .00070000
 4500.    498.229   496.850    1.379      1.088      600.0     .00070000
 5000.    497.879   496.500    1.379      1.088      600.0     .00070000
 5500.    497.529   496.150    1.379      1.088      600.0     .00070000
 6000.    497.179   495.800    1.379      1.088      600.0     .00070000
 6500.    496.829   495.450    1.379      1.088      600.0     .00070000
 7000.    496.479   495.100    1.379      1.088      600.0     .00070000
 7500.    496.129   494.750    1.379      1.088      600.0     .00070000
 8000.    495.779   494.400    1.379      1.088      600.0     .00070000
 8500.    495.429   494.050    1.379      1.088      600.0     .00070000
 9000.    495.079   493.700    1.379      1.088      600.0     .00070000
 9500.    494.729   493.350    1.379      1.088      600.0     .00070000
10000.    494.379   493.000    1.379      1.088      600.0     .00070000
10500.    494.029   492.650    1.379      1.088      600.0     .00070000
11000.    493.679   492.300    1.379      1.088      600.0     .00070000
11500.    493.329   491.950    1.379      1.088      600.0     .00070000
12000.    492.979   491.600    1.379      1.088      600.0     .00070000
12500.    492.629   491.250    1.379      1.088      600.0     .00070000
13000.    492.279   490.900    1.379      1.088      600.0     .00070000
13500.    491.929   490.550    1.379      1.088      600.0     .00070000
14000.    491.579   490.200    1.379      1.088      600.0     .00070000
14500.    491.229   489.850    1.379      1.088      600.0     .00070000
15000.    490.879   489.500    1.379      1.088      600.0     .00070000
15500.    490.529   489.150    1.379      1.088      600.0     .00070000
16000.    490.179   488.800    1.379      1.088      600.0     .00070000
16500.    489.829   488.450    1.379      1.088      600.0     .00070000
17000.    489.479   488.100    1.379      1.088      600.0     .00070000
17500.    489.129   487.750    1.379      1.088      600.0     .00070000
18000.    488.779   487.400    1.379      1.088      600.0     .00070000
18500.    488.429   487.050    1.379      1.088      600.0     .00070000
19000.    488.079   486.700    1.379      1.088      600.0     .00070000
19500.    487.729   486.350    1.379      1.088      600.0     .00070000
20000.    487.379   486.000    1.379      1.088      600.0     .00070000
20500.    487.029   485.650    1.379      1.088      600.0     .00070000
21000.    486.679   485.300    1.379      1.088      600.0     .00070000
21500.    486.329   484.950    1.379      1.088      600.0     .00070000
22000.    485.979   484.600    1.379      1.088      600.0     .00070000
22500.    485.629   484.250    1.379      1.088      600.0     .00070000
23000.    485.279   483.900    1.379      1.088      600.0     .00070000
23500.    484.929   483.550    1.379      1.088      600.0     .00070000
24000.    484.579   483.200    1.379      1.088      600.0     .00070001
24500.    484.229   482.850    1.379      1.088      600.0     .00070000
25000.    483.879   482.500    1.379      1.088      599.9     .00070000
```

```
     AFTER      1.000 HOURS, CONDITIONS ARE :

DISTANCE WAT.SURF THALWEG    DEPTH    VELOCITY  DISCHARGE  FRIC. SLOPE

    0.     502.072   500.000     2.072      .724     600.0     .00018111
  500.     502.001   499.650     2.351     1.004     944.3     .00029488
 1000.     501.866   499.300     2.566     1.202    1233.8     .00037653
 1500.     501.688   498.950     2.738     1.355    1484.1     .00043951
 2000.     501.477   498.600     2.877     1.481    1703.8     .00049150
 2500.     501.239   498.250     2.989     1.586    1895.7     .00053614
 3000.     500.978   497.900     3.078     1.677    2064.7     .00057682
 3500.     500.697   497.550     3.147     1.756    2210.7     .00061477
 4000.     500.396   497.200     3.196     1.826    2333.4     .00065086
 4500.     500.076   496.850     3.226     1.886    2433.5     .00068622
 5000.     499.738   496.500     3.238     1.939    2510.9     .00072173
 5500.     499.381   496.150     3.231     1.984    2564.7     .00075798
 6000.     499.006   495.800     3.206     2.022    2592.7     .00079523
 6500.     498.610   495.450     3.160     2.051    2592.9     .00083374
 7000.     498.194   495.100     3.094     2.071    2563.2     .00087376
 7500.     497.757   494.750     3.007     2.080    2501.8     .00091551
 8000.     497.296   494.400     2.896     2.077    2406.7     .00095890
 8500.     496.812   494.050     2.762     2.060    2275.7     .00100308
 9000.     496.304   493.700     2.604     2.023    2106.7     .00104554
 9500.     495.772   493.350     2.422     1.961    1899.4     .00108098
10000.     495.220   493.000     2.220     1.867    1658.3     .00109979
10500.     494.658   492.650     2.008     1.737    1395.5     .00108692
11000.     494.104   492.300     1.804     1.574    1135.9     .00102826
11500.     493.583   491.950     1.633     1.404     917.5     .00093317
12000.     493.114   491.600     1.514     1.266     767.0     .00083827
12500.     492.695   491.250     1.445     1.177     680.4     .00077132
13000.     492.309   490.900     1.409     1.130     636.6     .00073369
13500.     491.942   490.550     1.392     1.106     616.1     .00071513
14000.     491.585   490.200     1.385     1.096     606.9     .00070659
14500.     491.231   489.850     1.381     1.091     602.9     .00070281
15000.     490.880   489.500     1.380     1.089     601.2     .00070118
15500.     490.529   489.150     1.379     1.088     600.5     .00070049
16000.     490.179   488.800     1.379     1.088     600.2     .00070020
16500.     489.829   488.450     1.379     1.088     600.1     .00070008
17000.     489.479   488.100     1.379     1.088     600.0     .00070003
17500.     489.129   487.750     1.379     1.088     600.0     .00070001
18000.     488.779   487.400     1.379     1.088     600.0     .00070000
18500.     488.429   487.050     1.379     1.088     600.0     .00070000
19000.     488.079   486.700     1.379     1.088     600.0     .00070000
19500.     487.729   486.350     1.379     1.088     600.0     .00070000
20000.     487.379   486.000     1.379     1.088     600.0     .00070000
20500.     487.029   485.650     1.379     1.088     600.0     .00070000
21000.     486.679   485.300     1.379     1.088     600.0     .00070000
21500.     486.329   484.950     1.379     1.088     600.0     .00070000
22000.     485.979   484.600     1.379     1.088     600.0     .00070000
22500.     485.629   484.250     1.379     1.088     600.0     .00070000
23000.     485.279   483.900     1.379     1.088     600.0     .00070000
23500.     484.929   483.550     1.379     1.088     600.0     .00070000
24000.     484.579   483.200     1.379     1.088     600.0     .00070000
24500.     484.229   482.850     1.379     1.088     600.0     .00070000
25000.     483.879   482.500     1.379     1.088     600.0     .00070000
```

```
***** HYDROGRAPHS *****


HYDROGRAPH AT STATION    13  DISTANCE =      6000.

      TIME            DEPTH        DISCHARGE

      .000            1.379            600.0
      .050            1.379            600.0
      .100            1.379            600.0
      .150            1.379            600.0
      .200            1.379            600.0
      .250            1.379            600.1
      .300            1.380            600.8
      .350            1.382            604.1
      .400            1.392            616.6
      .450            1.422            654.8
      .500            1.499            751.8
      .550            1.653            949.3
      .600            1.893           1264.1
      .650            2.190           1663.8
      .700            2.499           2079.1
      .750            2.769           2421.6
      .800            2.970           2630.3
      .850            3.098           2714.0
      .900            3.173           2720.1
      .950            3.206           2676.5
     1.000            3.206           2592.7
     1.050            3.177           2480.2
     1.100            3.128           2350.3
     1.150            3.061           2209.4
     1.200            2.981           2063.9
     1.250            2.892           1921.6
     1.300            2.800           1789.7
     1.350            2.710           1672.8
     1.400            2.623           1571.2
     1.450            2.540           1481.1
     1.500            2.460           1399.1
     1.550            2.383           1324.0
     1.600            2.310           1256.1
     1.650            2.241           1194.4
     1.700            2.175           1138.0
     1.750            2.113           1086.6
     1.800            2.055           1039.6
     1.850            1.999            996.7
     1.900            1.947            957.5
     1.950            1.899            921.7
     2.000            1.853            889.1
```

```
***** MAXIMUM CONDITIONS *****

  DISTANCE       TIME       DEPTH   VELOCITY  DISCHARGE FRICTION SLOPE

        0.       .500       3.984      2.635     4200.0        .00117032
      500.       .550       3.916      2.585     3941.9        .00116357
     1000.       .600       3.822      2.534     3858.7        .00116065
     1500.       .600       3.753      2.516     3681.2        .00115978
     2000.       .650       3.679      2.474     3584.4        .00116009
     2500.       .700       3.605      2.449     3427.8        .00116122
     3000.       .700       3.538      2.411     3334.5        .00116301
     3500.       .750       3.478      2.383     3210.4        .00116530
     4000.       .800       3.420      2.343     3096.1        .00116724
     4500.       .850       3.364      2.316     2999.8        .00116738
     5000.       .900       3.310      2.277     2900.3        .00117204
     5500.       .950       3.257      2.246     2806.5        .00117295
     6000.       .950       3.206      2.214     2720.1        .00116791
     6500.      1.000       3.160      2.178     2639.7        .00116335
     7000.      1.050       3.115      2.145     2569.2        .00116213
     7500.      1.100       3.072      2.117     2501.8        .00115411
     8000.      1.150       3.029      2.088     2437.2        .00114007
     8500.      1.200       2.989      2.060     2375.2        .00113462
     9000.      1.250       2.950      2.032     2315.8        .00112712
     9500.      1.300       2.913      2.006     2259.5        .00111491
    10000.      1.350       2.878      1.981     2206.1        .00109979
    10500.      1.400       2.844      1.957     2155.7        .00108692
    11000.      1.450       2.812      1.934     2108.3        .00107891
    11500.      1.500       2.782      1.913     2063.6        .00106841
    12000.      1.550       2.753      1.893     2021.6        .00105661
    12500.      1.600       2.726      1.873     1982.0        .00104437
    13000.      1.650       2.700      1.854     1945.0        .00103219
    13500.      1.700       2.675      1.836     1910.1        .00102036
    14000.      1.800       2.652      1.819     1877.2        .00100988
    14500.      1.850       2.631      1.802     1846.3        .00100153
    15000.      1.900       2.610      1.786     1817.0        .00099302
    15500.      1.950       2.591      1.772     1789.7        .00098453
    16000.      2.000       2.572      1.758     1765.0        .00097673
    16500.      2.000       2.547      1.745     1741.5        .00096855
    17000.      2.000       2.514      1.733     1719.0        .00096063
    17500.      2.000       2.470      1.721     1690.8        .00095300
    18000.      2.000       2.417      1.709     1650.7        .00094566
    18500.      2.000       2.352      1.698     1597.9        .00093864
    19000.      2.000       2.277      1.682     1531.8        .00093193
    19500.      2.000       2.190      1.657     1452.3        .00092554
    20000.      2.000       2.094      1.623     1360.0        .00091944
    20500.      2.000       1.991      1.578     1256.6        .00091363
    21000.      2.000       1.882      1.521     1145.6        .00090809
    21500.      2.000       1.774      1.455     1032.3        .00089739
    22000.      2.000       1.672      1.381      923.6        .00087412
    22500.      2.000       1.584      1.306      827.4        .00084070
    23000.      2.000       1.513      1.239      749.5        .00080332
    23500.      2.000       1.461      1.185      692.3        .00076918
    24000.      2.000       1.427      1.146      653.9        .00074284
    24500.      2.000       1.406      1.120      629.9        .00072337
    25000.      2.000       1.403      1.092      612.7        .00070000
```

A.5 Program Listing

The following is a listing of the computer program developed to solve unsteady flow. It has been compiled using Microsoft Fortran version 4.0 on an IBM XT compatible personal computer. The adaptation made for chapter 5 has not been included. These adaptations involved changing the ice roughness and thickness at one section at each time step. The new values of ice roughness and thickness and the first section to be changed are added to the datafile. At each subsequent time step, the next downstream section is given the new values.

```
C
C
C
C     ************************************************************
C     *                                                          *
C     *                                                          *
C     *            PROGRAM TO SOLVE UNSTEADY FLOW                *
C     *                                                          *
C     *             (D. Williamson, June 1989)                   *
C     *                                                          *
C     *                                                          *
C     ************************************************************
C
C
C
C
C
C
C
C     ------------------------------------------------------------
C
C
C       DIMENSION ARRAYS
C
C
C     ------------------------------------------------------------
C
C
      IMPLICIT REAL*8(A-H,L,O-Z)
C
C
      DIMENSION VLI(50),TI(50),RKB(200),THALW(200),VLO(50),TO(50)
      INTEGER J(1000),NPTS(200),NH(10)
      DIMENSION YN(200),VN(200),YO(200),VO(200),SF(200),Q1(200)
      DIMENSION U(1000),L(1000),RES(500),TP(50),RKI(200),TCK(200)
      DIMENSION X(200,20),EL(200,20),SO(200),AR(200),XX(200)
      DIMENSION VM(200),YM(200),QM(200),TM(200),SFM(200)
      DIMENSION TIM(300),QH(10,300),YH(10,300)
      COMMON/ONE/NPTS,X,EL
      COMMON/TWO/THALW,AR,XX,TCK
      COMMON/THREE/YN,VN,SF,NXS
      COMMON/FOUR/RKB,RKI
      COMMON/FIVE/DER,NRF,NTXS,G,RMN
      COMMON/SIX/BW,RM
C
C     VLI      = INFLOW HYDROGRAPH ORDINATE
C     VLO      = OUTFLOW HYDROGRAPH ORDINATE
C     TI       = TIME ASSOCIATED WITH EACH INFLOW ORDINATE
C     TO       = TIME ASSOCIATED WITH EACH OUTFLOW ORDINATE
C     YN       = DEPTH OF WATER FLOW
C     VN       = AVERAGE VELOCITY OF WATER FLOW
C     YO       = DEPTH OF WATER FLOW AT LAST TIME STEP
C     VO       = AVERAGE VELOCITY OF WATER FLOW AT LAST TIME STEP
C     SF       = FRICTION SLOPE
```

```
C     YM       = MAXIMUM DEPTH CALCULATED
C     VM       = MAXIMUM VELOCITY CALCULATED
C     QM       = MAXIMUM DISCHARGE CALCULATED
C     TM       = TIME TO MAXIMUM DEPTH
C     TIM      = TIME
C     QH       = MATRIX CONTAINING DISCHARGE HYDROGRAPH DATA
C     YH       = MATRIX CONTAINING DEPTH HYDROGRAPH DATA
C     J        = MATRIX POINTER
C     U        = MATRIX VALUES BELOW DIAGONAL
C     L        = MATRIX VALUES ABOVE DIAGONAL
C     RES      = MATRIX SOLUTION VECTOR
C     TP       = TIMES AT WHICH PROFILES ARE PRINTED
C     NH       = STATIONS AT WHICH HYDROGRAPHS ARE PRINTED
C     X        = LATERAL CROSS SECTION VALUES
C     EL       = VERTICAL CROSS SECTION VALUES
C     SO       = BED SLOPE ARRAY
C     AR       = CROSS SECTION AREA ARRAY
C     XX       = LONGITUDINAL DISTANCE ARRAY
C     TCK      = ICE THICKNESS
C     RKB      = ROUGHNESS OF BOTTOM OF ICE
C     RKI      = ROUGHNESS OF CHANNEL BED
C     THALW    = THALWEG PROFILE
C     NPTS     = POINTS AT A CROSS SECTION
C
C
C
C     ----------------------------------------------------
C
C
C        INPUT
C
C
C     ----------------------------------------------------
C
C
      READ(4,*)NXS,NIO,NOO,MAXIT,NTP,NHYD,NHT
      WRITE(8,8000)NXS,NIO,NOO,MAXIT,NTP,NHYD,NHT
 8000 FORMAT(//5X,'NXS   =    ',I10/5X,'NIO   =    ',I10/5X,
     *'NOO   =    ',I10/5X,'MAXIT =    ',I10/5X,
     *'NTP   =    ',I10/5X,'NHYD  =    ',I10/5X,'NHT   =    ',I10/)
C
C     NXS      = NUMBER OF CROSS SECTIONS
C     NIO      = NUMBER OF INFLOW ORDINATES
C     NOO      = NUMBER OF OUTFLOW ORDINATES
C     MAXIT    = TOTAL NUMBER OF TIME INCREMENTS
C     NTP      = NUMBER OF PRINTOUTS
C     NHYD     = NUMBER OF OUTPUT HYDROGRAPHS
C     NHT      = NUMBER OF TIME INCREMENTS BETWEEN HYDROGRAPH POINTS
C
C
C
      READ(4,*)NUBC,NDBC,NDBG,NRF,NTXS,NINIT
      WRITE(8,8001)NUBC,NDBC,NDBG,NRF,NTXS,NINIT
 8001 FORMAT(/5X,'NUBC   =    ',I10/5X,'NDBC   =    ',I10/5X,
     *'NDBG  =   ',I10/5X,'NRF   =   ',I10/5X,
     *'NTXS  =   ',I10/5X,'NINIT =   ',I10/)
C
C      NUBC      = INTEGER TO CONTROL U/S BOUNDARY CONDITION
C           NBC=1 ... INFLOW HYDROGRAPH - DISCHARGE
C           NBC=2 ... INFLOW HYDROGRAPH - DEPTH
C      NDBC      = INTEGER TO CONTROL D/S BOUNDARY CONDITION
C           NBC=1 ... UNIFORM FLOW
C           NBC=2 ... CRITICAL FLOW
C           NBC=3 ... FIXED ELEVATION
C           NBC=4 ... KNOWN HYDROGRAPH
C      NDBG      = INTEGER TO CONTROL OUTPUT TO SCREEN
C           NDBG=0 ... NO OUTPUT
C           NDBG=1 ... OUTPUT TIME, DISCHARGE, AND ITERATION #
C      NRF       = INTEGER TO CONTROL TYPE OF ROUGHNESS COMPUTATION
C           NRF=1 ... ROUGHNESS HEIGHT IN METRES
C           NRF=2 ... MANNING ROUGHNESS COEFFICIENT
C      NTXS      = INTEGER TO CONTROL TYPE OF CROSS SECTION
C           NTXS=1 ... IRREGULAR CROSS SECTION
C           NTXS=2 ... TRAPEZOIDAL CROSS SECTION
C      NINIT     = INTEGER TO CONTROL INITIAL PROFILE CALCULATIONS
C           NINIT=O ... INITIAL PROFILE CALCULATED FROM INPUT
C           NINIT=1 ... STEADY FLOW COMPUTATIONS PERFORMED
C                       (NOT TO BE USED WHEN NBC = 4)
C
C
      READ(4,*)DT,SOD,TH,G,DER,TOL
      WRITE(8,8002)DT,SOD,TH,G,DER,TOL
 8002 FORMAT(/5X,'DT    =   ',F10.4/5X,'SOD  =   ',F10.7/5X,'TH    =  '
     *,F10.5/5X,'G     =   ',F10.5/5X,'DER  =   ',F10.5/5X,'TOL   =  '
     *,F10.5/)
      DT=DT*3600.
      RMN=1.
      IF(G.GT.30.)RMN=1.486
C
C     DT       = TIME INCREMENT (hours)
C     SOD      = D/S SLOPE USED IN INITIAL PROFILE COMPUTATIONS
C     TH       = VALUE OF THETA TO CONTROL IMPLICIT SOLUTION
C     G        = ACCELERATION DUE TO GRAVITY (METRIC/IMPERIAL)
C     DER      = RANGE USED TO CALCULATE DERIVATIVES
C     TOL      = CONVERGENCE CRITERIA
C
C
C     READ INFLOW HYDROGRAPH
C
C
      DO 10 I=1,NIO
      READ(4,*)VLI(I),TI(I)
      WRITE(8,8003)I,VLI(I),TI(I)
 8003 FORMAT(/5X,'I    =   ',I5,5X,'VLI(I) =   ',F10.3,5X,'TI(I) =  '
     *,F10.3)
 10   CONTINUE
C
C
```

```
C     READ OUTFLOW HYDROGRAPH
C
C
      IF(NDBC.LT.3)GOTO 16
      DO 15 I=1,NOO
      READ(4,*)VLO(I),TO(I)
      WRITE(8,8004)I,VLO(I),TO(I)
 8004 FORMAT(/5X,'I    =  ',I5,5X,'VLO(I) =  ',F10.3,5X,'TO(I) =  '
     *,F10.3)
 15   CONTINUE
 16   CONTINUE
C
C
C
C     READ PRINTOUT TIMES
C
C
      IF(NTP.EQ.0)GOTO 38
      READ(4,*)(TP(I),I=1,NTP)
C
C
C     READ HYDROGRAPH OUTPUT LOCATIONS
C
C
 38   CONTINUE
      IF(NHYD.EQ.0)GOTO 39
      READ(4,*)(NH(I),I=1,NHYD)
C
C
C     READ CROSS SECTION PROPERTIES
C
C
 39   CONTINUE
      IF(NTXS.EQ.2)GOTO 41
      DO 30 I=1,NXS
      READ(4,*)XX(I),YO(I),Q1(I),TCK(I),RKB(I),RKI(I),NPTS(I)
      DO 40 I2=1,NPTS(I)
      READ(4,*)X(I,I2),EL(I,I2)
 40   CONTINUE
 30   CONTINUE
      GOTO 42
 41   CONTINUE
      READ(4,*)BW,RM,BEL,SC
      DO 43 I=1,NXS
      READ(4,*)XX(I),YO(I),Q1(I),TCK(I),RKB(I),RKI(I)
 43   CONTINUE
 42   CONTINUE
C
C
C     ------------------------------------------------------
C
C
C        PERFORM PRELIMINARY COMPUTATIONS
C
```

```
C
C     -----------------------------------------------------------
C
C
C
C
C     DETERMINE THALWEG  AND SLOPE
C
C
      NX=NXS-1
      IF(NTXS.EQ.2)GOTO 51
      DO 50 I=1,NXS
      THALW(I)=EL(I,1)
      DO 60 I2=2,NPTS(I)
      IF  (EL(I,I2).LT.THALW(I))THALW(I)=EL(I,I2)
 60   CONTINUE
 50   CONTINUE
      DO 70 I=1,NX
      SO(I)=(THALW(I)-THALW(I+1))/(XX(I+1)-XX(I))
 70   CONTINUE
      GOTO 69
 51   CONTINUE
      THALW(1)=BEL
      DO 61 I=2,NXS
      DX=XX(I)-XX(I-1)
      SO(I-1)=SC
      THALW(I)=THALW(I-1)-DX*SC
 61   CONTINUE
C
C
C     DETERMINE YO,VO
C
C
 69   CONTINUE
      IF(NINIT.EQ.1)GOTO 65
      DO 80 I=1,NXS
      Y=YO(I)
      CALL PROP(I,Y,A1,R,B)
      CALL ROUGH(I,RK)
      VO(I)=Q1(I)/A1
      AR(I)=A1
      CC=2.5*DLOG(12.*R/RK)
      SF(I)=VO(I)*VO(I)/(G*R*CC*CC)
      IF(NRF.EQ.2)SF(I)=RK*RK*VO(I)*VO(I)/R**(4./3.)/RMN/RMN
 80   CONTINUE
      GOTO 66
 65   CONTINUE
      IF(NUBC.EQ.2)STOP
      IF(NDBC.EQ.4)STOP
      CALL  INIT(NXS,VLI(1),TOL,NDBC,NDBG,SOD,YO,VO,SF)
      DO 67 I=1,NXS
      Q1(I)=VLI(1)
 67   CONTINUE
 66   CONTINUE
```

```
      DO 85 JJ=1,NHYD
      QH(JJ,1)=Q1(NH(JJ))
      YH(JJ,1)=YO(NH(JJ))
 85   CONTINUE
      IH=1
      DO 90 I=1,NXS
      YN(I)=YO(I)
      VN(I)=VO(I)
      YM(I)=YO(I)
      VM(I)=VO(I)
      QM(I)=Q1(I)
      TM(I)=0.
      SFM(I)=SF(I)
 90   CONTINUE
      TN=0.
      CALL OUTPUT(TN)
C
C
C     DETERMINE MATRIX POINTER ARRAY
C
C
      MT=MAXIT+1
      N1=1
      NN=2*NXS
      J(1)=1
      J(2)=3
      DO 45 I=3,NN
      J(I)=J(I-1)+3
 45   CONTINUE
      IF(NDBC.EQ.1)J(NN)=J(NN)+1
C
C
C     ----------------------------------------------------
C
C
C       CALCULATE MATRIX AT EACH TIME STEP
C
C
C     ----------------------------------------------------
C
C
      IF(MAXIT.EQ.0)STOP
      DO 1000 IT=1,MAXIT
      TT=IT*DT
      TN=TT/3600.
      IF(NDBG.NE.1)GOTO 71
      WRITE(6,6000)TN
 6000 FORMAT(//5X,'TIME = ',F12.3,' HOURS'/)
C
C
C     DETERMINE VALUE AT U/S NODE
C
C
 71   CONTINUE
```

```
      DO 75 I=1,NIO
      IF(TN.GT.TI(I))GOTO 75
      NT=I
      GOTO 76
 75   CONTINUE
 76   CONTINUE
      VIN=VLI(NT-1)+(VLI(NT)-VLI(NT-1))*(TN-TI(NT-1))/(TI(NT)-TI(NT-
      IF(NDBG.NE.1)GOTO 79
      IF(NUBC.EQ.1)WRITE(6,6010)VIN
      IF(NUBC.EQ.2)WRITE(6,6011)VIN
 6010 FORMAT(5X,'QIN = ',F12.0/)
 6011 FORMAT(5X,'YIN = ',F12.3/)
C
C
C     DETERMINE VALUE AT D/S NODE
C
C
      IF(NDBC.LT.3)GOTO 82
      DO 77 I=1,NOO
      IF(TN.GT.TO(I))GOTO 77
      NT=I
      GOTO 78
 77   CONTINUE
 78   CONTINUE
      VOUT=VLO(NT-1)+(VLO(NT)-VLO(NT-1))*(TN-TO(NT-1))/(TO(NT)-TO(NT
 82   CONTINUE
C
C
C     MATRIX POSITION COUNTER
C
C
 79   CONTINUE
      ITER=0
 55   CONTINUE
      ITER=ITER+1
      IF(NDBG.NE.1)GOTO 81
      WRITE(6,6001)ITER
 6001 FORMAT(5X,'ITERATION # ',I5)
 81   CONTINUE
      DO 100 I=1,NN
      IF(I.NE.1) GOTO 200
      IF(NUBC.EQ.2)GOTO 150
C
C
C     ----------------------------------------------------
C
C
C       UPSTREAM BOUNDARY NODE CALCULATION
C
C
C     ----------------------------------------------------
C
C
C     DISCHARGE
```

```
C
C
      YNB=YN(1)
      VNB=VN(1)
      QNB=VIN
      CALL PROP(I,YNB,A,R,B)
      RES(1)=QNB-VNB*A
      CALL DERIV(I,YNB,DAY,DB,DRY)
      U(1)=VNB*DAY
      U(2)=A
      L(1)=1.
      GOTO 100
C
C
C     DEPTH
C
C
  150 CONTINUE
      YNB=VIN
      RES(1)=YNB-YN(1)
      U(1)=1.
      U(2)=0.
      L(1)=1.
      GOTO 100
C
C
C     ---------------------------------------------------------
C
C
C        CONTINUITY EQUATION CALCULATION AT EACH NODE
C
C
C     ---------------------------------------------------------
C
C
  200 IF(I.EQ.NN) GOTO 300
      NC=2*INT(I/2)
      IF(NC.NE.I) GOTO 250
      NI=I/2
      NI1=NI+1
      YN1=YN(NI)
      YN2=YN(NI1)
      YO1=YO(NI)
      YO2=YO(NI1)
      VN1=VN(NI)
      VN2=VN(NI1)
      VO1=VO(NI)
      VO2=VO(NI1)
      DX=XX(NI1)-XX(NI)
      CALL PROP(NI,YN1,AN1,R,BN1)
      CALL PROP(NI,YO1,AO1,R,BO1)
      CALL PROP(NI1,YN2,AN2,R,BN2)
      CALL PROP(NI1,YO2,AO2,R,BO2)
      BP=TH*(BN2+BN1)+(1.-TH)*(BO2+BO1)
      APP=TH*(AN2+AN1)+(1.-TH)*(AO2+AO1)
      APN=TH*(AN2-AN1)+(1.-TH)*(AO2-AO1)
      VPP=TH*(VN2+VN1)+(1.-TH)*(VO2+VO1)
      VPN=TH*(VN2-VN1)+(1.-TH)*(VO2-VO1)
      YS=YN2+YN1-YO2-YO1
      RES(I)=-1.*(1./(4.*DT)*BP*YS+.5/DX*(APP*VPN+VPP*APN))
      CALL DERIV(NI,YN1,DA1,DB1,DRY)
      CALL DERIV(NI1,YN2,DA2,DB2,DRY)
      L(J(I)-1)=.25*TH/DT*DB1*YS+.25/DT*BP+.5*TH/DX*DA1*(VPN-VPP)
      U(J(I))=-.5*TH/DX*(APP-APN)
      U(J(I+1)-1)=.25*TH/DT*DB2*YS+.25/DT*BP+.5*TH/DX*DA2*(VPN+VPP)
      U(J(I+2)-2)=.5*TH/DX*(APP+APN)
      L(J(I))=1.
      IF(I.NE.2)L(J(I)-2)=0.
      GOTO 100
C
C
C     -----------------------------------------------------
C
C
C       MOMENTUM EQUATION CALCULATION AT EACH NODE
C
C
C     -----------------------------------------------------
C
C
  250 NP=INT(I/2)
      NP1=NP+1
      YN1=YN(NP)
      YN2=YN(NP1)
      YO1=YO(NP)
      YO2=YO(NP1)
      VN1=VN(NP)
      VN2=VN(NP1)
      VO1=VO(NP)
      VO2=VO(NP1)
      CALL PROP(NP,YN1,A,RN1,B)
      CALL ROUGH(NP,RK1)
      AR(NP)=A
      CN1=2.5*DLOG(12.*RN1/RK1)
      SN1=VN1*VN1/(G*RN1*CN1*CN1)
      IF(NRF.EQ.2)SN1=RK1*RK1*VN1*VN1/RN1**(4./3.)/RMN/RMN
      SF(NP)=SN1
      CALL PROP(NP1,YN2,A,RN2,B)
      CALL ROUGH(NP1,RK2)
      AR(NP1)=A
      CN2=2.5*DLOG(12.*RN2/RK2)
      SN2=VN2*VN2/(G*RN2*CN2*CN2)
      IF(NRF.EQ.2)SN2=RK2*RK2*VN2*VN2/RN2**(4./3.)/RMN/RMN
      SF(NP1)=SN2
      CALL PROP(NP,YO1,A,RO1,B)
      CO1=2.5*DLOG(12.*RO1/RK1)
      SO1=VO1*VO1/(G*RO1*CO1*CO1)
      IF(NRF.EQ.2)SO1=RK1*RK1*VO1*VO1/RO1**(4./3.)/RMN/RMN
      CALL PROP(NP1,YO2,A,RO2,B)
      CO2=2.5*DLOG(12.*RO2/RK2)
      SO2=VO2*VO2/(G*RO2*CO2*CO2)
      IF(NRF.EQ.2)SO2=RK2*RK2*VO2*VO2/RO2**(4./3.)/RMN/RMN
      DX=XX(NP1)-XX(NP)
      VS=(VN1+VN2-VO1-VO2)/(2.*DT)
      VPP=TH*(VN2+VN1)+(1.-TH)*(VO2+VO1)
      VPN=TH*(VN2-VN1)+(1.-TH)*(VO2-VO1)
      YJ1=TH*(YN2+.92*TCK(NP1)-YN1-.92*TCK(NP))
      YJ2=(1.-TH)*(YO2+.92*TCK(NP1)-YO1-.92*TCK(NP))
      YP=G/DX*(YJ1+YJ2)
      SP=G/2.*(TH*(SN2+SN1)+(1.-TH)*(SO2+SO1))
      SPO=G*SO(NP)
      RES(I)=-1.*(VS+.5/DX*(VPP*VPN)+YP+SP-SPO)
      CALL DERIV(NP,YN1,DAY,DBY,DR1)
      CALL DERIV(NP1,YN2,DAY,DBY,DR2)
      SY1=(-5./CN1-1.)*VN1*VN1/(G*RN1*RN1*CN1*CN1)*DR1
      IF(NRF.EQ.2)SY1=-4./3.*RK1*RK1*VN1*VN1/RN1**(7./3.)*DR1/RMN/RM
      SY2=(-5./CN2-1.)*VN2*VN2/(G*RN2*RN2*CN2*CN2)*DR2
      IF(NRF.EQ.2)SY2=-4./3.*RK2*RK2*VN2*VN2/RN2**(7./3.)*DR2/RMN/RM
      SV1=2.*VN1/(CN1*CN1*G*RN1)
      IF(NRF.EQ.2)SV1=2.*VN1*RK1*RK1/RN1**(4./3.)/RMN/RMN
      SV2=2.*VN2/(CN2*CN2*G*RN2)
      IF(NRF.EQ.2)SV2=2.*VN2*RK2*RK2/RN2**(4./3.)/RMN/RMN
      L(J(I)-2)=G*TH*(.5*SY1-1./DX)
      L(J(I)-1)=.5/DT+.5*TH/DX*(VPN-VPP)+G/2.*TH*SV1
      U(J(I))=G*TH*(.5*SY2+1./DX)
      U(J(I+1)-1)=.5/DT+.5*TH/DX*(VPN+VPP)+G/2.*TH*SV2
      U(J(I)-2)=0.
      L(J(I))=1.
      GOTO 100
C
C
C     ----------------------------------------------------
C
C
C        DOWNSTREAM BOUNDARY NODE CALCULATION
C
C
C     ----------------------------------------------------
C
C
 300  CONTINUE
      IF(NDBC.EQ.2)GOTO 350
      IF(NDBC.EQ.3)GOTO 400
      IF(NDBC.EQ.4)GOTO 450
C
C
C        OPTION 1 - UNIFORM FLOW D/S B.C.
C
C
      YN1=YN(NX)
      YN2=YN(NXS)
      Y1=YN(NX)+.92*TCK(NX)
      Y2=YN(NXS)+.92*TCK(NXS)
      VN1=VN(NX)
      VN2=VN(NXS)
      DX=XX(NXS)-XX(NX)
      CALL PROP(NX,YN1,A,RN1,B)
      CALL PROP(NXS,YN2,A,RN2,B)
      CALL ROUGH(NX,RK1)
      CALL ROUGH(NXS,RK2)
      CN1=2.5*DLOG(12.*RN1/RK1)
      CN2=2.5*DLOG(12.*RN2/RK2)
      SS=SO(NX)+(Y1-Y2)/DX
      SF2=2.*SS-SF(NX)
      RES(I)=CN2*DSQRT(G*RN2*SF2)-VN2
      IF(NRF.EQ.2)RES(I)=RMN*RN2**(2./3.)*DSQRT(SF2)/RK2-VN2
      CALL DERIV(NX,YN1,DA1,DB1,DR1)
      CALL DERIV(NXS,YN2,DA2,DB2,DR2)
      SY1=(-5./CN1-1.)*VN1*VN1/(G*RN1*RN1*CN1*CN1)*DR1
      IF(NRF.EQ.2)SY1=-4./3.*RK1*RK1/RMN/RMN*VN1*VN1/RN1**(7./3.)*DF
      SV1=2.*VN1/(CN1*CN1*G*RN1)
      IF(NRF.EQ.2)SV1=2.*RK1*RK1/RMN/RMN*VN1/RN1**(4./3.)
      DSC=-.5*CN2*DSQRT(G*RN2/SF2)
      DRC=(-2.5-CN2/2.)*DSQRT(G*SF2/RN2)
      DSM=-.5*RMN/RK2*RN2**(2./3.)/DSQRT(SF2)
      DRM=-2./3.*RMN/RK2/RN2**(1./3.)*DSQRT(SF2)
      L(J(I)-3)=DSC*(2./DX-SY1)
      IF(NRF.EQ.2)L(J(I)-3)=DSM*(2./DX-SY1)
      L(J(I)-2)=-1.*DSC*SV1
      IF(NRF.EQ.2)L(J(I)-2)=-1.*DSM*SV1
      L(J(I)-1)=DRC*DR2-DSC*2./DX
      IF(NRF.EQ.2)L(J(I)-1)=DRM*DR2-DSM*2./DX
      U(J(I))=1.
      U(J(I)-3)=0.
      L(J(I))=1.
      GOTO 100
C
C
C        OPTION 2 - CRITICAL FLOW D/S B.C.
C
C
  350 CONTINUE
      Y=YN(NXS)
      V VN(NXS)
      CALL PROP(NXS,Y,A,R,B)
      CALL DERIV(NXS,Y,DAY,DBY,DRY)
      RES(I)=-1.*(V*V*B-G*A)
      L(J(I)-2)=0.
      L(J(I)-1)=V*V*DBY-G*DAY
      U(J(I))=2.*V*B
      L(J(I))=1.
      GOTO 100
C
C
C        OPTION 3 - GIVEN ELEVATION D/S B.C.
C
```

```
C
 400   CONTINUE
       YND=VOUT
       RES(I)=YND-YN(NXS)
       L(J(I)-2)=0.
       L(J(I)-1)=1.
       U(J(I))=0.
       L(J(I))=1.
       GOTO 100
C
C
C         OPTION 4 - GIVEN DISCHARGE D/S B.C.
C
C
 450   CONTINUE
       YND=YN(NXS)
       VND=VN(NXS)
       QND=VOUT
       CALL PROP(I,YND,A,R,B)
       RES(I)=QND-VND*A
       CALL DERIV(I,YND,DAY,DB,DRY)
       L(J(I)-2)=0.
       L(J(I)-1)=VND*DAY
       U(J(I))=A
       L(J(I))=1.
  100 CONTINUE
C
C
C      ----------------------------------------------------
C
C
C         SOLVE MATRIX
C
C
C      ----------------------------------------------------
C
C
       CALL UACTL(U,L,RES,J,NN)
       DO 500 II=1,NXS
       YN(II)=YN(II)+RES(2*II-1)
       VN(II)=VN(II)+RES(2*II)
  500 CONTINUE
C
C
C         CHECK FOR CONVERGENCE
C
C
       NK=0
       DO 600 II=1,NN
       IF(DABS(RES(II)).GT.TOL)NK=1
  600 CONTINUE
       IF(NK.EQ.1)GOTO 55
C
C
```

```
C     ---------------------------------------------------
C
C
C       CALCULATE MAXIMUMS AND HYDROGRAPHS
C
C
C     ---------------------------------------------------
C
C
      NCMP=NHT*INT(IT/NHT)
      IF(IT.NE.NCMP)GOTO 606
      IH=IH+1
      DO 605 JJ=1,NHYD
      QH(JJ,IH)=VN(NH(JJ))*AR(NH(JJ))
      YH(JJ,IH)=YN(NH(JJ))
      TIM(IH)=TN
 605  CONTINUE
 606  CONTINUE
      DO 700 II=1,NXS
      QN=VN(II)*AR(II)
      IF(YN(II).LE.YM(II))GOTO 610
      YM(II)=YN(II)
      TM(II)=TT/3600.
 610  IF(VN(II).LE.VM(II))GOTO 620
      VM(II)=VN(II)
 620  IF(QN.LE.QM(II))GOTO 630
      QM(II)=QN
 630  IF(SF(II).LE.SFM(II))GOTO 650
      SFM(II)=SF(II)
 650  YO(II)=YN(II)
      VO(II)=VN(II)
 700  CONTINUE
C
C
C     ---------------------------------------------------
C
C
C       CHECK FOR OUTPUT
C
C
C     ---------------------------------------------------
C
C
      IF(N1.GT.NTP)GOTO 900
      IF(TN.LT.TP(N1))GOTO 900
      CALL OUTPUT(TN)
      N1=N1+1
 900  CONTINUE
 1000 CONTINUE
      CALL HYDPUT(NHYD,NH,QH,YH,TIM,IH)
      CALL MAXPUT(YM,VM,QM,TM,SFM,NXS)
      STOP
      END
C
```

```
C
C     XXXXXXXXXXXXXXXXXXXXXXXXXXXXXXXXXXXXXXXXXXXXXXXXXXXXXX
C     XXXXXXXXXXXXXXXXXXXXXXXXXXXXXXXXXXXXXXXXXXXXXXXXXXXXXX
C
C     END OF MAIN PROGRAM
C
C     XXXXXXXXXXXXXXXXXXXXXXXXXXXXXXXXXXXXXXXXXXXXXXXXXXXXXX
C     XXXXXXXXXXXXXXXXXXXXXXXXXXXXXXXXXXXXXXXXXXXXXXXXXXXXXX
C
C
C
C
C
C
C
C
C     ******************************************************
C     *                                                    *
C     *                                                    *
C     *    SUBROUTINE TO CALCULATE DERIVATIVES             *
C     *                                                    *
C     *                                                    *
C     ******************************************************
C
C
      SUBROUTINE DERIV(I,YN,DA,DB,DR)
      IMPLICIT REAL*8(A-H,L,O-Z)
      COMMON/FIVE/DER,NRF,NTXS,G,RMN
      CALL PROP(I,YN,A1,R1,T1)
      YD=YN+DER
      CALL PROP(I,YD,A2,R2,T2)
      DA=(A2-A1)/DER
      DB=(T2-T1)/DER
      DR=(R2-R1)/DER
      RETURN
      END
C
C
C     ******************************************************
C     *                                                    *
C     *                                                    *
C     *    SUBROUTINE TO CALCULATE SECTION PROPERTIES      *
C     *                                                    *
C     *                                                    *
C     ******************************************************
C
C
      SUBROUTINE PROP(NCS,Y,A,R,TW)
      IMPLICIT REAL*8(A-H,L,O-Z)
      COMMON/ONE/NPTS(200),X(200,20),EL(200,20)
      COMMON/TWO/THALW(200),AR(200),XX(200),TCK(200)
      COMMON/FIVE/DER,NRF,NTXS,G,RMN
      COMMON/SIX/BW,RM
      IF(NTXS.NE.2)GOTO 50
      A=BW*Y+RM*Y*Y
      TW=BW+2.*RM*Y
      P=BW+2.*DSQRT(1.+RM*RM)*Y
      R=A/(P+TW)
      IF(TCK(NCS).EQ.0.)R=A/P
      RETURN
 50   CONTINUE
      A=0.0
      TW=0.0
      P=0.0
      R=0.0
      I=0
      EY=THALW(NCS)+Y
C
  100 I=I+1
      IF(I-NPTS(NCS))102,101,101
  101 R=A/P
      IF(TCK(NCS).EQ.0.)GOTO 107
      R=A/(P+TW)
 107  CONTINUE
      RETURN
  102 IF(EY-EL(NCS,I))104,104,103
  103 IF(EY-EL(NCS,I+1))200,200,300
  104 IF(EY-EL(NCS,I+1))105,105,200
  105 DA=0.0
      DT=0.0
      DP=0.0
      GO TO 400
C
  200 S=(X(NCS,I+1)-X(NCS,I))/(EL(NCS,I+1)-EL(NCS,I))
      X1=EL(NCS,I+1)-EY
      IF(X1)202,201,201
C
  201 X1=EY-EL(NCS,I)
  202 DT=S*X1
      X2=ABS(X1)
      DA=DT*X2*0.5
      DP=X2*DSQRT(1.0+(S*S))
      GO TO 400
C
  300 DT=X(NCS,I+1)-X(NCS,I)
      X1=EY-EL(NCS,I)
      X2=EL(NCS,I)-EL(NCS,I+1)
      DA=DT*(X1+(X2*0.5))
      DP=DSQRT((DT*DT)+(X2*X2))
C
  400 A=A+DA
      TW=TW+DT
      P=P+DP
      GO TO 100
      END
C
C
C
```

```
C     ***********************************************************
C     *                                                         *
C     *                                                         *
C     *    SUBROUTINE TO CALCULATE UNIFORM FLOW PROFILE         *
C     *                                                         *
C     *                                                         *
C     ***********************************************************
C
C
C
      SUBROUTINE INIT(NXS,Q,TOL,NBC,NDBG,SOD,YO,VO,SF)
      IMPLICIT REAL*8(A-H,L,O-Z)
      DIMENSION YO(200),VO(200),SF(200)
      COMMON/TWO/THALW(200),AR(200),XX(200),TCK(200)
      COMMON/FIVE/DER,NRF,NTXS,G,RMN
C
C
C
      NX=NXS-1
      Y0=YO(NXS)
      IF((NBC.EQ.1).AND.(NRF.EQ.2))GOTO 510
      IF(NBC.EQ.2)GOTO 600
      IF(NBC.EQ.3)GOTO 800
C
C     ----------------------------------------------------------
C
C     OPTION # 1 - UNIFORM FLOW (USING C* METHOD)
C
C     ----------------------------------------------------------
C
      IF(SOD.EQ.0.)SOD=(THALW(NX)-THALW(NXS))/(XX(NXS)-XX(NX))
      ITER=0
 100  CONTINUE
      IF(NDBG.NE.1)GOTO 110
      ITER=ITER+1
      WRITE(6,6000)NXS,ITER,Y0
 6000 FORMAT(5X,'SECT.',I3,5X,'ITER #',I3,5X,'Y  =',F8.3)
 110  CONTINUE
      CALL PROP(NXS,Y0,A,R,B)
      CALL ROUGH(NXS,RK)
      CC=2.5*DLOG(12.*R/RK)
      V=CC*DSQRT(G*R*SOD)
      Z=Q-V*A
      CALL DERIV(NXS,Y0,DA,DB,DR)
      DZ=-2.5*A*V/R/CC*DR-V*DA-.5*CC*A*DSQRT(G*SOD/R)*DR
      Y=Y0-Z/DZ
      IF(DABS(Y-Y0).LT.TOL)GOTO 200
      Y0=Y
      GOTO 100
 200  CONTINUE
      YO(NXS)=Y
      VO(NXS)=V
      SF(NXS)=V*V/(G*R*CC*CC)
      AR(NXS)=A
      GOTO 450
C
C     ----------------------------------------------------
C
C     OPTION # 1 - UNIFORM FLOW (USING MANNING'S EQUATION)
C
C     ----------------------------------------------------
C
 510  CONTINUE
      IF(SOD.EQ.0.)SOD=(THALW(NX)-THALW(NXS))/(XX(NXS)-XX(NX))
      ITER=0
 520  CONTINUE
      IF(NDBG.NE.1)GOTO 530
      ITER=ITER+1
      WRITE(6,6000)NXS,ITER,Y0
 530  CONTINUE
      CALL PROP(NXS,Y0,A,R,B)
      CALL ROUGH(NXS,RK)
      V=R**(2./3.)*DSQRT(SOD)*RMN/RK
      Z=Q-V*A
      CALL DERIV(NXS,Y0,DA,DB,DR)
      DZ=-V*DA-2./3.*A/R*V*DR
      Y=Y0-Z/DZ
      IF(DABS(Y-Y0).LT.TOL)GOTO 540
      Y0=Y
      GOTO 520
 540  CONTINUE
      YO(NXS)=Y
      VO(NXS)=V
      SF(NXS)=V*V*RK*RK/R**(4./3.)/RMN/RMN
      AR(NXS)=A
      GOTO 450
C
C     ----------------------------------------------------
C
C     OPTION # 2 - CRITICAL FLOW
C
C     ----------------------------------------------------
C
 600  CONTINUE
      ITER=0
 700  CONTINUE
      IF(NDBG.NE.1)GOTO 710
      ITER=ITER+1
      WRITE(6,6000)NXS,ITER,Y0
 710  CONTINUE
      CALL PROP(NXS,Y0,A,R,B)
      Z=Q*Q-G*A*A*A/B
      CALL DERIV(NXS,Y0,DA,DB,DR)
      DZ=G*A*A/B*(A/B*DB-3.*DA)
      Y=Y0-Z/DZ
      IF(DABS(Y-Y0).LT.TOL)GOTO 750
      Y0=Y
      GOTO 700
 750  CONTINUE
      YO(NXS)=Y
      VO(NXS)=Q/A
      CALL ROUGH(NXS,RK)
      CC=2.5*DLOG(12.*R/RK)
      SF(NXS)=VO(NXS)*VO(NXS)/(G*R*CC*CC)
      IF(NRF.EQ.2)SF(NXS)=VO(NXS)*VO(NXS)*RK*RK/R**(4./3.)/RMN/RMN
      AR(NXS)=A
      GOTO 450
C
C     ----------------------------------------------------
C
C     OPTION # 3 - FIXED ELEVATION
C
C     ----------------------------------------------------
C
 800  CONTINUE
      YO(NXS)=Y0
      CALL PROP(NXS,Y0,A,R,B)
      VO(NXS)=Q/A
      CALL ROUGH(NXS,RK)
      CC=2.5*DLOG(12.*R/RK)
      SF(NXS)=VO(NXS)*VO(NXS)/(G*R*CC*CC)
      IF(NRF.EQ.2)SF(NXS)=VO(NXS)*VO(NXS)*RK*RK/R**(4./3.)/RMN/RMN
      AR(NXS)=A
      GOTO 450
C
C     ----------------------------------------------------
C
C     STANDARD STEP GRADUALLY VARIED FLOW
C
C     ----------------------------------------------------
C
 450  CONTINUE
      DO 300 I=1,NX
      N=NXS-I
      DZ=THALW(N+1)-THALW(N)
      Y1=YO(N+1)
      V1=VO(N+1)
      S1=SF(N+1)
      DX=XX(N+1)-XX(N)
      ITER=0
      Y2=Y1
 350  CONTINUE
      ITER=ITER+1
      IF(NDBG.NE.1)GOTO 210
      WRITE(6,6000)N,ITER,Y2
 210  CONTINUE
      CALL PROP(N,Y2,A,R,B)
      CALL ROUGH(N,RK)
      C=2.5*DLOG(12.*R/RK)
      V2=Q/A
      S2=V2*V2/(G*R*C*C)
      IF(NRF.EQ.2)S2=V2*V2*RK*RK/R**(4./3.)/RMN/RMN
      DTK=.92*(TCK(N+1)-TCK(N))
      RES=DZ+Y1-Y2+DTK+DX/2.*(S1+S2)+(V1*V1-V2*V2)/2./G
      CALL DERIV(N,Y2,DAY,DBY,DRY)
      DSY=V2*V2*DX/(2.*G*R*R*C*C)*((-1.-5./C)*DRY-2.*R/A*DAY)
      IF(NRF.EQ.2)DSY=S2*DX*(-2./3./R*DRY-1./A*DAY)
      DY=DSY+V2*Q/A/A/G*DAY-1.
      YN2=Y2-RES/DY
      IF(DABS(YN2-Y2).LT.TOL)GOTO 400
      Y2=YN2
      GOTO 350
  400 CONTINUE
      YO(N)=YN2
      VO(N)=V2
      SF(N)=S2
      AR(N)=A
  300 CONTINUE
C
C
C
      RETURN
      END
C
C
C     ******************************************************
C     *                                                    *
C     *                                                    *
C     *    SUBROUTINE TO SOLVE MATRIX                      *
C     *                                                    *
C     *                                                    *
C     ******************************************************
C
C
      SUBROUTINE UACTL (A,C,B,JDIAG,NEQ)
      IMPLICIT REAL*8(A-H,L,O-Z)
      DIMENSION        A(1), B(1), C(1), JDIAG(1)
C
C        FACTOR A TO UT*D*U, REDUCE B TO Y
C
      JR=0
      DO 300 J=1,NEQ
      JD=JDIAG(J)
      JH=JD-JR
      IF (JH .LE. 1) GO TO 300
      IS=J+1-JH
      IE=J-1
      K=JR+1
      ID=0
C
C        REDUCE ALL EQUATIONS EXCEPT DIAGONAL
C
      DO 200 I=IS,IE
      IR=ID
      ID=JDIAG(I)
      IH=MIN0(ID-IR-1,I-IS)
      IF (IH.EQ.0) GO TO 150
      A(K)=A(K)-DOT(A(K-IH), C(ID-IH), IH)
      C(K)=C(K)-DOT(C(K-IH), A(ID-IH), IH)
 150  IF (A(ID) .NE. 0.0) C(K)=C(K)/A(ID)
 200  K=K+1
C
C        REDUCE DIAGONAL TERM
C
      A(JD)=A(JD)-DOT(A(JR+1), C(JR+1), JH-1)
C
C        FORWARD REDUCE THE R.H.S.
C
 250  B(J)=B(J)-DOT(C(JR+1), B(IS), JH-1)
 300  JR=JD
C
C        BACK SUBSTITUTION
C
      J=NEQ
      JD=JDIAG(J)
 500  IF (A(JD) .NE. 0.0) B(J)=B(J)/A(JD)
      D=B(J)
      J=J-1
      IF (J .LE. 0) RETURN
      JR=JDIAG(J)
      IF ((JD-JR) .LE. 1) GO TO 700
      IS=J-JD+JR+2
      K=JR-IS+1
      DO 600 I=IS,J
 600  B(I)=B(I)-A(I+K)*D
 700  JD=JR
      GO TO 500
C
      END
      FUNCTION DOT (A,B,N)
      IMPLICIT REAL*8(A-H,L,O-Z)
      DIMENSION A(1),B(1)
      DOT=0.0
      DO 100 I=1,N
     DOT=DOT+A(I)*B(I)
 100  CONTINUE
      RETURN
      END
C
C
C     *****************************************************
C     *                                                   *
C     *                                                   *
C     *    SUBROUTINE TO CALCULATE COMPOSITE ROUGHNESS    *
C     *                                                   *
C     *                                                   *
C     *****************************************************
C
C
      SUBROUTINE ROUGH(N,RK)
      IMPLICIT REAL*8(A-H,L,O-Z)
      COMMON/FOUR/RKB(200),RKI(200)
      COMMON/TWO/THALW(200),AR(200),XX(200),TCK(200)
      COMMON/FIVE/DER,NRF,NTXS,G,RMN
      IF(NRF.EQ.2)GOTO 100
      RK=((RKB(N)**(1./3.)+RKI(N)**(1./3.))/2.)**3
      GOTO 200
  100 CONTINUE
      RK=DSQRT((RKB(N)*RKB(N)+RKI(N)*RKI(N))/2.)
  200 CONTINUE
      IF(TCK(N).EQ.0.)RK=RKB(N)
      RETURN
      END
C
C
C     ******************************************************
C     *                                                    *
C     *                                                    *
C     *     SUBROUTINE TO PRINT PROFILES                   *
C     *                                                    *
C     *                                                    *
C     ******************************************************
C
C
      SUBROUTINE OUTPUT(TN)
      IMPLICIT REAL*8(A-H,L,O-Z)
      COMMON/THREE/YN(200),VN(200),SF(200),NXS
      COMMON/TWO/THALW(200),AR(200),XX(200),TCK(200)
      WRITE(7,7001)TN
 7001 FORMAT(//5X,'AFTER ',F10.3,' HOURS, CONDITIONS ARE : '//)
      WRITE(7,7002)
 7002 FORMAT(5X,'  DISTANCE WAT. SURF   THALWEG',
     *'      DEPTH  VELOCITY DISCHARGE    FRIC. SLOPE'/)
      DO 85 I=1,NXS
      WL=YN(I)+THALW(I)+.92*TCK(I)
      QS=VN(I)*AR(I)
      WRITE(7,7004)XX(I),WL,THALW(I),YN(I),VN(I),QS,SF(I)
 7004 FORMAT(5X,F10.0,4F10.3,F10.1,F14.8)
 85   CONTINUE
      RETURN
      END
C
C
C     ******************************************************
C     *                                                    *
C     *                                                    *
C     *     SUBROUTINE TO PRINT MAXIMUM CONDITIONS         *
C     *                                                    *
C     *                                                    *
C     ******************************************************
C
C
      SUBROUTINE MAXPUT(YM,VM,QM,TM,SFM,NXS)
      IMPLICIT REAL*8(A-H,L,O-Z)
      DIMENSION YM(200),VM(200),QM(200),TM(200),SFM(200),SFN(200)
      COMMON/TWO/THALW(200),AR(200),XX(200),TCK(200)
      WRITE(7,7010)
 7010 FORMAT(////5X,'***** MAXIMUM CONDITIONS *****'//)
      WRITE(7,7011)
 7011 FORMAT(5X,'  DISTANCE       TIME      DEPTH  VELOCITY',
     *' DISCHARGE FRICTION SLOPE'/)
      DO 100 I=1,NXS
      WRITE(7,7012)XX(I),TM(I),YM(I),VM(I),QM(I),SFM(I)
 7012 FORMAT(5X,F10.0,3F10.3,F10.1,F15.8)
 100  CONTINUE
      RETURN
      END
C
C
C     ****************************************************
C     *                                                  *
C     *                                                  *
C     *     SUBROUTINE TO PRINT HYDROGRAPHS              *
C     *                                                  *
C     *                                                  *
C     ****************************************************
C
C
      SUBROUTINE HYDPUT(NHYD,NH,QH,YH,TIM,IH)
      IMPLICIT REAL*8(A-H,L,O-Z)
      DIMENSION NH(10),QH(10,200),YH(10,200),TIM(200)
      COMMON/TWO/THALW(200),AR(200),XX(200),TCK(200)
      WRITE(7,7700)
 7700 FORMAT(////5X,'***** HYDROGRAPHS *****'//)
      DO 100 I=1,NHYD
      WRITE(7,7701)NH(I),XX(NH(I))
 7701 FORMAT(//5X,'HYDROGRAPH AT STATION ',I5,'  DISTANCE = ',F10.0/
      WRITE(7,7702)
 7702 FORMAT(5X,'       TIME           DEPTH       DISCHARGE'/)
      DO 200 J=1,IH
      WRITE(7,7703)TIM(J),YH(I,J),QH(I,J)
 7703 FORMAT(5X,F10.3,F15.3,F15.1)
 200  CONTINUE
 100  CONTINUE
      RETURN
      END
```

APPENDIX B : DATA FOR DIAGNOSTIC PLOTS

Table B.1 - Ch. 3

	Tp'	Tb'	Q'	Fo	x'	Y/Yo	Sf/So	Cw/Vo
Fig. 3.3	1	2	3	0.3	1	1.67	1.33	3.40
	5					1.88	1.10	2.27
	20					1.92	1.03	1.42
	1		5			2.20	1.51	3.93
	5					2.54	1.17	2.69
	20					2.60	1.06	1.86
	1		7			2.67	1.66	4.44
	5					3.10	1.23	2.93
	20					3.19	1.09	2.13
Fig. 3.4	0.5	2	3	0.3	1	1.51	1.50	3.55
			5			1.95	1.81	3.84
			9			2.69	2.17	4.15
	1		3			1.67	1.33	3.23
			5			2.20	1.51	3.57
			9			3.08	1.78	3.84
	10		3			1.91	1.06	1.82
			5			2.59	1.10	2.27
			9			3.68	1.18	2.69

Table B.1 - continued

	Tp'	Tb'	Q'	Fo	x'	Y/Yo	Sl/So	Cw/Vo
Fig. 3.5	1	2	3	0.3	1	1.67		
		6				1.79		
		10				1.83		
		2	5			2.20		
		6				2.39		
		10				2.45		
		2	7			2.67		
		6				2.90		
		10				2.98		
Fig. 3.6	1	2	3	0.1	1			3.47
				0.3				3.29
				0.5				2.84
			5	0.1				3.97
				0.3				3.60
				0.5				3.04
			7	0.1				4.29
				0.3				3.73
				0.5				3.20

Table B.2 - Ch. 4

	X'	L'	Y'	Fo	x'	Y/Yo	Sl/So	Cw/Vo
Fig. 4.3 and 4.4a	1	0.2	2	0.3	1	1.46		
	5					1.85		
	20					2.00		
	1		4			2.43		
	5					3.30		
	20					3.92		
	1		6			3.42		
	5					4.58		
	20					5.72		
Fig. 4.5 and 4.4b,c	5	0.2	2	0.1	1		1.97	7.22
				0.3			1.54	4.96
				0.5			1.39	3.14
			4	0.1			4.12	9.18
				0.3			2.74	6.15
				0.5			2.18	3.89
			6	0.1			6.99	10.31
				0.3			3.97	6.99
				0.5			2.73	4.71
Fig. 4.6	5	0.1	2	0.1	1		1.99	7.82
		0.5					1.92	6.82
		1					1.84	6.18
		0.1		0.3			1.58	5.01
		0.5					1.50	4.77
		1					1.44	4.08
		0.1		0.5			1.40	3.26
		0.5					1.38	3.09
		1					1.35	2.98

APPENDIX C : DATA FOR PREDICTIVE PLOTS

Table C.1 - Ch.3

			Tb'=2		Tb'=4	
Q'	Tp'	xSo/Yo	Y/Yo	Q/Qo	Y/Yo	Q/Qo
3	0.2	0.00	1.59	3.00	1.65	3.00
		0.96	1.29	1.75	1.45	2.06
		1.91	1.18	1.39	1.34	1.73
		2.87	1.14	1.28	1.27	1.55
		3.82	1.12	1.22	1.23	1.45
		4.78	1.11	1.19	1.20	1.38
		5.73	1.09	1.17	1.18	1.34
		6.69	1.09	1.16	1.17	1.31
		7.65	1.08	1.14	1.16	1.29
		8.60	1.08	1.13	1.15	1.27
		9.56	1.07	1.13	1.14	1.25
3	1	0.00	1.80	3.00	1.82	3.00
		0.96	1.67	2.54	1.75	2.67
		1.91	1.58	2.27	1.70	2.51
		2.87	1.51	2.08	1.66	2.40
		3.82	1.45	1.93	1.63	2.30
		4.78	1.41	1.83	1.60	2.23
		5.73	1.38	1.74	1.57	2.16
		6.69	1.35	1.68	1.55	2.11
		7.65	1.33	1.63	1.53	2.06
		8.60	1.31	1.59	1.51	2.01
		9.56	1.30	1.56	1.49	1.97
3	5	0.00	1.91	3.00	1.91	3.00
		1.02	1.88	2.91	1.89	2.94
		2.05	1.86	2.84	1.88	2.90
		3.07	1.84	2.80	1.87	2.86
		4.09	1.82	2.75	1.86	2.84
		5.12	1.81	2.71	1.86	2.82
		6.14	1.79	2.68	1.85	2.80
		7.16	1.78	2.64	1.84	2.78
		8.19	1.77	2.61	1.84	2.76
		9.21	1.76	2.58	1.83	2.75
		10.24	1.75	2.55	1.83	2.73

Table C.1 - continued

α	Tp'	xSo/Yo	Sf/So	Cw/Vo
3	0.2	0.00	1.94	
		0.96	1.49	4.83
		1.91	1.22	4.52
		2.87	1.12	4.14
		3.82	1.08	3.83
		4.78	1.06	3.57
		5.73	1.05	3.38
		6.69	1.04	3.18
		7.65	1.03	3.06
		8.60	1.03	2.94
		9.56	1.03	2.84
3	1	0.00	1.35	
		0.96	1.34	3.54
		1.91	1.32	3.43
		2.87	1.28	3.29
		3.82	1.24	3.20
		4.78	1.21	3.11
		5.73	1.18	3.04
		6.69	1.15	2.99
		7.65	1.14	2.94
		8.60	1.12	2.90
		9.56	1.11	2.86
3	5	0.00	1.09	
		1.02	1.09	2.18
		2.05	1.09	2.56
		3.07	1.09	2.56
		4.09	1.09	2.56
		5.12	1.09	2.49
		6.14	1.09	2.44
		7.16	1.10	2.43
		8.19	1.10	2.43
		9.21	1.10	2.41
		10.24	1.10	2.39

Table C.1 - continued

			Tb'=2		Tb'=4	
Q'	Tp'	xSo/Yo	Y/Yo	Q/Qo	Y/Yo	Q/Qo
5	0.2	0.00	2.05	5.00	2.15	5.00
		0.96	1.57	2.62	1.84	3.26
		1.91	1.36	1.83	1.64	2.56
		2.87	1.28	1.57	1.51	2.16
		3.82	1.23	1.46	1.44	1.92
		4.78	1.20	1.39	1.39	1.78
		5.73	1.18	1.34	1.35	1.69
		6.69	1.17	1.31	1.32	1.63
		7.65	1.16	1.29	1.30	1.57
		8.60	1.15	1 27	1.28	1.53
		9.56	1.14	1.25	1.27	1.50
5	1	0.00	2.39	5.00	2.43	5.00
		0.96	2.20	4.19	2.33	4.40
		1.91	2.06	3.65	2.25	4.09
		2.87	1.95	3.30	2.19	3.86
		3.82	1.86	3.00	2.13	3.67
		4.78	1.78	2.76	2.08	3.51
		5.73	1.72	2.58	2.04	3.38
		6.69	1.67	2.43	2.00	3.26
		7.65	1.63	2.32	1.96	3.15
		8.60	1.59	2.23	1.93	3.06
		9.56	1.56	2.15	1.90	2.97
5	5	0.00	2.58	5.00	2.58	5.00
		1.02	2.54	4.84	2.57	4.88
		2.05	2.51	4.74	2.55	4.81
		3.07	2.49	4.62	2.53	4.75
		4.09	2.46	4.55	2.52	4.70
		5.12	2.44	4.48	2.51	4.65
		6.14	2.42	4.42	2.50	4.62
		7.16	2.40	4.35	2.49	4.58
		8.19	2.38	4.29	2.48	4.55
		9.21	2.36	4.24	2.47	4.52
		10.24	2.35	4.18	2.46	4.49

Table C.1 - continued

α	Tp'	xSo/Yo	Sf/So	Cw/Vo
5	0.2	0.00	2.40	
		0.96	1.92	5.60
		1.91	1.46	5.06
		2.87	1.25	4.62
		3.82	1.17	4.30
		4.78	1.12	4.00
		5.73	1.10	3.77
		6.69	1.08	3.56
		7.65	1.07	3.40
		8.60	1.06	3.27
		9.56	1.05	3.16
5	1	0.00	1.56	
		0.96	1.54	4.09
		1.91	1.54	3.87
		2.87	1.52	3.67
		3.82	1.46	3.54
		4.78	1.41	3.43
		5.73	1.36	3.38
		6.69	1.31	3.29
		7.65	1.28	3.25
		8.60	1.25	3.19
		9.56	1.22	3.16
5	5	0.00	1.16	
		1.02	1.15	2.67
		2.05	1.15	2.98
		3.07	1.15	2.98
		4.09	1.16	2.87
		5.12	1.16	2.80
		6.14	1.16	2.76
		7.16	1.17	2.70
		8.19	1.17	2.65
		9.21	1.18	2.64
		10.24	1.18	2.61

Table C.1 - continued

			Tb'=2		Tb'=4	
Q'	Tp'	xSo/Yo	Y/Yo	Q/Qo	Y/Yo	Q/Qo
7	0.2	0.00	2.44	7.00	2.57	7.00
		0.96	1.82	3.64	2.18	4.54
		1.91	1.52	2.32	1.92	3.47
		2.87	1.40	1.88	1.75	2.82
		3.82	1.34	1.69	1.63	2.43
		4.78	1.30	1.59	1.56	2.20
		5.73	1.27	1.52	1.51	2.05
		6.69	1.25	1.47	1.47	1.95
		7.65	1.23	1.43	1.43	1.87
		8.60	1.22	1.40	1.41	1.81
		9.56	1.20	1.38	1.39	1.75
7	1	0.00	2.89	7.00	2.95	7.00
		0.96	2.66	5.89	2.82	6.16
		1.91	2.48	5.12	2.72	5.71
		2.87	2.35	4.59	2.64	5.36
		3.82	2.22	4.13	2.57	5.08
		4.78	2.11	3.75	2.50	4.84
		5.73	2.02	3.45	2.45	4.64
		6.69	1.95	3.21	2.39	4.45
		7.65	1.89	3.03	2.34	4.29
		8.60	1.85	2.88	2.30	4.14
		9.56	1.80	2.76	2.26	4.00
7	5	0.00	3.15	7.00	3.16	7.00
		1.02	3.11	6.78	3.14	6.85
		2.05	3.07	6.63	3.11	6.75
		3.07	3.03	6.50	3.09	6.65
		4.09	3.01	6.39	3.08	6.57
		5.12	2.98	6.29	3.06	6.51
		6.14	2.95	6.19	3.05	6.44
		7.16	2.93	6.10	3.04	6.40
		8.19	2.90	6.00	3.02	6.35
		9.21	2.88	5.92	3.01	6.30
		10.24	2.86	5.83	3.00	6.26

Table C.1 - continued

Q	Tp'	xSo/Yo	Sf/So	Cw/Vo
7	0.2	0.00	2.77	
		0.96	2.34	5.91
		1.91	1.71	5.45
		2.87	1.39	4.98
		3.82	1.26	4.62
		4.78	1.19	4.32
		5.73	1.15	4.04
		6.69	1.12	3.86
		7.65	1.10	3.65
		8.60	1.09	3.51
		9.56	1.08	3.39
7	1	0.00	1.72	
		0.96	1.69	4.62
		1.91	1.70	4.17
		2.87	1.71	3.94
		3.82	1.66	3.79
		4.78	1.60	3.67
		5.73	1.54	3.57
		6.69	1.48	3.51
		7.65	1.42	3.46
		8.60	1.38	3.42
		9.56	1.34	3.37
7	5	0.00	1.21	
		1.02	1.21	2.89
		2.05	1.21	3.26
		3.07	1.21	3.26
		4.09	1.21	3.11
		5.12	1.22	2.98
		6.14	1.22	2.90
		7.16	1.23	2.85
		8.19	1.24	2.81
		9.21	1.24	2.78
		10.24	1.25	2.73

Table C.2 - Ch.4

Y^*	X^*	xSo/Yo	Y/Yo	Q/Qo
2	0.2	0.00	1.96	7.40
		0.24	1.53	3.05
		0.48	1.46	2.25
		0.96	1.39	1.90
		1.91	1.31	1.64
		2.87	1.27	1.53
		3.82	1.24	1.46
		4.78	1.22	1.41
		5.73	1.20	1.37
		7.65	1.18	1.32
		9.56	1.16	1.29
2	1	0.00	1.78	3.92
		0.51	1.54	2.56
		1.02	1.47	2.20
		2.03	1.39	1.83
		3.05	1.35	1.69
		4.06	1.31	1.61
		5.08	1.29	1.55
		6.09	1.27	1.51
		8.12	1.24	1.45
		10.15	1.22	1.40
2	5	0.00	1.94	4.07
		0.20	1.91	3.22
		0.51	1.88	3.05
		1.02	1.85	2.94
		2.03	1.80	2.76
		3.05	1.76	2.63
		4.06	1.72	2.53
		5.08	1.69	2.44
		6.09	1.66	2.37
		8.12	1.61	2.25
		10.15	1.58	2.16
2	20	0.00	2.01	3.19
		0.20	2.01	3.19
		0.41	2.01	3.19
		1.02	2.01	3.18
		2.05	2.00	3.18
		3.07	2.00	3.17
		4.09	2.00	3.16
		5.12	1.99	3.16
		6.14	1.99	3.15
		8.19	1.98	3.13
		10.24	1.98	3.11

Table C.2 - continued

Y'	Fo	xSo/Yo	Sf/So	Cw/Vo
2	0.1	0.00	6.15	
		0.12	3.96	
		0.24	3.01	
		0.48	2.42	
		0.96	1.82	8.06
		1.91	1.47	5.94
		2.87	1.32	5.13
		3.82	1.25	4.57
		4.78	1.20	4.25
		5.73	1.17	3.99
		6.69	1.14	3.76
		7.65	1.13	3.59
		8.60	1.10	3.44
		9.56	1.04	3.32
2	0.3	0.00	2.83	
		0.10	2.32	
		0.20	2.15	
		0.51	1.87	
		1.02	1.58	4.26
		2.03	1.40	4.08
		3.05	1.34	3.83
		4.06	1.30	3.65
		5.08	1.27	3.50
		6.09	1.24	3.35
		7.11	1.22	3.26
		8.12	1.21	3.18
		9.14	1.19	3.11
		10.15	1.16	3.05
2	0.5	0.00	1.64	
		0.20	1.55	
		0.41	1.48	
		1.02	1.39	3.44
		2.05	1.32	3.35
		3.07	1.29	3.26
		4.09	1.26	3.18
		5.12	1.25	3.10
		6.14	1.23	3.03
		7.16	1.21	2.97
		8.19	1.20	2.91
		9.21	1.19	2.88
		10.24	1.17	2.83

Table C.2 - continued

Y*	X*	xSo/Yo	Y/Yo	Q/Qo
4	0.2	0.00	3.86	29.86
		0.24	2.81	10.19
		0.48	2.61	7.26
		0.96	2.41	5.60
		1.91	2.16	4.17
		2.87	2.01	3.52
		3.82	1.91	3.15
		4.78	1.83	2.90
		5.73	1.78	2.72
		7.65	1.69	2.47
		9.56	1.63	2.31
4	1	0.00	3.12	13.53
		0.51	2.61	6.86
		1.02	2.46	5.82
		2.03	2.29	4.49
		3.05	2.17	3.94
		4.06	2.09	3.62
		5.08	2.02	3.38
		6.09	1.97	3.21
		8.12	1.88	2.95
		10.15	1.82	2.76
4	5	0.00	3.50	13.60
		0.20	3.45	9.56
		0.51	3.39	9.00
		1.02	3.30	8.29
		2.03	3.16	7.57
		3.05	3.04	6.93
		4.06	2.95	6.48
		5.08	2.87	6.12
		6.09	2.79	5.82
		8.12	2.68	5.35
		10.15	2.58	5.00
4	20	0.00	3.96	9.99
		0.20	3.96	9.97
		0.41	3.96	9.96
		1.02	3.94	9.92
		2.05	3.92	9.84
		3.07	3.90	9.76
		4.09	3.88	9.67
		5.12	3.85	9.57
		6.14	3.83	9.48
		8.19	3.78	9.28
		10.24	3.73	9.08

Table C.2 - continued

Y'	Fo	xSo/Yo	Sf/So	Cw/Vo
4	0.1	0.00	10.19	
		0.12	8.33	
		0.24	6.12	
		0.48	5.15	
		0.96	3.76	10.22
		1.91	2.61	7.88
		2.87	2.11	6.79
		3.82	1.86	6.11
		4.78	1.69	5.54
		5.73	1.58	5.19
		6.69	1.51	4.86
		7.65	1.44	4.62
		8.60	1.40	4.41
		9.56	1.36	4.22
4	0.3	0.00	4.97	
		0.10	3.77	
		0.20	3.78	
		0.51	3.43	
		1.02	3.06	5.67
		2.03	2.29	5.37
		3.05	2.12	4.94
		4.06	2.01	4.75
		5.08	1.91	4.56
		6.09	1.82	4.38
		7.11	1.75	4.26
		8.12	1.69	4.15
		9.14	1.64	4.05
		10.15	1.60	3.96
4	0.5	0.00	2.67	
		0.20	2.56	
		0.41	2.45	
		1.02	2.18	3.98
		2.05	1.94	3.98
		3.07	1.82	3.89
		4.09	1.77	3.73
		5.12	1.76	3.61
		6.14	1.73	3.61
		7.16	1.70	3.56
		8.19	1.66	3.52
		9.21	1.62	3.47
		10.24	1.58	3.44

Table C.2 - continued

Y'	X'	xSo/Yo	Y/Yo	Q/Qo
6	0.2	0.00	5.77	63.67
		0.24	4.17	19.27
		0.48	3.85	17.91
		0.96	3.42	11.50
		1.91	2.96	7.83
		2.87	2.70	6.17
		3.82	2.53	5.27
		4.78	2.40	4.70
		5.73	2.30	4.30
		7.65	2.16	3.78
		9.56	2.06	3.45
6	1	0.00	4.59	27.68
		0.51	3.69	15.42
		1.02	3.51	12.40
		2.03	3.24	8.50
		3.05	3.07	7.36
		4.06	2.95	6.65
		5.08	2.85	6.15
		6.09	2.77	5.78
		8.12	2.63	5.23
		10.15	2.53	4.84
6	5	0.00	4.92	27.97
		0.20	4.85	18.30
		0.51	4.75	16.90
		1.02	4.59	15.80
		2.03	4.37	13.90
		3.05	4.21	12.39
		4.06	4.07	11.45
		5.08	3.95	10.70
		6.09	3.84	10.12
		8.12	3.67	9.21
		10.15	3.52	8.53
6	20	0.00	5.76	18.95
		0.20	5.75	18.91
		0.41	5.74	18.86
		1.02	5.71	18.73
		2.05	5.66	18.49
		3.07	5.61	18.25
		4.09	5.56	17.99
		5.12	5.51	17.73
		6.14	5.45	17.46
		8.19	5.35	16.92
		10.24	5.26	16.39

Table C.2 - continued

Y'	Fo	xSo/Yo	Sf/So	Cw/Vo
6	0.1	0.00	12.12	
		0.12	10.76	
		0.24	9.03	
		0.96	5.78	12.36
		1.91	4.28	9.67
		2.87	3.20	8.62
		3.82	2.61	7.46
		4.78	2.27	6.73
		5.73	2.06	6.19
		6.69	1.91	5.81
		7.65	1.80	5.49
		8.60	1.71	5.23
		9.56	1.64	5.02
6	0.3	0.00	5.89	
		0.10	5.06	
		0.20	4.36	
		0.51	3.95	
		2.03	3.57	6.38
		3.05	3.05	5.89
		4.06	2.72	5.52
		5.08	2.58	5.32
		6.09	2.44	5.19
		7.11	2.33	5.03
		8.12	2.22	4.89
		9.14	2.14	4.76
		10.15	2.06	4.66
6	0.5	0.00	3.21	
		0.20	2.95	
		0.41	2.72	
		1.02	2.73	5.12
		2.05	2.55	4.65
		3.07	2.32	4.55
		4.09	2.35	4.37
		5.12	2.24	4.31
		6.14	2.18	4.18
		7.16	2.21	4.12
		8.19	2.14	4.08
		9.21	2.06	4.05
		10.24	1.99	4.00